Distribution Systems Planning Considering Distributed Generation and Energy Storage Systems

ALEJANDRO VALENCIA DÍAZ

UNIVERSIDAD TECNOLÓGICA DE PEREIRA
Faculty of Engineering - Electric Engineering program
Master in Electrical Engineering
PEREIRA, RISARALDA, COLOMBIA
2020

Distribution Systems Planning Considering Distributed Generation and Energy Storage Systems

Thesis submitted as a partial requirement to receive the grade of:
Master in Electrical Engineering

Advisor: Ramón Alfonso Gallego Rendón, Ph.D.

Co-advisor: Ricardo Alberto Hincapié Isaza, Ph.D.

UNIVERSIDAD TECNOLÓGICA DE PEREIRA
Faculty of Engineering - Electric Engineering program
Master in Electrical Engineering
PEREIRA, RISARALDA, COLOMBIA
2020

Dedication

- To my mother María Lida Diaz Noreña, my father Carlos Alfonso Valencia Cañas, and my brother Santiago Valencia Diaz whom supported me in all the difficult moments of this process and were always aware of my well-being.

The autor.

Acknowledgments

- To the advisor of this project Ph.D. Ramón A. Gallego Rendón and to the co-advisor Ph.D. Ricardo A. Hincapié Isaza for giving me their support, trust, and guidance, to make this achievement possible.
- To all the professors of the Program of Electrical Engineering and Master in Electrical Engineering for their valuable contributions to my professional development.

The autor.

Abstract

This thesis presents a new methodology for optimal integrated planning of medium and low voltage distribution systems with distributed generation (DG) in the low voltage network, and integration of energy storage systems (ESSs). This problem is formulated as a mixed integer non-linear problem and is solved using a simulated annealing algorithm (SA) with a novel neighborhood search method based on the Zbus matrix (NSZM). The NSZM method uses sensitivity factors based on the Zbus matrix for reducing the neighborhood size in order to find attractive solutions based on the electrical information of the Zbus matrix. Hence, the solution space is explored more efficiently in order to find a joint global solution that establishes a balanced benefit for the planning of both networks.

This methodology is compared to a bilevel approach used in the literature to verify its efficiency. The bilevel approach solved the optimal integrated planning of medium and low voltage distribution systems with a penetration of DG in the low voltage network using a real distribution system. The obtained results show the importance of considering both networks simultaneously in the planning of the electric distribution system, as well as the use of the Zbus matrix for sensitivity analysis, which allows finding answers with lower global costs.

Subsequent to the validation of the methodology, the ESSs are integrated in the distribution system planning problem (DSP) of the both networks considering DG. The obtained results show the importance of integrating ESSs in the DSP problem due to the maximization of the profit from the energy purchase and sale. Furthermore, the results show the impact of considering ESSs in the MV network instead of LV network.

Contents

List of Figures

List of Tables

Nomenclature

Chapter 3

Parameters

$C_{ij,p}^{EP}$	Fixed cost to expand the capacity of an existing primary feeder between nodes $i-j$, type p [$].
$C_{ij,c}^{ES}$	Fixed cost to expand the capacity of an existing secondary circuit between nodes $i-j$, type c [$].
C_{s}^{ESS}	Fixed cost to expand the capacity of an existing substation type s [$].
$C_{ij,p}^{NP}$	Fixed cost of a new primary feeder between nodes $i-j$, type p [$].
$C_{ij,c}^{NS}$	Fixed cost of a new secondary circuit between nodes $i-j$, type c [$].
C_{s}^{NSS}	Fixed cost of a new substation type s [$].
C_{d}^{NDT}	Fixed cost of a new DT type d [$].
C_{g}^{NDG}	Fixed cost of a new DG type g [$].
C_{b}^{NESS}	Fixed cost of a new ESS type b [$].
$O_{\&}M_{b}^{fx}$	Fixed operation and maintenance cost of a new ESS type b [$/year].
$k1$	Factor which converts to present value.
$k2_{l}$	Energy purchase cost [$/kWh] for each load level l.
$k3$	Energy sale cost [$/kWh].
ΔT_{l}	Time duration of each load level l [h].
I_{p}^{max}	Maximum current limit of a primary wire type p [A].
I_{c}^{max}	Maximum current limit of a secondary wire type c [A].
NL	Number of load levels.
D_{year}	Number of days of the year.
ϕ_{b}	Charge/discharge slope of a ESS type b [%/kWh].
η_{b}	Power injection/extraction efficiency of a ESS type b [%].
SoC_{i}^{0}	Initial state of charge of a ESS at node i [%].
SoC_{i}^{F}	Final state of charge of a ESS at node i [%].
V_{nom}^{P}	Nominal voltage of the primary network.
V_{nom}^{S}	Nominal voltage of the secondary network.

a_0	Coefficient corresponding to constant power.
a_1	Coefficient corresponding to constant current.
a_2	Coefficient corresponding to constant impedance.
$Z^P_{ij,p}$	Impedance of the primary feeder between nodes $i-j$, type p [Ω].
$Z^S_{ij,c}$	Impedance of the secondary circuit between nodes $i-j$, type c [Ω].
G^P_{ij}	Conductance of the primary feeder between nodes $i-j$ [S].
B^P_{ij}	Susceptance of the primary feeder between nodes $i-j$ [S].
S^{max}_d	Maximum power limit of a DT type d [kVA].
S^{max}_g	Maximum power limit of a DG type g [kVA].
S^{max}_s	Maximum power limit of a substation type s [kVA].
S^{maxc}_b	Maximum extraction power limit of a ESS type b [kVA].
S^{maxd}_b	Maximum injection power limit of a ESS type b [kVA].
$S^{PD}_{i,l}$	Primary demand at node i, for a load level l [kVA].
$S^{SD}_{i,l}$	Secondary demand at node i, for a load level l [kVA].
V^{max}_i	Maximum voltage limit at node i [kV].
V^{min}_i	Minimum voltage limit at node i [kV].
SoC^{max}_i	Maximum state of charge of a ESS at node i [%].
SoC^{min}_i	Minimum state of charge of a ESS at node i [%].

Variables

$\gamma^{EP}_{ij,p}$	Binary decision variable to expand the capacity of an existing primary feeder between nodes $i-j$, type p.
$\gamma^{ES}_{ij,c}$	Binary decision variable to expand the capacity of an existing secondary circuit between nodes $i-j$, type c.
$\gamma^{ESS}_{i,s}$	Binary decision variable to expand the capacity of an existing substation at node i, type s.
$\gamma^{NDT}_{i,d}$	Binary decision variable to install a new DT at node i, type d.
$\gamma^{NDG}_{i,g}$	Binary decision variable to install a new DG at node i, type g.
$\gamma^{NP}_{ij,p}$	Binary decision variable to install a new primary feeder between nodes $i-j$, type p.
$\gamma^{NS}_{ij,c}$	Binary decision variable to install a new secondary circuit between nodes $i-j$, type c.

$\gamma_{i,s}^{NSS}$	Binary decision variable to install a new substation at node i, type s.
$\gamma_{i,b}^{NESS}$	Binary decision variable to install a new ESS at node i, type b.
$\varphi_{i,l}^{NESS}$	Binary decision variable for the operation state of the ESS at node i, for a load level l.
$I_{ij,l}^{P}$	Current flow in primary branch $i-j$, for a load level l [A].
$I_{ij,l}^{S}$	Current flow in secondary branch $i-j$ for a load level l [A].
$S_{i,l}^{DT}$	Power injected to a DT at node i, for a load level l [kVA].
$S_{i,l}^{DG}$	Power injected by a DG at node i, for a load level l [kVA].
$S_{i,l}^{S}$	Power injected by a substation at node i, for a load level l [kVA].
$S_{i,l}^{ESS}$	Power injected or extracted by a ESS at node i, for a load level l [kVA].
$S_{i,l}^{ESSD}$	Power injected by a ESS at node i, for a load level l [kVA].
$S_{i,l}^{ESSC}$	Power extracted by a ESS at node i, for a load level l [kVA].
$SoC_{i,l}$	State of charge of the ESS at node i, for a load level l [%].
$V_{i,l}^{BUS}$	Bus voltage at node i, for a load level l [kV].
$I_{i,l}^{BUS}$	Bus current at node i, for a load level l [A].
$ZIP_{i,l}^{P}$	ZIP load model at primary node i, for a load level l.
$ZIP_{i,l}^{S}$	ZIP load model at secondary node i, for a load level l.
Z_{ij}^{BUS}	Zbus matrix [Ω].
Sets	
Ω_{EP}	Set formed by existing primary feeders.
Ω_{ES}	Set formed by existing secondary circuits.
Ω_{ESS}	Set formed by existing substations.
Ω_{NDT}	Set formed by new DTs.
Ω_{NDG}	Set formed by new DGs.
Ω_{NESS}	Set formed by new ESSs.
Ω_{NL}	Set formed by the load levels.
Ω_{NP}	Set formed by new primary feeders.
Ω_{NS}	Set formed by new secondary circuits.
Ω_{NSS}	Set formed by new substations.
Ω_{PF}	Set formed by new and existing primary feeders.
Ω_{PN}	Set formed by nodes of primary network.

Ω_{SC}	Set formed by new and existing secondary circuits.
Ω_{SN}	Set formed by nodes of secondary circuits.
Ω_{N}	Set formed by nodes of primary and secondary networks.
Ω_{SS}	Set formed by new and existing substations.
Ω_{TDT}	Set formed by types of DTs.
Ω_{TDG}	Set formed by types of DGs.
Ω_{TESS}	Set formed by types of ESSs.
Ω_{TP}	Set formed by types of primary feeders.
Ω_{TS}	Set formed by types of secondary circuits.
Ω_{TSS}	Set formed by types of substations.

Chapter 4

Parameters

$k1$	Factor which converts to present value.
$k2_l$	Energy purchase cost [$/kWh] for each load level l.
$k3$	Energy sale cost [$/kWh].
ΔT_l	Time duration of each load level l [h].
S_{base}	Base apparent power of the system [kVA].
NL	Number of load levels.
D_{year}	Number of days of the year.
$\phi_{i,b}$	Charge/discharge slope of a ESS type b [%/kWh] at node i.
$\eta_{i,b}$	Power injection/extraction efficiency of a ESS type b at node i [pu].
SoC_i^0	Initial state of charge of a ESS at node i [%].
SoC_i^F	Final state of charge of a ESS at node i [%].
V_{ref}^{pu}	Magnitude of the voltage at node slack [pu].
θ_{ref}^{rad}	Angle of the voltage at node slack [rad].
a_0	Coefficient corresponding to constant power.
a_1	Coefficient corresponding to constant current.
a_2	Coefficient corresponding to constant impedance.
G_{ij}^P	Conductance of the primary feeder between nodes $i-j$ [pu].
B_{ij}^P	Susceptance of the primary feeder between nodes $i-j$ [pu].

$P_{i,g}^{max}$	Maximum active power limit of a DG at node i, type g [pu].
$P_{i,b}^{maxc}$	Maximum extraction limit of active power of a ESS at node i, type b [pu].
$P_{i,b}^{maxd}$	Maximum injection limit of active power of a ESS at node i, type b [pu].
$P_{i,l}^{D}$	Active demand at node i, for a load level l [pu].
$Q_{i,l}^{D}$	Reactive demand at node i, for a load level l [pu].
V_{i}^{max}	Maximum voltage limit at node i [pu].
V_{i}^{min}	Minimum voltage limit at node i [pu].
SoC_{i}^{max}	Maximum state of charge of a ESS at node i [%].
SoC_{i}^{min}	Minimum state of charge of a ESS at node i [%].
R_{ij}^{BUS}	Real part of the Zbus matrix [pu].
X_{ij}^{BUS}	Imaginary part of the Zbus matrix [pu].
Variables	
$P_{i,l}^{DG}$	Active power injected by a DG at node i, for a load level l [pu].
$P_{i,l}^{S}$	Active power injected by a substation at node i, for a load level l [pu].
$Q_{i,l}^{S}$	Reactive power injected by a substation at node i, for a load level l [pu].
$P_{i,l}^{ESS}$	Active power injected or extracted by a ESS at node i, for a load level l [pu].
$P_{i,l}^{ESSD}$	Active power injected by a ESS at node i, for a load level l [pu].
$P_{i,l}^{ESSC}$	Active power extracted by a ESS at node i, for a load level l [pu].
$SoC_{i,l}$	State of charge of the ESS at node i, for a load level l [%].
$V_{i,l}^{BUS}$	Bus voltage magnitude at node i, for a load level l [pu].
$I_{i,l}^{BUS}$	Bus current magnitude at node i, for a load level l [pu].
$\theta_{i,l}^{V}$	Bus voltage angle at node i, for a load level l [rad].
$\theta_{i,l}^{I}$	Bus current angle at node i, for a load level l [rad].
$ZIP_{i,l}$	ZIP load model in per unit representation at node i, for a load level l.
Sets	
Ω_{NL}	Set formed by the load levels.
Ω_{N}	Set formed by nodes of primary and secondary networks.
Ω_{TDG}	Set formed by types of DGs.
Ω_{TESS}	Set formed by types of ESSs.
Ω_{DG}	Set formed by DGs nodes.
Ω_{B}	Set formed by ESSs nodes.

Chapter 1

Introduction

1.1 Motivation

Distribution system planning (DSP) is a set of strategies that allows determining how many, where, and when elements can be installed in an electric network to satisfy the growing demand for a specific time horizon [1]. Traditionally, DSP is employed for upgrading existing elements and installing new electric circuits (medium and low voltage – MV/LV) and sources (substations and distribution transformers (DTs)) [2, 3]. Due to the combinatorial nature (NP-complete) of the DSP problem, both voltage levels (MV/LV) have been solved separately, allowing a reduced searching space but not leading to a joint global solution [4, 5]. In this context, several methodologies and different mathematical models have been proposed [6]. The number of papers regarding DSP for medium voltage [1, 2, 6–19] is higher than for low voltage [20–26]. Moreover, only a few of them consider both levels in an integrated way [3–5, 27–29].

Nowadays, the electric power sector has been presented an energetic change due to the emergence of new technologies, such as distributed generators (DGs), energy storage systems

(ESSs), and electric vehicles (EVs), which have produced technical, economic, and environmental benefits [1,30,31]. For this reason, incorporating DGs and ESSs into the DSP problem is desired. There are more papers considering DGs and ESSs in the DSP for MV [30, 32–37] than for LV [38–40]. For the integrated DSP of primary and secondary networks, only two have integrated DGs [5, 29], and only integrates DGs, ESSs, and EVs [41].

1.2 Problem Description

DSP is a complex mixed integer nonlinear optimization problem [29]. Classic optimization, and heuristic and metaheuristic methods have been used to solve DSP; classic optimization guarantees an optimal global solution but requires excessive computational effort due to the combinatorial complexity of DSP [4, 5]. Heuristic and metaheuristic methods can find near-global solutions, reducing the computational effort [4, 29]. As consequence, a metaheuristic is used to solve the DSP problem considering DGs and ESSs. This way, simulated annealing (SA) is applied because it has been employed in problems with similar mathematical complexity [9, 42, 43].

SA is a stochastic optimization algorithm that can converge asymptotically to the optimal global solution with probability one [44]. Although this may turn out to be computationally expensive, it is a valuable feature of the algorithm. Nevertheless, quick answers can be obtained for the SA algorithm with adequate cooling schemes and reduced neighborhoods which may yield a bunch of near or even globally optimal solutions. These neighborhoods can be reduced by using sensitivity factors based on the Zbus matrix in order to reduced computational efforts and obtained good quality solutions.

The Zbus matrix reflects important electrical characteristics of the network due its relation between voltages and current injections in a system [45]. This electrical information can be used through sensitivity factors to reduce the solution space obtained by the neighborhood

structure (branch exchange, upgrading existing elements, and the location of DGs and DTs) in order to find good quality solutions in quick times.

The integration of DGs and ESSs in the DSP problem increases its mathematical complexity due to the variability and intermittency of the DGs and the optimal charge and discharge operation of the ESSs. Therefore, it is needed to develop more robust models in order to solve the DSP problem considering ESSs. These models need to reduced computational efforts for the solving of the optimal charge and discharge operation of the ESSs and considering multiple scenarios due to the variability and intermittency of the DGs.

1.3 State of the Art

Despite the benefits provided by the Zbus matrix due its electrical information of the network, the Zbus matrix has not been used to solve the DSP problem. On the other hand, the Zbus has been used for different applications in the literature, such as load flow [46], reconfiguration of networks [47], and DGs location [48].

1.3.1 DSP for MV networks

In the literature, different papers used several mathematical models, objective functions, time stages, and solution techniques for the planning of MV networks [6]. Some authors presented integer linear approximation models to find near optimal solutions, such as the proposed in [7]. In order to find real optimal solutions, mixed integer nonlinear programming (MINLP) models were presented and solved using metaheuristic solution techniques for large scale MV networks, such as the genetic algorithm (GA) proposed in [10]. Other authors used different metaheuristics to solve the DSP problem, such as simulated annealing (SA), tabu search (TS), and GA [9, 11, 13].

Multi planning stages are considered in the DSP of MV networks for a time horizon to considered growth in the demand. In [8], authors used GAs in the optimal multistage planning of MV networks. Multiobjective functions allow to consider non-supplied energy under contingencies in the DSP problem to improve reliability. In [15], authors proposed a multiobjective multistage DSP using TS.

More accurate linear models were proposed to guarantee global optimal solutions, such as the mixed integer linear programming (MILP) model presented in [12] and solved using OSL solver in GAMS. Other authors presented different MILP models, such as the proposed in [16–19].

Nowadays, new technologies such as DGs and ESSs are integrated to distribution systems due to their benefits. As consequence, some papers considered the location and sizing of DGs and ESSs in the DSP of MV networks [30, 32–37]. Some authors used GAs to solve the DSP problem considering DGs [32, 34]. Other authors used a bilevel approach which combines an improved GA and a MILP model to solve the DSP problem considering DGs and ESSs [35]. These technologies introduce the need of considering different scenarios due to the variability and intermittency of the DGs and charge/discharge schemes of the ESSs. As consequence, some authors considered different scenarios using a probabilistic MILP model, such as in [30]. In [36], the authors proposed a stochastic methodology to consider different scenarios. Other authors used a mixed-integer second-order cone programming (MISOCP) to consider DGs and ESSs, such as in [37].

1.3.2 DSP for LV networks

Low voltage networks are three-phase and large size, due to these characteristics, the DSP problem becomes computationally expensive to solve. As consequence, most of the papers in the literature regarding DSP for low voltage are solved using metaheuristic techniques and

one time stage [6]. Some authors used evolutionary algorithms to solve the DSP problem in a large size LV network, such as in [20], and some others used to solve the DSP problem in a three-phase LV network, such as in [21].

Other authors used heuristic techniques with a micro optimization approach to solve the DSP of LV networks separately in small zones [22]. After micro optimization is done, the authors used TS with Voronoi's diagram with a macro optimization approach to solve the DSP of the complete LV network with the results of the micro optimization [23]. In [24], authors also used TS to solved the DSP of a three-phase LV network.

Electric utilities have different information about their customers due to the socioeconomic strata. Besides, these companies establish different technical requirements for the LV networks. This information and requirements need to be considered in the DSP problem of LV networks [25, 26]. In [25], the authors proposed a statistical methodology that uses a fractal-based algorithm to solve the DSP of a real UK distribution system. The authors considered all the information and requirements of the electric company. Other authors used the TS algorithm using diversified demand from the electric companies to solve the DSP of a LV network, such as in [26].

Nowadays, new technologies as DGs and ESSs are integrated to distribution systems but only DGs are considered into the DSP of LV networks. As consequence, some papers considered the location and sizing of DGs in the DSP for LV networks [38–40]. In [38], the authors used a GA to solve the DSP for a real three-phase LV network considering DGs and the reliability of the network. In [39], authors used a TS algorithm to solve the DSP for a three-phase LV network considering DGs and the reliability of the network. Other authors used clustering techniques to solve the DSP for a rural LV network, such as in [40].

1.3.3 Integrated DSP for MV and LV networks

Integrated DSP for both networks leads to a joint global solution but becomes computationally expensive to solve. As consequence, most of the paper regarding this integrated DSP used metaheuristic techniques to solve the problem [3–5, 28, 29, 41]. In [27], the authors used a MILP model to solve the DSP of both networks in an integrated way. Other authors used continuous constrained nonlinear programming methods to solve the integrated DSP problem, such as in [28].

In [4], the authors used a discrete particle swarm optimization (DPSO) method to solve the integrated DSP problem. Other authors used a new metaheuristic technique called biogeography-based optimization (BBO) and compared its efficiency with GA and PSO, such as in [3].

Currently, new technologies such as DGs, ESSs and EVs are incorporated to distribution systems, but only three papers considered them in the integrated DSP for both networks [5, 29, 41]. In [29], the authors used an imperialist competitive algorithm to solve the integrated DSP problem of both networks considering DGs. Other authors used TS and a bilevel optimization approach to solve the integrated DSP problem considering DGs, such as in [5]. In [41], the authors used a general variable neighborhood search metaheuristic (GVNS), along with the Chu-Beasley Genetic Algorithm (CBGA) to solve the integrated DSP problem considering DGs, ESSs and EVs. Nevertheless, it is needed to develop more robust models in order to solve the integrated DSP problem of both networks considering DGs and ESSs.

1.4 Contributions

The main contributions of this thesis are presented as follows:

- Proposal of a specialized simulated annealing algorithm which uses a novel neighborhood search method based on the Zbus matrix for solving the integrated DSP problem of both networks (primary and secondary) as one system. The Zbus matrix establishes an electrical relation between the primary and secondary nodes, where a change in one network is reflected in the electrical characteristics of the other one. As consequence, the results show that a joint global solution is found.

- A novel neighborhood search method based on the Zbus matrix (NSZM) is used to explore the solution space for the SA algorithm. The NSZM method uses sensitivity factors based on the Zbus matrix for reducing the neighborhood size in order to find attractive solutions in quick times. Hence, the solution space is explored more efficiently in order to find the optimal global solution.

- A new sensitivity analysis based on the Zbus matrix for solving the allocation and sizing of DGs and ESSs is proposed. The difference in relation to other papers from the literature is that the impact of DGs and ESSs in the technical losses of both networks is measured in an easy way. As a consequence, the solution space is explored efficiently in order to find better solutions.

- A new nonlinear model based on the Zbus matrix is used for the optimal power flow to evaluate operative conditions of the solutions considering ESSs and DGs. This nonlinear model finds the optimal operation of charge and discharge of the ESSs considering the operative conditions of the network and DGs.

- A new decomposition method is used to solve the optimal power flow considering ESSs and DGs. This method allows to find the optimal operation of charge and discharge of the ESSs in quick times. Hence, the proposed methodology is robust and accurate when ESSs and DGs are considered.

1.4.1 Research results

- Authors: Alejandro Valencia Diaz, Ramón Alfonso Gallego Rendón, Ricardo Alberto Hincapié Isaza. Title: Use of energy storage systems in the optimal operation of distribution networks. Accepted in: Ciencia e Ingeniería Neogranadina Vol. 29 Núm. 2 (2019).

- Authors: Alejandro Valencia Diaz, Ricardo Alberto Hincapié Isaza, Ramón Alfonso Gallego Rendón. Title: Integrated planning of MV/LV distribution systems with DG using single solution based metaheuristics with a novel neighborhood search method based on the Zbus matrix. Under revision: International Journal of Electrical Power & Energy Systems.

1.5 Structure of the Thesis

This thesis is organized as follows. The mathematical formulation of the problem is presented in Chapter 2. This Chapter describes three mathematical models: 1) the DSP for MV and LV networks, 2) the DSP for MV and LV networks considering DGs, and 3) the DSP for MV and LV networks considering DGs and ESSs. The second model is used to validate the solution methodology with the specialized literature. Chapter 3 describes the application of the Zbus matrix into the DSP problem. Chapter 4 presents the methodology based on the Zbus matrix used to solve the DSP problem considering DGs and ESSs. This Chapter presents the methodology used to solve the mathematical models presented in Chapter 2. The numerical results are presented in Chapter 5, where a test system is used to validate the presented methodology with results reported in the specialized literature. Chapter 6 presents the conclusions and future work.

Chapter 2

Problem Formulation and Modeling

The mathematical formulation of the DSP is a mixed-integer nonlinear problem. It is nonlinear due to the multiplication of variables in the equations of Kirchhoff's laws and the presence of the square of the voltage in the constant impedance term of the ZIP load model. Additionally, the model is mixed-integer because it has both integer and continuous variables (decision variables, current magnitudes, voltage levels, etc.). New technologies such as DGs and ESSs, introduce new constraints and variables to the DSP model. Furthermore, the objective function and some constraints are modified since these technologies change the paradigm of the DSP problem.

Three models are formulated in this chapter. The first model considers the DSP for MV and LV networks. This model considers in the objective function the inversion and operative costs of both networks; and presents the constraints that models the DSP problem. The second model considers the DGs in the DSP problem. This model introduces the inversion cost of new DGs in the objective function. Besides, a few constraints are modified and introduced from the first model. The third model considers DGs and ESSs in the DSP problem. This model introduces the inversion cost and the fixed operational and maintenance costs of new

ESSs. The operative cost in the objective function is changed by the profit from the energy purchase and sale. Furthermore, some constraints are modified and introduced from the second model.

2.1 DSP for MV and LV networks

The first mathematical model is presented in (2.1)–(2.20). The primary and secondary networks are represented by a single-phase model. Eq. (2.1) is the objective function which minimizes the investment and operative costs of the primary and secondary networks. The objective function is the present value of eight terms. Terms 1 and 2 are the installation and upgrading costs of the new and existing primary feeders, respectively. Terms 3 and 4 are the installation and upgrading costs of the new and existing substations, respectively. Term 5 is the cost of installing new DTs. Terms 6 and 7 are the installation and upgrading costs of the new and existing secondary circuits, respectively. Term 8 is the operative cost of the networks (technical energy losses in primary feeders, secondary circuits, and distribution transformers).

$$
\begin{aligned}
min = \Bigg\{ & \sum_{ij \in \Omega_{NP}} \sum_{p \in \Omega_{TP}} C_{ij,p}^{NP} \gamma_{ij,p}^{NP} + \sum_{ij \in \Omega_{EP}} \sum_{p \in \Omega_{TP}} C_{ij,p}^{EP} \gamma_{ij,p}^{EP} + \\
& \sum_{i \in \Omega_{NSS}} \sum_{s \in \Omega_{TSS}} C_{s}^{NSS} \gamma_{i,s}^{NSS} + \sum_{i \in \Omega_{ESS}} \sum_{s \in \Omega_{TSS}} C_{s}^{ESS} \gamma_{i,s}^{ESS} + \\
& \sum_{i \in \Omega_{NDT}} \sum_{d \in \Omega_{TDT}} C_{d}^{NDT} \gamma_{i,d}^{NDT} + \sum_{ij \in \Omega_{NS}} \sum_{c \in \Omega_{TS}} C_{ij,c}^{NS} \gamma_{ij,c}^{NS} + \\
& \sum_{ij \in \Omega_{ES}} \sum_{c \in \Omega_{TS}} C_{ij,c}^{ES} \gamma_{ij,c}^{ES} + k1 \sum_{l=1}^{NL} k2_l \, \mathbb{R}\mathrm{e} \left[\sum_{i \in \Omega_{SS}} S_{i,l}^{S} - \right. \\
& \left. \left(\sum_{i \in \Omega_{PN}} S_{i,l}^{PD} ZIP_{i,l}^{P} + \sum_{i \in \Omega_{SN}} S_{i,l}^{SD} ZIP_{i,l}^{S} \right) \right] \Delta T_l \Bigg\}
\end{aligned}
\tag{2.1}
$$

Subject to:

$$S_{i,l}^{S} = S_{i,l}^{DT} + S_{i,l}^{PD} ZIP_{i,l}^{P} + V_{i,l}^{BUS} \left(I_{i,l}^{BUS}\right)^{*} \quad \forall i \in \Omega_{PN};\ \forall l \in \Omega_{NL} \tag{2.2}$$

$$S_{i,l}^{DT} = S_{i,l}^{SD} ZIP_{i,l}^{S} + V_{i,l}^{BUS} \left(I_{i,l}^{BUS}\right)^{*} \quad \forall i \in \Omega_{SN};\ \forall l \in \Omega_{NL} \tag{2.3}$$

$$ZIP_{i,l}^{P} = a_0 + a_1 \left(\frac{V_{i,l}^{BUS}}{V_{nom}^{P}}\right) + a_2 \left(\frac{V_{i,l}^{BUS}}{V_{nom}^{P}}\right)^2 \quad \forall i \in \Omega_{PN};\ \forall l \in \Omega_{NL} \tag{2.4}$$

$$ZIP_{i,l}^{S} = a_0 + a_1 \left(\frac{V_{i,l}^{BUS}}{V_{nom}^{S}}\right) + a_2 \left(\frac{V_{i,l}^{BUS}}{V_{nom}^{S}}\right)^2 \quad \forall i \in \Omega_{SN};\ \forall l \in \Omega_{NL} \tag{2.5}$$

$$V_{i,l}^{BUS} = V_{nom}^{P} + \sum_{j \in \Omega_N} Z_{ij}^{BUS} I_{j,l}^{BUS} \qquad \forall i \in \Omega_{PN};\ \forall l \in \Omega_{NL} \tag{2.6}$$

$$V_{i,l}^{BUS} = V_{nom}^{S} + \sum_{j \in \Omega N} Z_{ij}^{BUS} I_{j,l}^{BUS} \qquad \forall i \in \Omega_{SN};\ \forall l \in \Omega_{NL} \tag{2.7}$$

$$I_{i,l}^{BUS} = \sum_{ij \in \Omega_{PF}} I_{ij,l}^{P} \qquad \forall i \in \Omega_{SS};\ \forall l \in \Omega_{NL} \tag{2.8}$$

$$I_{ij,l}^{P} = \left(\frac{V_{i,l}^{BUS} - V_{j,l}^{BUS}}{Z_{ij,p}^{P}}\right) \left(\gamma_{ij,p}^{NP} + \gamma_{ij,p}^{EP}\right) \quad \forall ij \in \Omega_{PF};\ \forall l \in \Omega_{NL};\ \forall p \in \Omega_{TP} \tag{2.9}$$

$$I_{ij,l}^{S} = \left(\frac{V_{i,l}^{BUS} - V_{j,l}^{BUS}}{Z_{ij,c}^{S}}\right) \left(\gamma_{ij,c}^{NS} + \gamma_{ij,c}^{ES}\right) \quad \forall ij \in \Omega_{SC};\ \forall l \in \Omega_{NL};\ \forall c \in \Omega_{TS} \tag{2.10}$$

$$0 \leq \left|I_{ij,l}^{P}\right| \leq \sum_{p \in \Omega_{TP}} \left(\gamma_{ij,p}^{NP} + \gamma_{ij,p}^{EP}\right) I_{p}^{max} \qquad \forall ij \in \Omega_{PF};\ \forall l \in \Omega_{NL} \tag{2.11}$$

$$0 \leq \left|I_{ij,l}^{S}\right| \leq \sum_{c \in \Omega_{TS}} \left(\gamma_{ij,c}^{NS} + \gamma_{ij,c}^{ES}\right) I_{c}^{max} \qquad \forall ij \in \Omega_{SC};\ \forall l \in \Omega_{NL} \tag{2.12}$$

$$0 \leq \left|S_{i,l}^{S}\right| \leq \sum_{s \in \Omega_{TSS}} \left(\gamma_{i,s}^{NSS} + \gamma_{i,s}^{ESS}\right) S_{s}^{max} \qquad \forall i \in \Omega_{SS};\ \forall l \in \Omega_{NL} \tag{2.13}$$

$$S_{i,l}^{DT} = V_{i,l}^{BUS} \left(\sum_{ki \in \Omega_{PF}} I_{ki,l}^{P} - \sum_{im \in \Omega_{PF}} I_{im,l}^{P} \right)^{*} \gamma_{i,d}^{NDT} \qquad \forall i \in \Omega_{NDT};\ \forall l \in \Omega_{NL} \tag{2.14}$$

$$0 \leq \left|S_{i,l}^{DT}\right| \leq \sum_{d \in \Omega_{TDT}} \gamma_{i,d}^{NDT} S_{d}^{max} \qquad \forall i \in \Omega_{NDT};\ \forall l \in \Omega_{NL} \tag{2.15}$$

$$V_{i}^{min} \leq \left|V_{i,l}^{BUS}\right| \leq V_{i}^{max} \qquad \forall i \in \Omega_{N};\ \forall l \in \Omega_{NL} \tag{2.16}$$

$$\sum_{p \in \Omega_{TP}} \left(\gamma_{ij,p}^{NP} + \gamma_{ij,p}^{EP}\right) \leq 1 \qquad \forall ij \in \Omega_{PF} \tag{2.17}$$

$$\sum_{c \in \Omega_{TS}} \left(\gamma_{ij,c}^{NS} + \gamma_{ij,c}^{ES}\right) \leq 1 \qquad \forall ij \in \Omega_{SC} \tag{2.18}$$

$$\sum_{s \in \Omega_{TSS}} \left(\gamma_{i,s}^{NSS} + \gamma_{i,s}^{ESS}\right) \leq 1 \qquad \forall i \in \Omega_{SS} \tag{2.19}$$

$$\sum_{d \in \Omega_{TDT}} \gamma_{i,d}^{NDT} \leq 1 \qquad \forall i \in \Omega_{NDT} \tag{2.20}$$

The set of constraints is presented in (2.2)–(2.20). Eqs. (2.2) and (2.3) represent the nodal balance given by Kirchhoff's laws for both networks. Eqs. (2.4) and (2.5) use the ZIP model for demands in both networks. Eqs. (2.6) and (2.7) use Ohm's law to calculate the nodal voltage using the Zbus matrix. Eq. (2.8) uses the Kirchhoff's first law to calculate the nodal currents in substations. Eqs. (2.9) and (2.10) calculate the currents in the primary feeders and secondary circuits, respectively. Eqs. (2.11), (2.12) and (2.13) are the operating limits of the primary feeders, secondary circuits, and substations, respectively. Eq. (2.14) determines the injected power in each DT. Eq. (2.15) is the operating limits of the DTs. Eq. (2.16) is the voltage limit in all nodes of both networks. Eqs. (2.17)–(2.20) ensure that only one type of wire, substation, and DT can be installed in the same place, respectively.

2.2 DSP for MV and LV networks considering DGs

The mathematical formulation of the DSP considering DGs is similar to the previous one, only some constraints are modified and some are added due to the DGs. Eqs. (2.1) and (2.3) are modified and replaced by Eqs. (2.21) and (2.22), and Eqs. (2.23) and (2.24) are added. Eq. (2.21) is the objective function which minimizes the investment and operative costs of the primary and secondary networks considering DGs. The objective function is the present value of nine terms. Terms 1 to 8 are the same of Eq. (2.1), and term 9 is the installation cost of new DGs.

$$
\begin{aligned}
min = \Bigg\{ & \sum_{ij\in\Omega_{NP}} \sum_{p\in\Omega_{TP}} C_{ij,p}^{NP}\gamma_{ij,p}^{NP} + \sum_{ij\in\Omega_{EP}} \sum_{p\in\Omega_{TP}} C_{ij,p}^{EP}\gamma_{ij,p}^{EP} + \\
& \sum_{i\in\Omega_{NSS}} \sum_{s\in\Omega_{TSS}} C_{s}^{NSS}\gamma_{i,s}^{NSS} + \sum_{i\in\Omega_{ESS}} \sum_{s\in\Omega_{TSS}} C_{s}^{ESS}\gamma_{i,s}^{ESS} + \\
& \sum_{i\in\Omega_{NDT}} \sum_{d\in\Omega_{TDT}} C_{d}^{NDT}\gamma_{i,d}^{NDT} + \sum_{ij\in\Omega_{NS}} \sum_{c\in\Omega_{TS}} C_{ij,c}^{NS}\gamma_{ij,c}^{NS} + \\
& \sum_{ij\in\Omega_{ES}} \sum_{c\in\Omega_{TS}} C_{ij,c}^{ES}\gamma_{ij,c}^{ES} + k1 \sum_{l=1}^{NL} k2_l \, \mathbb{R}\mathrm{e} \left[\sum_{i\in\Omega_{SS}} S_{i,l}^{S} - \right. \\
& \left. \left(\sum_{i\in\Omega_{PN}} S_{i,l}^{PD} ZIP_{i,l}^{P} + \sum_{i\in\Omega_{SN}} S_{i,l}^{SD} ZIP_{i,l}^{S} \right) \right] \Delta T_l + \\
& \sum_{i\in\Omega_{NDG}} \sum_{g\in\Omega_{TDG}} C_{g}^{NDG}\gamma_{i,g}^{NDG} \Bigg\}
\end{aligned}
\tag{2.21}
$$

$$
S_{i,l}^{DT} + S_{i,l}^{DG} = S_{i,l}^{SD} ZIP_{i,l}^{S} + V_{i,l}^{BUS} \left(I_{i,l}^{BUS} \right)^{*} \quad \forall i \in \Omega_{SN};\ \forall l \in \Omega_{NL} \tag{2.22}
$$

$$
0 \leq \left| S_{i,l}^{DG} \right| \leq S_{g}^{max} \gamma_{i,g}^{NDG} \qquad \forall i \in \Omega_{NDG};\ \forall l \in \Omega_{NL};\ \forall g \in \Omega_{TDG} \tag{2.23}
$$

$$
\sum_{g\in\Omega_{TDG}} \gamma_{i,g}^{NDG} \leq 1 \qquad \forall i \in \Omega_{NDG} \tag{2.24}
$$

Eq. (2.22) represents the nodal balance given by Kirchhoff's laws for LV network considering DGs. Eq. (2.23) is the operating limits of the DGs. Eq. (2.24) ensures that only one type of DG can be installed in the same place. The second mathematical model is presented in (2.21),(2.2),(2.22),(2.4)–(2.15),(2.23),(2.16)–(2.20),(2.24).

Objective function:

$$
\left\{ F_{Obj} = Eq.\ (2.21) \right\}
$$

Subject to:

$$\Big\{ Eqs.\ (2.2), (2.22), (2.4) - (2.15), (2.23), (2.16) - (2.20), (2.24) \Big\}$$

2.3 DSP for MV and LV networks considering DGs and ESSs

The mathematical formulation of the DSP considering ESSs has some changes from the previous models. ESSs are integrated to maximize the profits from the energy purchase and sale due to the charge and discharge scheme of these. As consequence, the objective function and some constraints are modified, and some others are added. Eqs. (2.21), (2.2) and (2.22) are modified and replaced by Eqs. (2.25), (2.26) and (2.27). Eqs. (2.28)–(2.35) are added.

Eq. (2.25) is the objective function which minimizes the investment and operative costs of the primary and secondary networks considering DGs and ESSs, and maximizes the profits from the energy purchase and sale. The maximize term can be converted to minimize by multiplying for minus one.

The objective function is the present value of nine terms. Terms 1 to 7, and 9 are the same of Eq. (2.21). Term 8 is the profit from the energy purchase and sale. Moreover, this term also considers the operative cost of the networks (technical energy losses in primary feeders, secondary circuits, distribution transformers, and energy storage systems). The value of this term is negative due to the change from maximize to minimize. Term 10 considered the installation cost and the fixed operational and maintenance costs of new ESSs.

$$
\begin{aligned}
min = \Bigg\{ & \sum_{ij\in\Omega_{NP}} \sum_{p\in\Omega_{TP}} C_{ij,p}^{NP}\gamma_{ij,p}^{NP} + \sum_{ij\in\Omega_{EP}} \sum_{p\in\Omega_{TP}} C_{ij,p}^{EP}\gamma_{ij,p}^{EP} + \\
& \sum_{i\in\Omega_{NSS}} \sum_{s\in\Omega_{TSS}} C_{s}^{NSS}\gamma_{i,s}^{NSS} + \sum_{i\in\Omega_{ESS}} \sum_{s\in\Omega_{TSS}} C_{s}^{ESS}\gamma_{i,s}^{ESS} + \\
& \sum_{i\in\Omega_{NDT}} \sum_{d\in\Omega_{TDT}} C_{d}^{NDT}\gamma_{i,d}^{NDT} + \sum_{ij\in\Omega_{NS}} \sum_{c\in\Omega_{TS}} C_{ij,c}^{NS}\gamma_{ij,c}^{NS} + \\
& \sum_{ij\in\Omega_{ES}} \sum_{c\in\Omega_{TS}} C_{ij,c}^{ES}\gamma_{ij,c}^{ES} + k1 \sum_{l=1}^{NL} \Bigg[k2_l \left(\sum_{i\in\Omega_{SS}} \mathbb{R}\mathrm{e}\left\{ S_{i,l}^{S} \right\} \right) \Delta T_l - \\
& k3\, \mathbb{R}\mathrm{e} \left(\sum_{i\in\Omega_{PN}} S_{i,l}^{PD} ZIP_{i,l}^{P} + \sum_{i\in\Omega_{SN}} S_{i,l}^{SD} ZIP_{i,l}^{S} \right) \Delta T_l \Bigg] D_{year} + \\
& \sum_{i\in\Omega_{NDG}} \sum_{g\in\Omega_{TDG}} C_{g}^{NDG}\gamma_{i,g}^{NDG} + \sum_{i\in\Omega_{NESS}} \sum_{b\in\Omega_{TESS}} \Big(C_{b}^{NESS} + \\
& k1\, O_{\&} M_{b}^{fx} \Big) \gamma_{i,b}^{NESS} \Bigg\}
\end{aligned}
\tag{2.25}
$$

$$
S_{i,l}^{S} + S_{i,l}^{ESS} = S_{i,l}^{DT} + S_{i,l}^{PD} ZIP_{i,l}^{P} + V_{i,l}^{BUS} \left(I_{i,l}^{BUS} \right)^{*} \quad \forall i \in \Omega_{PN};\ \forall l \in \Omega_{NL} \tag{2.26}
$$

$$
S_{i,l}^{DT} + S_{i,l}^{DG} + S_{i,l}^{ESS} = S_{i,l}^{SD} ZIP_{i,l}^{S} + V_{i,l}^{BUS} \left(I_{i,l}^{BUS} \right)^{*} \quad \forall i \in \Omega_{SN};\ \forall l \in \Omega_{NL} \tag{2.27}
$$

$$
S_{i,l}^{ESS} = S_{i,l}^{ESSD} - S_{i,l}^{ESSC} \qquad \forall i \in \Omega_{NESS};\ \forall l \in \Omega_{NL} \tag{2.28}
$$

$$
\begin{gathered}
SoC_{i,l} = SoC_{i,l-1} - \phi_b \left(\frac{1}{\eta_b} S_{i,l}^{ESSD} - \eta_b S_{i,l}^{ESSC} \right) \Delta T_l \quad \forall i \in \Omega_{NESS}; \\
\forall l \in \Omega_{NL};\ \forall b \in \Omega_{TESS}
\end{gathered}
\tag{2.29}
$$

$$
SoC_{i,l} = SoC_{i}^{0} \qquad l = 0;\ \forall i \in \Omega_{NESS} \tag{2.30}
$$

$$SoC_{i,l} = SoC_i^F \qquad l = NL;\ \forall i \in \Omega_{NESS} \tag{2.31}$$

$$0 \leq S_{i,l}^{ESSC} \leq S_b^{maxc} \gamma_{i,b}^{NESS} \varphi_{i,l}^{NESS} \quad \forall i \in \Omega_{NESS};\ \forall l \in \Omega_{NL};\ \forall b \in \Omega_{TESS} \tag{2.32}$$

$$0 \leq S_{i,l}^{ESSD} \leq S_b^{maxd} \gamma_{i,b}^{NESS} \left(1 - \varphi_{i,l}^{NESS}\right) \quad \forall i \in \Omega_{NESS};\ \forall l \in \Omega_{NL};\ \forall b \in \Omega_{TESS} \tag{2.33}$$

$$SoC_i^{min} \leq SoC_{i,l} \leq SoC_i^{max} \quad \forall i \in \Omega_{NESS};\ \forall l \in \Omega_{NL} \tag{2.34}$$

$$\sum_{b \in \Omega_{TESS}} \gamma_{i,b}^{NESS} \leq 1 \qquad \forall i \in \Omega_{NESS} \tag{2.35}$$

Eqs. (2.26) and (2.27) represent the nodal balance given by Kirchhoff's laws for MV and LV networks considering ESSs. Eqs. (2.28)–(2.35) model the integration of ESSs into the DSP model, where if $\varphi_{i,l}^{NESS} = 0$ the ESSs are injecting power and if $\varphi_{i,l}^{NESS} = 1$ the ESSs are extracting power. Eq. (2.28) considers the charge and discharge power of the ESSs as two different variables. Eq. (2.29) is the state of charge of the ESSs, this constraint considers the efficiency of charge and discharge of the ESSs. Eqs. (2.30) and (2.31) are the initial and final state of charge of the ESSs. Eqs. (2.32) and (2.33) are the operating limits of the charge and discharge power of the ESSs. Eq. (2.34) is the capacity limits of the ESSs. Eq. (2.35) ensures that only one type of ESS can be installed in the same place. The third mathematical model is presented in (2.25),(2.26)–(2.31),(2.4)–(2.15),(2.23),(2.32)–(2.34),(2.16)–(2.20),(2.24),(2.35).

Objective function:

$$\left\{ F_{Obj} = Eq.\ (2.25) \right\}$$

Subject to:

$$\left\{ Eqs.\ (2.26) - (2.31), (2.4) - (2.15), (2.23), (2.32) - (2.34), (2.16) - (2.20), (2.24), (2.35) \right\}$$

Chapter 3

Zbus Matrix

The Zbus matrix represents the relation between current injections and voltages in a system. This matrix is formed by diagonal and off-diagonal elements that represent the electrical information of the network. The diagonal elements of Zbus are the equivalent impedances between each bus and the reference bus, which are the same as the Thevenin impedances of each bus [45]. The off-diagonal elements are called transfer impedances and define the ratio of change for the voltage at a certain bus caused by a current injection at another bus (i.e., bus k). As consequence, the Zbus matrix reflects important electrical characteristics of the network, such as information for the neighborhood structure (branch exchange, upgrading existing elements, and the location of DGs, ESSs and DTs to minimize operative costs). Besides its electrical information, the Zbus matrix also contains and reflects some topological characteristics of the network. Thus, the Zbus matrix is used as sensitivity factors for reducing the neighborhood size of the solution method (SA). Moreover, the Zbus matrix is used for the analysis of the impact of DGs and ESSs in the technical losses of both network and for the solution of load flow to evaluate operative conditions of the solutions. Therefore, the Zbus matrix is used as the main basis of the methodology proposed to solve the DSP problem.

3.1 Constructive algorithm of the Zbus matrix

The Zbus matrix can be found by inverting the Ybus matrix. The disadvantage of this method is that inverting the Ybus matrix for large networks is computationally intensive. Therefore, it is better to build the Zbus by analyzing the relations between the currents and the voltages.

The constructive algorithm starts by adding branches from the reference node 0 until all the n nodes of the network are connected. In each step, a $m \times m$ partial Zbus matrix of the partial network of m buses and the reference node 0 is obtained. This procedure to find the Zbus matrix using a construction algorithm is described in [49]. This algorithm is only for radial networks and is shown in Fig. 3.1.

When a new element $p - q$ is added to the partial network, a new bus q is incorporated to the partial network and the new resultant Zbus matrix is of dimension $(m + 1) \times (m + 1)$. To determine the new Zbus matrix requires only the calculation of the elements in the new row and column.

$$\begin{aligned} Z_{qi}^{BUS} &= Z_{pi}^{BUS} \\ Z_{iq}^{BUS} &= Z_{ip}^{BUS} \end{aligned} \qquad i = 1, 2, ..., m;\ i \neq q \tag{3.1}$$

$$Z_{qq}^{BUS} = Z_{pq}^{BUS} + z_{pq}^{primitive} \tag{3.2}$$

$$\begin{aligned} Z_{qi}^{BUS} &= 0 \\ Z_{iq}^{BUS} &= 0 \end{aligned} \qquad i = 1, 2, ..., m;\ i \neq q \tag{3.3}$$

$$Z_{qq}^{BUS} = z_{pq}^{primitive} \tag{3.4}$$

The Eqs. (3.1) and (3.2) represents the adding of the element $p - q$ in the partial bus impedance matrix. The Eqs. (3.3) and (3.4) represents the adding of the element $p - q$ in the partial bus impedance matrix when p is the reference node.

Zbus matrix construction algorithm

```
1: begin
2:     while All nodes are not connected in the network do
3:         Add new element p − q
4:         if Node p is the reference node then
5:             Use Eq. (3.3);
6:             Use Eq. (3.4);
7:         else
8:             Use Eq. (3.1);
9:             Use Eq. (3.2);
10:        end if
11:        Partial Zbus matrix
12:    end while
13:    Final Zbus matrix
14: end
```

Figure 3.1: Constructive algorithm of the Zbus matrix.

3.2 Modifications of the Zbus matrix to reflect changes in the network

The Zbus matrix can be modified to reflect changes in the network without the need to build it again. These changes may be the addition or removal of elements and variation in the impedances of elements. These modifications are described in [49].

For adding an element, two options can happen: add a branch or a link. When a branch $p - q$ is added, a new bus q is incorporated to the network adding a new row and column

in the Zbus matrix. The Eqs. (3.1) and (3.2) are used to calculated the elements of the new row and column.

When a link $p-q$ is added, no new bus is added to the network. Therefore, the dimensions of the Zbus matrix are unchanged, but all the elements in the matrix must be recalculated to incorporate the effect of the added link. To include the link in the Zbus matrix, the Eqs. (3.5) and (3.6) are used. When these equations are applied, a new row and column is added to the Zbus matrix, hence, a fictitious node l is added.

$$\begin{aligned} Z_{li}^{BUS} &= Z_{pi}^{BUS} - Z_{qi}^{BUS} \\ Z_{il}^{BUS} &= Z_{ip}^{BUS} - Z_{iq}^{BUS} \end{aligned} \qquad i = 1, 2, ..., m;\ i \neq l \tag{3.5}$$

$$Z_{ll}^{BUS} = Z_{pl}^{BUS} - Z_{ql}^{BUS} + z_{pq}^{primitive} \tag{3.6}$$

For recalculating the elements of the Zbus matrix, Kron's reduction is used. This procedure was proposed by Kron [50], and is based on the elimination of a node in a matrix where the independent variable of this node is equal to zero. Eq. (3.7) represents the elimination of the row and column of the fictitious bus l by using the reduction of Kron.

$$Z_{modified}^{BUS} = Z_{n\times n}^{BUS} - \frac{\overline{Z}_{n\times l}^{BUS}\overline{Z}_{l\times n}^{BUS}}{Z_{ll}^{BUS}} \tag{3.7}$$

For removing an element $p-q$, the next procedure is applied. Between $p-q$ there is added, in parallel, a link whose impedance is equal to the negative of the impedance of the element $p-q$ to be removed, then the procedure explained before to recalculate the Zbus matrix is applied.

The procedure to change the impedance of an element $p-q$ is next. Between $p-q$ there is added, in parallel, a link whose impedance is such that the equivalent impedance of the two

elements in $p-q$ is the desired value, then the elements of the Zbus matrix are recalculated. Eq. (3.8) gives the value of the impedance added in the link $p-q$ to obtain the new value of impedance from the old value.

$$z_{pq}^{change} = \frac{z_{pq}^{old} z_{pq}^{new}}{z_{pq}^{old} - z_{pq}^{new}} \tag{3.8}$$

3.3 Topological information of the network provided by the Zbus matrix

The Zbus matrix provides physical information of the network by comparing some elements of the matrix with each other. The physical information obtained from the Zbus matrix is the next: Identification of terminal nodes, nodes upstream from a specific node, nodes downstream from a specific node, and send and receipt nodes. This information is useful for the neighborhood structure used to solve the DSP problem.

The neighborhood structure is applied to explore the search solution space of the problem in order to find the optimal global solution. The neighborhood structure modifies the topology from the current solution in order to explore the solution space. When these changes in the topologies are applied, it is important to know the physical information of the network to keep making changes for the neighborhood structure. A mishandling of the neighborhood structure can lead to expensive computational efforts, forbidden topologies and bad quality solutions. Therefore, the Zbus matrix is used to know the physical information of the current solutions in order to optimize the neighborhood structure process. The physical information that can be obtained from the Zbus matrix is the next.

The procedure to know if a specific node is a terminal node is next. If the Eq. (3.9) is true for all $i = 1, 2, ..., n$, the node k is a terminal node.

$$Z_{kk}^{BUS} \neq Z_{ki}^{BUS} \quad i = 1, 2, ..., n;\ i \neq k \tag{3.9}$$

To know which nodes are upstream from a specific node, the next procedure is applied. If the Eq. (3.10) is true, the node i is a node upstream from the node k.

$$Z_{ii}^{BUS} = Z_{ki}^{BUS} \tag{3.10}$$

The procedure to know which nodes are downstream from a specific node is next. If the Eq. (3.11) is satisfied, the node i is downstream from the node k.

$$Z_{kk}^{BUS} = Z_{ki}^{BUS} \tag{3.11}$$

The procedure to identify which nodes are send and receipt nodes is next. If Eq. (3.12) is true, the node p is the receipt node and the node q is the send node. Otherwise, the node p is the send node and the node q is the receipt node.

$$Z_{pp}^{BUS} > Z_{qq}^{BUS} \tag{3.12}$$

3.4 Electrical information of the network provided by the Zbus matrix

Due to the matrix form of the Zbus, it is easy to obtain in a quick way some electrical variables, such as the voltages. These are obtained by using the Eq. (3.13). The voltages

obtained are used to calculate in approximated way other variables such as the electric current in the branches and the power in the DTs.

$$\overline{V}_{BUS} = \overline{V}_{slack} + Z_{BUS}\left(\frac{\overline{S}^{D}\overline{ZIP}}{\overline{V}_{slack}} + \frac{\overline{S}^{DG}}{\overline{V}_{slack}} + \frac{\overline{S}^{ESS}}{\overline{V}_{slack}}\right)^{*} \tag{3.13}$$

3.4.1 Impact of the DGs and ESSs on the active power losses of the network

The Zbus matrix provides electrical information of the network in order to reduce the neighborhood size. This electrical information is obtained by using sensitivity factors in order to lead to the optimal global solution with reduced computational efforts.

DGs and ESSs are power injections introduced in a distributed way in the network affecting the active power losses. Therefore, it is needed a sensitivity factor that measures the impact of a change in the bus current injected in a given bus k on the active power losses in the distribution system (i.e., $\partial P_{Losses}/\partial I_k^{BUS}$).

The sensitivity factor applied in order to reduce the neighborhood structure of DGs and ESSs is demonstrated as follows. Network losses can be calculated using the Zbus matrix as shown in Eq. (3.14). From Eq. (3.14) the active network losses can be determined as shown in Eq. (3.15).

$$S_{Losses} = \left(I^{BUS}\right)^{T} Z^{BUS}\left(I^{BUS}\right)^{*} \tag{3.14}$$

$$P_{Losses} = \sum_{i=1}^{n}\sum_{j=1}^{n}\left[R_{ij}^{BUS} I_i^{BUS} I_j^{BUS}\cos\left(\Theta_i - \Theta_j\right)\right] \tag{3.15}$$

Taking the derivative of P_{Losses}, in Eq. (3.15), with respect to I_k^{BUS}, yields Eq. (3.16).

$$\frac{\partial P_{Losses}}{\partial I_k^{BUS}} = 2\sum_{j=1}^{n}\left[R_{kj}^{BUS} I_j^{BUS}\cos\left(\Theta_k - \Theta_j\right)\right] \tag{3.16}$$

This sensitivity factor calculates the impact in the active network losses due different power injections of the DGs and ESSs. As consequence, this factor leads the neighborhood structure in order to find the best alternatives.

3.5 Load flow based on the Zbus matrix

The load flow is essential for knowing the operating conditions of each generated configuration. As a consequence, a load flow based on the Zbus Gauss method described in [49] is proposed. This load flow is based upon the principle of superposition applied to the system bus voltages. The bus voltages depend on two different types of sources: the specified incoming bus voltage of the distribution substation, and the current injection which is generated by the loads. New types of sources like DGs and ESSs can be included such as PQ nodes. The steps of this load flow algorithm are described as follows.

Step 1: Initialize bus voltage estimates and the Zbus matrix.

Step 2: Calculate the bus injection current using Eq. (3.17) for loads.

$$I_i^k = \left(\frac{S_i^D ZIP_i^k}{V_i^k}\right)^* + \left(\frac{S_i^{DG}}{V_i^k}\right)^* + \left(\frac{S_i^{ESS}}{V_i^k}\right)^* \tag{3.17}$$

Step 3: Calculate the new bus voltages applying the superposition principle using Eq. (3.18).

$$\overline{V}_{BUS}^{k+1} = \overline{V}_{slack} + Z_{BUS}\overline{I}_{BUS}^{k} \tag{3.18}$$

Step 4: Check for convergence using Eq. (3.18). If not converged go to step 2.

$$max\left\{|V_{BUS}^{k+1} - V_{BUS}^{k}|\right\} \leq Tolerance \tag{3.19}$$

Step 5: Calculate the rest of electric variables needed.

Chapter 4

Solution Methodology

As was mentioned in Chapter 2, the optimization problem is a mixed-integer nonlinear programming problem, and to solve it, a simulated annealing (SA) algorithm with a new neighborhood search method based on the Zbus matrix (NSZM) is used. The NSZM method explores the solution space for the SA algorithm using a defined neighborhood structure and sensitivity factors based on the Zbus matrix. The proposed methodology starts with an initial configuration for both networks (medium and low voltage) obtained using a constructive heuristic algorithm. It is essential to highlight that only feasible topologies in the initial configuration are allowed. Afterward, the Zbus matrix of this solution is obtained using a constructive algorithm explained in Chapter 3 (Section 3.1).

The NSZM method chooses one criterion of the neighborhood structure in order to explore the solution space. In the process, the NSZM method uses the current Zbus matrix to obtain information provided by the sensitivity factors in order to choose a new solution. Afterward, the current Zbus matrix is modified to reflect the changes made by the neighborhood structure. Then, the stochastic mechanism of the SA algorithm controls the transition between the solutions. The acceptance of new configurations obeys the following criteria: topologies

with decreasing objectives are always accepted, whereas configurations with higher costs can be accepted or not with a certain probability. The possibility of accepting solutions with an elevated cost avoids getting trapped in local minima.

The main aspects of the SA algorithm and the new NSZM method used in this thesis will be discussed below.

4.1 Codification

A codification scheme allows to represent the variables of a mathematical model into a vector. Therefore two different codification schemes are used in this thesis in order to represent two models: DSP of primary and secondary networks considering DGs and DSP of primary and secondary networks considering DGs and ESSs.

The codification employed for the primary and secondary DSP uses integer numbers, where each number (for all the elements) is associated to a different capacity. A zero indicates that the element is not installed.

4.1.1 DSP considering DGs

The DSP of primary and secondary networks considering DGs is encoded using the codification scheme illustrated in Fig. 4.1. This vector is divided into five parts. The first part contains the locations and sizes of the existing and new primary feeders (size $n_1 + n_2$); the second part contains the locations and sizes of the existing and new secondary circuits (size $n_3 + n_4$); the third part involves the locations and capacities of the DTs (size n_5); the fourth part contains the locations and sizes of the existing and new substations (size $n_6 + n_7$); and the fifth part contains the locations and capacities of the DGs (size n_8).

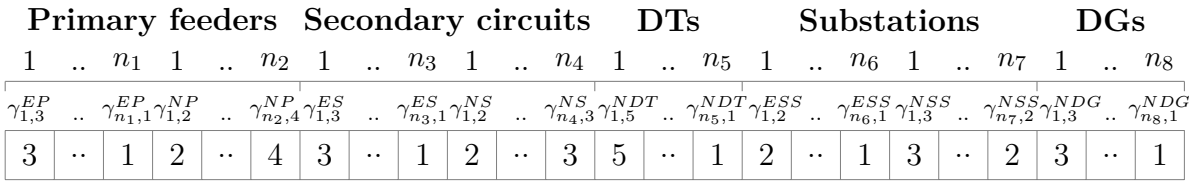

Figure 4.1: Codification scheme for primary and secondary DSP considering DGs.

4.1.2 DSP considering DGs and ESSs

The DSP of primary and secondary networks considering DGs and ESSs is encoded using the codification scheme illustrated in Fig. 4.2. This vector is divided into five parts. The first part contains the locations and sizes of the existing and new primary feeders (size $n_1 + n_2$); the second part contains the locations and sizes of the existing and new secondary circuits (size $n_3 + n_4$); the third part involves the locations and capacities of the DTs (size n_5); the fourth part contains the locations and sizes of the existing and new substations (size $n_6 + n_7$); the fifth part contains the locations and capacities of the ESSs (size n_8); and the six part contains the locations and capacities of the DGs (size n_9).

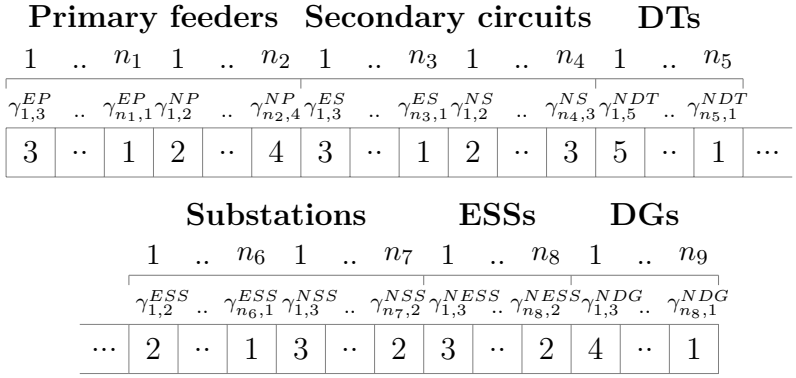

Figure 4.2: Codification scheme for primary and secondary DSP considering DGs and ESSs.

4.2 Initial configuration

The initial configuration for both networks (medium and low voltage) is obtained using a constructive heuristic algorithm. This algorithm begins from the existing source (substations), and in each step, a new branch (primary feeder, DT, or secondary circuit) is connected to the system. When a branch is added, the operating limits are checked (voltage regulation and capacities of the elements). This strategy stops when all demand nodes are connected to the network. It is essential to highlight that only feasible topologies in the initial configuration are allowed.

4.3 Neighborhood search method based on the Zbus matrix (NSZM)

This method explores the solution space using a defined neighborhood structure and sensitivity factors based on the Zbus matrix to find attractive solutions in quick times. The method uses an initial Zbus matrix to obtain a new Zbus matrix which represents a new solution for the SA algorithm. The NSZM method chooses one criterion of the neighborhood structure in order to explore the solution space. The criteria defined for the neighborhood structure uses the Eq. (3.13) and the sensitivity factor (SF) showed in Eq. (3.16) in order to choose a new solution. Afterward, the initial Zbus matrix is modified to reflect the changes made by the neighborhood structure.

The main aspects of the NSZM method are explained next.

4.3.1 Neighborhood structure

The neighborhood structure of the NSZM method uses the next criteria: the upgrading of existing substations, primary feeders and secondary circuits, installation of new substations, DTs and DGs, and branch exchange in both networks. From a current solution, a set of topologies are generated using one of the criteria explained. These configurations are called neighbors (or a neighborhood), and because the large amount they are, can be reduced to a defined number (reduced neighborhood) using sensitivity factors. The Zbus matrix is used for the sensitivity factors (SFs) for reducing the size of the neighborhood and choosing one topology from the neighborhood. The neighborhood structure considered is explained below.

- *Branch exchange*. The branch with $max\{\Delta V_{ij}\}$ is selected to connect the link. Then, the branch with $min\{I_{ij}\}$ of the loop formed is selected for removal. The currents of the loop are calculated using the Eq. (3.13).

- *DT installation*. A DT is chosen randomly from the three DTs with the largest capacities. If there are DTs disconnected nearby, one is chosen at random to be installed, and some loads are transferred from the first DT. Otherwise, the DT to be added is chosen at random from the disconnected DTs. Some loads need to be transferred to the new DT in order to comply radiality in the secondary circuits. Loads are transferred from the nearest existing DT to the new one. Loads are transferred by removing the circuit with $min\{I_{ij}\}$ of the loop formed. The currents of the loop are calculated using the Eq. (3.13). In the process, it is checked that the sizes of the DTs respect the operating limits.

- *DT removal.* The DT to be removed is chosen randomly from the three DTs with the smallest capacities. The loads of this DT need to be transferred to another existing DT. The DT chosen for receiving these loads is the nearest one with less capacity. If there is more than one such, the DT that is less overloaded is chosen. If there is more than

one DT that fulfills these conditions, the DT is chosen randomly from these. Loads are transferred by removing the circuit with $min\{I_{ij}\}$ of the loop formed. The currents of the loop are calculated using the Eq. (3.13).

- *Upgrading of existing branches and DTs.* Two alternatives are considered. In the first one, an element is chosen randomly from the three most overloaded elements, and the element is replaced by one with a bigger size. In the second one, an element is chosen randomly from the three least overloaded elements, and the element is replaced by one with a smaller size. One of these alternatives is chosen randomly. Primary feeders, secondary circuits, and DTs are chosen for upgrading capacity. One of these elements is selected randomly. Applying these criteria should ensure that the sections upstream do not present a smaller-size wire in the primary feeders and secondary circuits.

- *Installation and sizing of DGs and ESSs.* Four alternatives are considered: addition and removal of a DG or ESS and increasing and decreasing the size of a DG or ESS. One of these alternatives is chosen randomly. For each alternative, the sensitivity factor of Eq. (3.16) is applied, and the node which produces the minimum value is chosen. The sensitivity factor measures the impact of a change in the bus current injected in a given bus k on the active power losses in the distribution system (i.e., $\partial P_{Losses}/\partial I_k^{BUS}$). For the installation size of the DG or ESS, a random number from the types of DGs or ESSs is chosen and the sensitivity is applied.

Along the process, the neighborhood structure needs to know the physical information of the networks in order to make the changes proposed by the criteria. This information is obtained from the Zbus matrix as was explained in Chapter 3 (Section 3.3). After one of the criteria of the neighborhood structure is applied, the Zbus matrix is modified to reflect the changes made by the criterion.

4.3.2 Modifications of the Zbus matrix to reflect changes by the neighborhood structure

The Zbus matrix can be modified to reflect changes in the network caused by the neighborhood structure without the need to build it again (see Fig. 4.3). These changes may be the addition or removal of elements (feeders or circuits) for branch exchange, the addition or removal of elements (DTs or circuits) for DTs location, and changes in the impedances of elements (primary feeders, DTs, and secondary circuits) for upgrading or degrading the capacity. These modifications are described in Chapter 3 (Section 3.2).

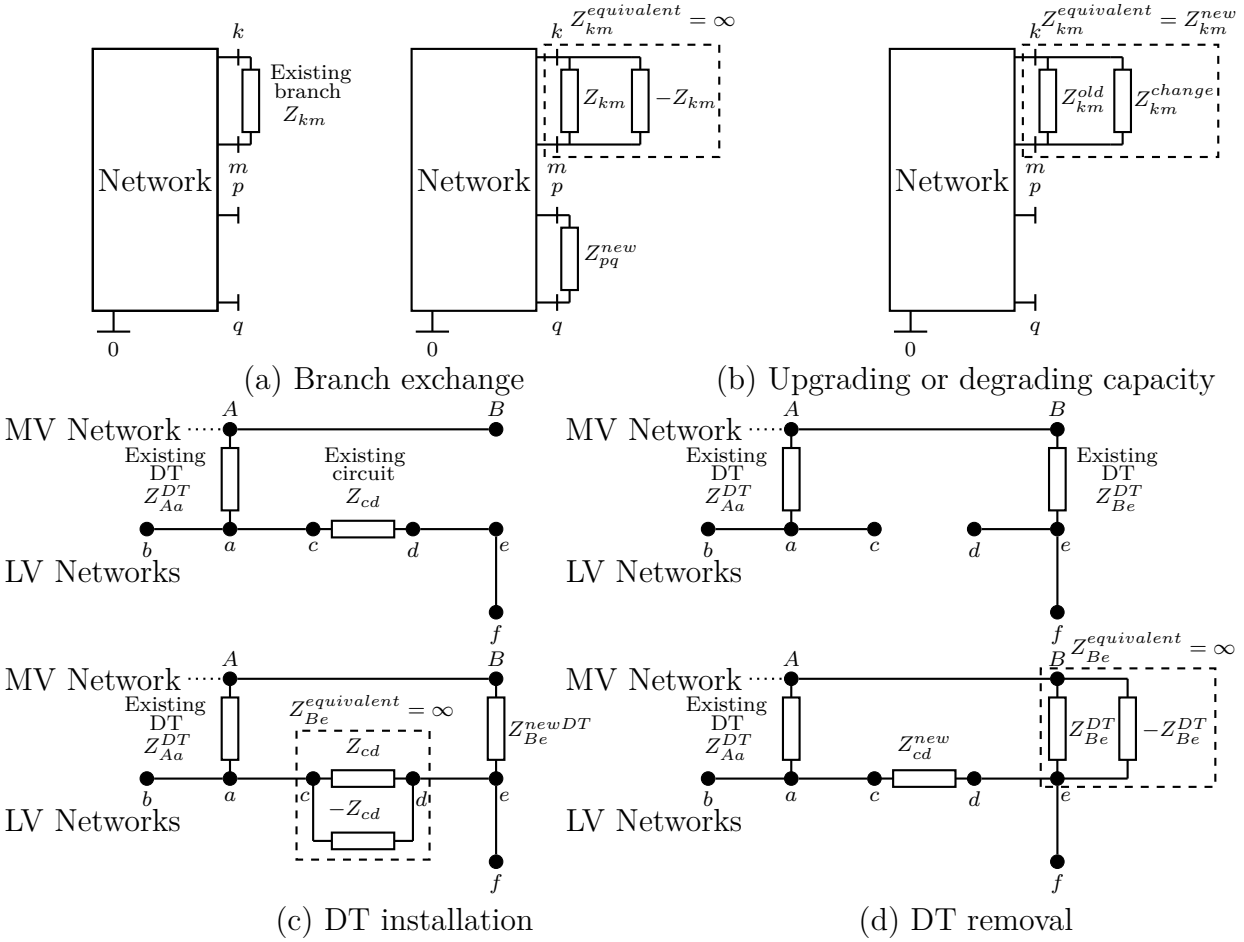

Figure 4.3: Zbus modification due to neighborhood criteria.

To calculate the new Zbus matrix produced by the neighborhood structure, the procedure is the following. For a branch exchange, the new element is added as a link between nodes $p-q$ (see Fig. 4.3a), and when it is added, the procedure explained before to recalculate the Zbus matrix is applied. After this, the element $k-m$ of the loop formed by the adding element $p-q$ is removed. Between $k-m$ there is added, in parallel, a link whose impedance is equal to the negative of the impedance of the element $k-m$ to be removed (see Fig. 4.3a), then the elements of the Zbus matrix are recalculated.

In per unit representation, the DTs are treated as lines. As consequence, the procedure described for branch exchange is the same for DTs location (adding a DT or removing a DT). For DTs installation, the new DT is added as a link between nodes $B-e$ (see Fig. 4.3c), and when it is added, the procedure explained before to recalculate the Zbus matrix is applied. After this, the circuit $c-d$ of the loop formed by the adding element $B-q$ is removed. Between $c-d$ there is added, in parallel, a link whose impedance is equal to the negative of the impedance of the circuit $c-d$ to be removed (see Fig. 4.3c), then the elements of the Zbus matrix are recalculated.

For the DTs removal, the procedure is quite the same. The new secondary circuit is added as a link between nodes $c-d$ (see Fig. 4.3d), and when it is added, the procedure explained before to recalculate the Zbus matrix is applied. Afterward, the existing DT $B-e$ is removed in order to comply radiality. Between $B-e$ there is added, in parallel, a link whose impedance is equal to the negative of the impedance of the circuit $B-e$ to be removed (see Fig. 4.3d), then the elements of the Zbus matrix are recalculated.

For upgrading or degrading the capacity of an element, the procedure is next. Between $k-m$ there is added, in parallel, a link whose impedance is such that the equivalent impedance of the two elements in $k-m$ is the desired value (see Fig. 4.3b), then the elements of the Zbus matrix are recalculated. Eq. (3.8) gives the value of the impedance added in the link $k-m$ to obtain the new value of impedance from the old value.

4.4 Evaluation of the configurations

During the procedure, the proposed configurations are evaluated using a load flow. When the DGs are considered into the DSP problem, the load flow used is the described in Section 3.5 due the DGs are treat as PQ nodes. Nevertheless, when the ESSs are considered into the DSP problem, it is needed an optimal power flow to determine the operation of the ESSs in order to maximize the profit from the energy purchase and sale.

The optimal power flow (OPF) proposed in this thesis is explained next.

4.4.1 Optimal Power Flow considering DGs and ESSs

The mathematical model proposed for the optimal power flow used in this thesis is based on the Zbus matrix. The constraints used in this OPF to represent the integration of ESSs were explained in the DSP mathematical model considering ESSs (Section 2.3). From that model, the Eqs. (2.28)–(2.34) are used and all the binary variables which reflect the inversion decisions of ESSs are eliminated. In Eqs. (2.32)–(2.33) the only binary variable left is $\varphi_{i,l}^{NESS}$ which represents the optimal operation of the ESSs, where if $\varphi_{i,l}^{NESS} = 0$ the ESSs are injecting power and if $\varphi_{i,l}^{NESS} = 1$ the ESSs are extracting power. This variable makes the mathematical formulation of the OPF a mixed-integer nonlinear problem. Hence, the Eqs. (2.32)–(2.33) are linearized in the Eqs. (4.15)–(4.16) to convert the OPF model into a nonlinear problem.

The OPF mathematical model is presented in the Eqs. (4.1)–(4.20). Per unit representation is applied to the optimal power flow model in order to represent the MV and LV networks as one. The Eq. (4.1) is the objective function which maximizes the utilities from the energy purchase and sale. The set of constraints is presented in (4.2)–(4.20). Eqs. (4.2) and (4.3) represent the active and reactive power nodal balance given by Kirchhoff's laws for both

networks, respectively. Eq. (4.4) represents the ZIP model in per unit representation for demands in both networks. Eqs. (4.5) and (4.6) use Ohm's law to calculate the real and imaginary part of the nodal voltage using the Zbus matrix. Eqs. (4.7) and (4.8) define the value of the voltage in the slack node in magnitude and angle. Eqs. (4.9) and (4.10) use the Kirchhoff's first law to calculate the real and imaginary part of the nodal currents in substations. Eq. (4.11) is the state of charge of the ESSs, this constraint considers the efficiency of charge and discharge of the ESSs. Eqs. (4.12) and (4.13) are the initial and final state of charge of the ESSs. Eqs. (4.14)–(4.17) ensure that the ESSs are not extracting and injecting power at the same time. Eq. (4.14) considers the charge and discharge power of the ESSs as two different variables. Eqs. (4.15) and (4.16) are the operating limits of the charge and discharge power of the ESSs. Eq. (4.18) is the capacity limits of the ESSs. Eq. (4.19) is the operating limits of the DGs. Eq. (4.20) is the voltage limit in all nodes of both networks.

$$max = k1D_{year} \sum_{l=1}^{NL} \left[k3 \sum_{i \in \Omega_N} P_{i,l}^{D} ZIP_{i,l} - k2_l \sum_{i \in \Omega_{SS}} P_{i,l}^{S} \right] \Delta T_l \, S_{base} \tag{4.1}$$

s.t.

$$\begin{aligned} P_{i,l}^{S} + P_{i,l}^{DG} + P_{i,l}^{ESS} =& P_{i,l}^{D} ZIP_{i,l} + V_{i,l}^{BUS} I_{i,l}^{BUS} \cos\left(\theta_{i,l}^{V} - \theta_{i,l}^{I}\right) \\ & \forall i \in \Omega_N; \ \forall l \in \Omega_{NL} \end{aligned} \tag{4.2}$$

$$Q_{i,l}^{S} = Q_{i,l}^{D} ZIP_{i,l} + V_{i,l}^{BUS} I_{i,l}^{BUS} \sin\left(\theta_{i,l}^{V} - \theta_{i,l}^{I}\right) \quad \forall i \in \Omega_N; \ \forall l \in \Omega_{NL} \tag{4.3}$$

$$ZIP_{i,l} = a_0 + a_1 V_{i,l}^{BUS} + a_2 \left(V_{i,l}^{BUS}\right)^2 \quad \forall i \in \Omega_N; \ \forall l \in \Omega_{NL} \tag{4.4}$$

$$V_{i,l}^{BUS}\cos\left(\theta_{i,l}^{V}\right) = V_{slack,l}^{BUS}\cos\left(\theta_{slack,l}^{V}\right) + \sum_{j\in\Omega N} I_{i,l}^{BUS}\left[R_{ij}^{BUS}\cos\left(\theta_{j,l}^{I}\right) - X_{ij}^{BUS}\sin\left(\theta_{j,l}^{I}\right)\right] \quad \forall i\in\Omega_N;\ \forall l\in\Omega_{NL};\ i\neq slack \tag{4.5}$$

$$V_{i,l}^{BUS}\sin\left(\theta_{i,l}^{V}\right) = V_{slack,l}^{BUS}\sin\left(\theta_{slack,l}^{V}\right) + \sum_{j\in\Omega N} I_{i,l}^{BUS}\left[R_{ij}^{BUS}\sin\left(\theta_{j,l}^{I}\right) + X_{ij}^{BUS}\cos\left(\theta_{j,l}^{I}\right)\right] \quad \forall i\in\Omega_N;\ \forall l\in\Omega_{NL};\ i\neq slack \tag{4.6}$$

$$V_{i,l}^{BUS} = V_{ref}^{p.u} \qquad i = slack;\ \forall l\in\Omega_{NL} \tag{4.7}$$

$$\theta_{i,l}^{V} = \theta_{ref}^{rad} \qquad i = slack;\ \forall l\in\Omega_{NL} \tag{4.8}$$

$$I_{i,l}^{BUS}\cos\left(\theta_{i,l}^{I}\right) = \sum_{ij\in\Omega_{PF}} G_{ij}^{P}\left[V_{i,l}^{BUS}\cos\left(\theta_{i,l}^{V}\right) - V_{j,l}^{BUS}\cos\left(\theta_{j,l}^{V}\right)\right] - B_{ij}^{P}\left[V_{i,l}^{BUS}\sin\left(\theta_{i,l}^{V}\right) - V_{j,l}^{BUS}\sin\left(\theta_{j,l}^{V}\right)\right] \qquad \forall i\in\Omega_{SS};\ \forall l\in\Omega_{NL} \tag{4.9}$$

$$I_{i,l}^{BUS}\sin\left(\theta_{i,l}^{I}\right) = \sum_{ij\in\Omega_{PF}} B_{ij}^{P}\left[V_{i,l}^{BUS}\cos\left(\theta_{i,l}^{V}\right) - V_{j,l}^{BUS}\cos\left(\theta_{j,l}^{V}\right)\right] + G_{ij}^{P}\left[V_{i,l}^{BUS}\sin\left(\theta_{i,l}^{V}\right) - V_{j,l}^{BUS}\sin\left(\theta_{j,l}^{V}\right)\right] \qquad \forall i\in\Omega_{SS};\ \forall l\in\Omega_{NL} \tag{4.10}$$

$$SoC_{i,l} = SoC_{i,l-1} - \phi_{i,b}\left(\frac{1}{\eta_{i,b}}P_{i,l}^{ESSD} - \eta_{i,b}P_{i,l}^{ESSC}\right)\Delta T_l\, S_{base} \qquad \forall i\in\Omega_B;\ \forall l\in\Omega_{NL};\ \forall b\in\Omega_{TESS} \tag{4.11}$$

$$SoC_{i,l} = SoC_i^0 \qquad l = 0;\ \forall i \in \Omega_B \tag{4.12}$$

$$SoC_{i,l} = SoC_i^F \qquad l = NL;\ \forall i \in \Omega_B \tag{4.13}$$

$$P_{i,l}^{ESS} = P_{i,l}^{ESSD} - P_{i,l}^{ESSC} \qquad \forall i \in \Omega_B;\ \forall l \in \Omega_{NL} \tag{4.14}$$

$$P_{i,l}^{ESSC} - P_{i,l}^{ESSD} \leq P_{i,b}^{maxc} \quad \forall i \in \Omega_B;\ \forall l \in \Omega_{NL};\ \forall b \in \Omega_{TESS} \tag{4.15}$$

$$P_{i,l}^{ESSD} - P_{i,l}^{ESSC} \leq P_{i,b}^{maxd} \quad \forall i \in \Omega_B;\ \forall l \in \Omega_{NL};\ \forall b \in \Omega_{TESS} \tag{4.16}$$

$$P_{i,l}^{ESSC} \geq 0;\ P_{i,l}^{ESSD} \geq 0 \quad \forall i \in \Omega_B;\ \forall l \in \Omega_{NL} \tag{4.17}$$

$$SoC_i^{min} \leq SoC_{i,l} \leq SoC_i^{max} \quad \forall i \in \Omega_B;\ \forall l \in \Omega_{NL} \tag{4.18}$$

$$0 \leq P_{i,l}^{DG} \leq P_{i,g}^{max} \qquad \forall i \in \Omega_{DG};\ \forall l \in \Omega_{NL};\ \forall g \in \Omega_{TDG} \tag{4.19}$$

$$V_i^{min} \leq V_{i,l}^{BUS} \leq V_i^{max} \qquad \forall i \in \Omega_N;\ \forall l \in \Omega_{NL};\ \ i \neq slack \tag{4.20}$$

Nonlinear problems such as the OPF presented are computational expensive in large scale

networks. Linearization methods can reduce computational efforts but are still computational expensive due the large amount of new constraints added. As consequence, the OPF model proposed in Eqs. (4.1)–(4.20) is solved using a new decomposition method.

This decomposition method splits in two steps. The first step considers that the cost of the energy purchase is bigger than the cost of the technical energy losses. Thus, the network losses are eliminated from the model presented in Eqs. (4.1)–(4.20). The Eqs. (4.1)–(4.2) are modified and replaced by Eqs. (4.21) and (4.22). Moreover, Eqs. (4.3)–(4.10) and (4.20) are eliminated. With these modification the nonlinear model is converted into a linear model.

$$max = k1 \sum_{l=1}^{NL} \left[k3 \sum_{i \in \Omega_N} P_{i,l}^{D} - k2_l \sum_{i \in \Omega_{SS}} P_{i,l}^{S} \right] \Delta T_l \, S_{base} \tag{4.21}$$

$$\sum_{i \in \Omega_N} \left(P_{i,l}^{S} + P_{i,l}^{DG} + P_{i,l}^{ESS} - P_{i,l}^{D} \right) = 0 \quad \forall l \in \Omega_{NL} \tag{4.22}$$

The linear model is presented in (4.21),(4.22),(4.11)–(4.19). In this linear model, the electrical variables and the reactive balance are removed. Eq. (4.21) is the objective function which maximizes the utilities from the energy purchase and sale. Eq. (4.22) represents the active power global balance given by Kirchhoff's laws for both networks.

Objective function:

$$\left\{ F_{Obj} = Eq.\ (4.21) \right\}$$

Subject to:

$$\left\{ Eqs.\ (4.22), (4.11) - (4.19) \right\}$$

The linear model results are the optimal operation of the ESSs. Afterward, the second step uses the load flow explained in Section 3.5 to consider the network losses due the operation of ESSs. The EESs are treated as nodes PQ. The results of this load flow are the objective function described in Eq. (4.1) and the operative conditions of the network.

This decomposition solution method only works for feasible solutions, but this is not a problem since unfeasible solutions are not desirable.

4.4.2 Fitness Function

The load flow results are the network losses to be summed in the objective function, and the operating limits to determine the feasible solutions. When the ESSs are considered, the load flow result is the profit from the energy purchase and sale instead of the network losses.

The objective function is used by the solution technique in order to compare the solutions and only feasible solutions need to be accepted. Under this premise, unfeasible solutions are penalized in their respective objective function. The sum of the objective function plus the penalty costs of the respective violated constraints is called the fitness function (F_{fit}), and is obtained as follows.

$$\begin{aligned} F_{fit} = & Eq.\ (2.1) + V_{MV} fpV_{MV} \Psi_{V_{MV}} + V_{LV} fpV_{LV} \Psi_{V_{LV}} + fpI_{MV} \Psi_{I_{MV}} + fpI_{LV} \Psi_{I_{LV}} + \\ & fpS_{MV} \Psi_{S_{MV}} + fpS_{LV} \Psi_{S_{LV}} \end{aligned} \tag{4.23}$$

The factors fpV, fpI and fpS are associated to the penalties for violation of voltage limits, and overloads in elements and sources (branches, DTs or substations). The terms with the subscripts MV and LV refer to the primary and secondary network, respectively. These factors are multiplied by a binary decision variable (Ψ). If any constraint is violated, this

variable is one, otherwise it is zero. The voltages penalties are also multiplied by the magnitude of the voltage violated (V). The units of these factors ensure that each term is expressed in monetary units.

4.5 Solution technique

SA is a stochastic optimization procedure that can converge asymptotically to the optimal global solution with probability one. A stochastic mechanism controls the transition between two successive configurations in the SA algorithm. The acceptance of new configurations obeys the following criteria: topologies with decreasing objectives are always accepted, whereas configurations with higher costs can be accepted or not with a certain probability. The possibility of accepting solutions with an elevated cost avoids getting trapped in local minima.

In this thesis, is proposed a specialized SA algorithm that uses the NSZM method to explore the solution space in order to provide attractive solutions that are evaluated by the stochastic mechanism of the SA algorithm. The pseudocode of the SA is shown in Fig. 4.4.

SA's pseudocode

```
1: begin
2:     Generate the initial configuration
3:     Initialize: Incumbent, T_0, N_0, k
4:     while stop criterion is not reached do
5:         for i = 1 to N_k do
6:             Obtain a solution from the NSZM method
7:             Evaluate objective function
8:             if best solution is improved then
9:                 Accept best solution;
10:            else
11:                if exp(ΔFo / T_k) > random[0, 1] then
12:                    Accept worst solution;
13:                else
14:                    Do not accept worst solution;
15:                end if
16:            end if
17:            if solution accepted is better than the incumbent then
18:                Update incumbent;
19:            end if
20:        end for
21:        T_{k+1} = α T_k
22:        N_{k+1} = β N_k
23:        k = k + 1
24:        The initial solution is now the incumbent solution
25:    end while
26:    Print results
27: end
```

Figure 4.4: Pseudocode of the specialized SA.

Simulated annealing models the process of annealing in metallurgy. This technique involves heating and controlled cooling of a material to increase the size of its crystals and reduce their defects. Heating and cooling the material affects both the temperature and the thermodynamic free energy. At a given temperature, SA sequentially moves from one configuration to the next until thermal equilibrium is reached.

The efficiency of the algorithm regarding both the quality of the final solutions as well as the number of iterations will depend on the choice of the parameters of the cooling scheme.

4.5.1 Cooling scheme

The procedures used in the calculation of the parameters are based on the idea of thermal equilibrium and are detailed below. The cooling scheme is defined by the following four parameters.

Initial temperature T_0

The initial temperature T_0 is determined in such a way that the number of configurations with higher costs that are accepted does not surpass a certain limit. If too many topologies with elevated costs are accepted, the search space will be guided to unattractive regions. Under this premise, the computational time would be increased, trying to return to attractive regions. The initial temperature is calculated as follows [51]:

$$T_0 = \frac{\mu}{-ln\left(\Phi\right)} F\left(x_0\right) \tag{4.24}$$

In Eq. (4.24), Φ (%/100) is the probability of accepting a solution that is worse, by a determined μ (%/100), than the objective function of the initial solution $F\left(x_0\right)$, (i.e., solutions that are $\mu = 1\%$ worse than the cost of the initial solution would be accepted with a probability of $\Phi = 13\%$).

Number of transitions N_k at temperature T_k

The number of transitions N_k should be such that a state of thermal near-equilibrium will be reached at a given temperature T_k. The number of transitions and the rate of change of the

temperature between two consecutive temperature levels are closely related. This way, if the temperature steps are too big, thermal equilibrium would be reached only with a high value of N_k; and if the temperature steps are too small, thermal equilibrium would be reached only with a low value of N_k. The initial number of transitions N_0 can be defined as the number of variables of the problem. To calculate the value of N_k for each temperature level, Eq. (4.25) is applied, where β is a constant greater than or equal to one.

$$N_{k+1} = \beta\, N_k \tag{4.25}$$

Rate of change of the temperature

The rate of cooling has a direct effect on the number of iterations required at each temperature level. Eq. (4.26) calculates the rate of change of the temperature, where α is a constant varying between 0.8 and 0.99.

$$T_{k+1} = \alpha\, T_k \tag{4.26}$$

Final temperature T_f

The stopping criterion is determined in such a way that at the optimal point the expected improvement in the objective function becomes negligible. Two stopping criteria are used: the first one assumes a fixed number of temperature levels T_k for the cooling process (a number between 6 and 50); and the second criterion stops when the incumbent solution is not improved for a predefined number of temperature levels.

4.6 General methodology

The procedure begins with the initial configuration, which is obtained as was explained in Section 4.2. After that, the Zbus matrix is obtained for the initial configuration as was explained in Chapter 3 (see Section 3.1). Then, the cooling scheme and incumbent are initialized. The cooling scheme is calculated as was explained in subsection 4.5.1 to start with the SA algorithm. The NSZM method uses the initial Zbus matrix in order to obtain a new solution for the SA algorithm (see Section 4.3). This new configuration represented by the Zbus matrix is evaluated using a load flow in order to determine its operative conditions. If the DSP problem only considers DGs, the load flow explained in Section 3.5 is used, but if the DSP problem considers DGs and ESSs, the decomposition method for the optimal power flow explained in Subsection 4.4.1 is used. Afterward, the objective function of this solution is determined by using the fitness function explained in Subsection 4.4.2. Then, the stochastic mechanism of the SA algorithm controls the transition between the solutions. The acceptance of new configurations obeys the following criteria: topologies with decreasing objectives are always accepted, whereas configurations with higher costs can be accepted or not with a certain probability. The possibility of accepting solutions with an elevated cost avoids getting trapped in local minima. Then, if the solution is better than the incumbent, the incumbent is updated. This procedure is repeated until N_k transitions are completed. For the next temperature level, T_k and N_k are updated as was explained in subsection 4.5.1. After a temperature level is completed, the initial Zbus matrix for the next temperature level is the incumbent Zbus matrix. The procedure ends when the stop criterion is reached (see subsection 4.5.1). Fig. 4.5 shows the flowchart of the proposed methodology.

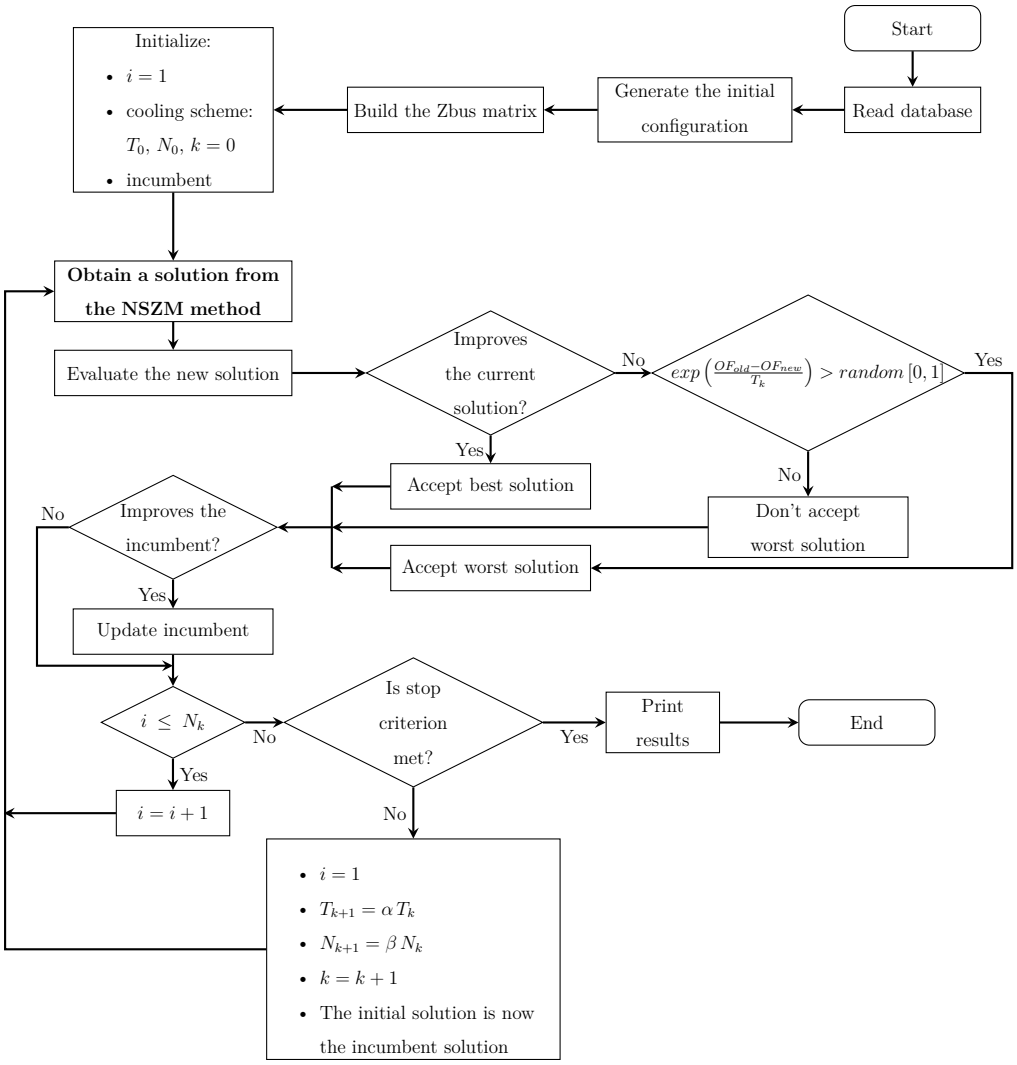

Figure 4.5: Flowchart of the proposed methodology.

Chapter 5

Application and Results

5.1 Description of the system

To validate the proposed methodology, the real distribution system of Fig. 5.1 is used. In this figure, existing and proposed branches are represented by solid and dashed lines respectively. Existing and proposed substations are represented by squares. The black points are the primary nodes, the white circles are the secondary nodes, and the white circles with a black point inside are nodes shared by both networks. The data system is different when ESSs are considered.

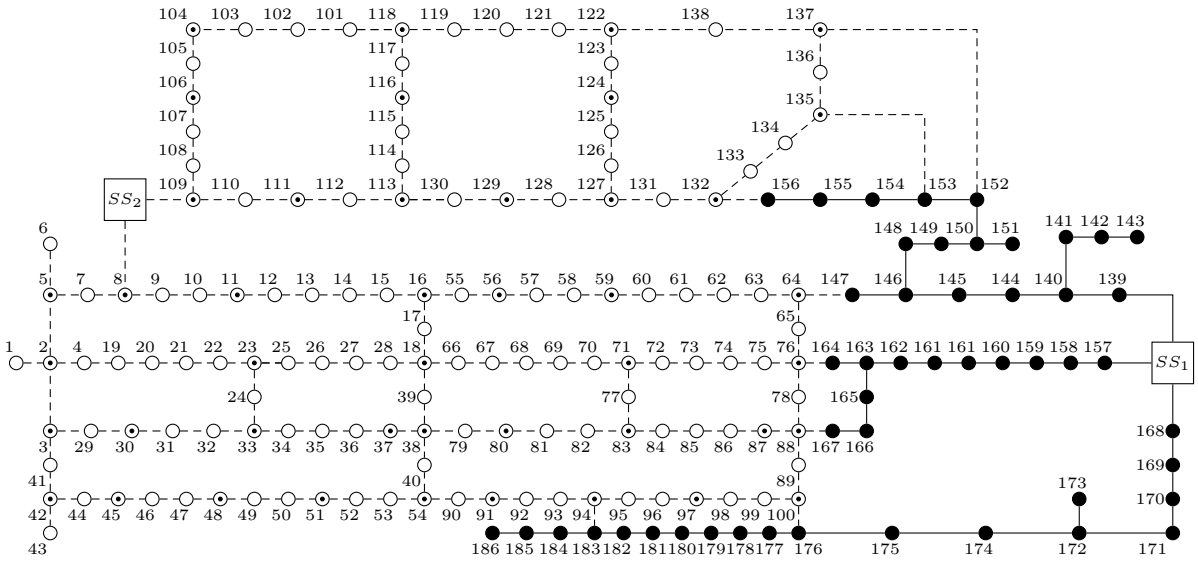

Figure 5.1: Integrated distribution system.

The full system database when only DGs are considered can be found in Appendix A.1, and the full system database when DGs and ESSs are considered can be found in Appendix A.2.

The battery type used for the ESSs is Sodium-Sulfur (NaS). The efficiency and the lifetime of this battery are $\eta_b = 90\%$ and 20 years, respectively [52]. The deep of discharge (DoD), the energy capital cost, and the operation and maintenance cost (O&M) are 100%, 320 [USD/kWh], and 80 (USD/kW-year), respectively [53]. Fig. 5.2 shows the behavior of the load and DGs curves used. The DGs curve used is a typical daily curve from a photovoltaic generator in the andean zone. Fig. 5.2 is used when DGs and ESSs are considered together.

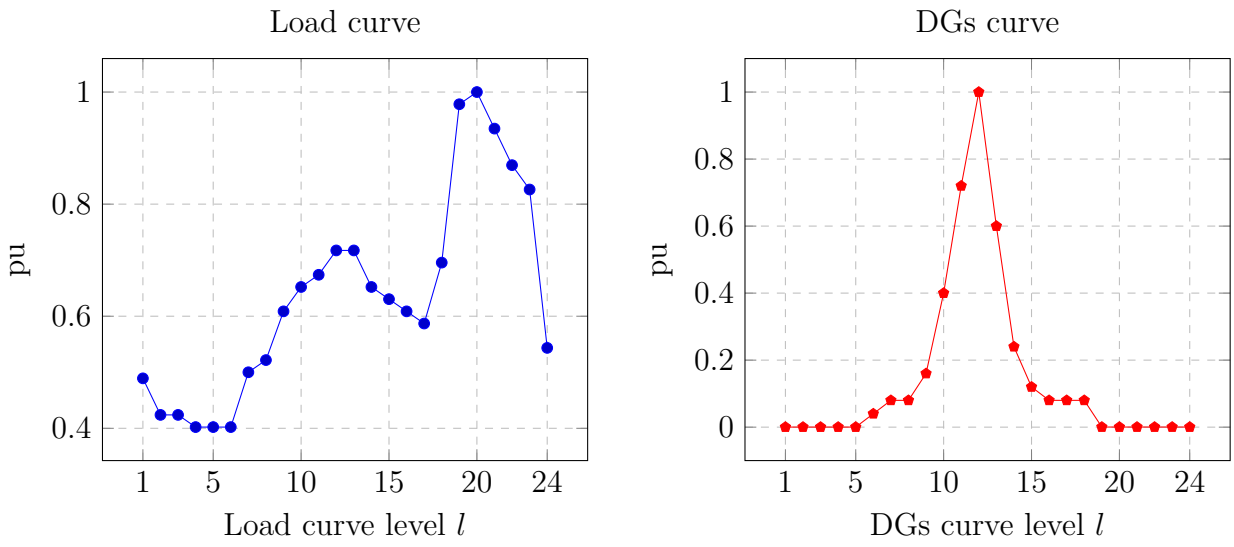

Figure 5.2: Daily behavior of the load and DGs curves in pu.

5.2 Integrated DSP of both networks considering DGs

To solve this problem, the methodology explained in Chapter 4 is used. The cooling scheme factors are 1%, 5%, 1.1, and 0.95 for μ, Φ, β, and α, respectively. The values of the penalty factors are defined as follows. Factors fpV_{MV} and fpV_{LV} are equal to 1000. Factors fpI_{MV} and fpI_{LV} are dynamic values equivalent to the cost of the next upgraded wire times 100. Factor fpS_{MV} is a dynamic value equivalent to the difference between the cost of the existing substation and the next upgraded substation, and factor fpS_{LV} is a dynamic value equivalent to the cost of the next upgraded DT. The two stopping criteria used are: 60 temperature levels for the cooling process, and 15 temperature levels if the best solution found is not improved. The test system used is shown in Fig. 5.1 and the full system database is found in Appendix A.1.

In order to verify the efficiency of the proposed methodology in this paper, four cases are studied: (1) integrated planning without DGs (case 2 in [5]), (2) integrated planning with

DG in the LV network (case 3 in [5]), (3) integrated planning without DGs, considering the copper losses in DTs, and (4) integrated planning with DG in the LV network, considering the copper losses in DTs. The two cases analyzed in [5], do not consider the copper losses of the DTs in the objective function since the DTs are the conflicting variables in the bilevel approach proposed. Cases (3) and (4) consider the copper losses of the DTs in the objective function since the methodology proposed in this thesis integrates the two networks into one.

The DGs are modeled as PQ nodes and their possible locations are based on the sensitivity analysis explained in Subsection 3.4.1.

5.2.1 Validation of the methodology

To validate the proposed methodology, the results are compared with the ones reported in [5], using the same design aspects than they employed. It is necessary to clarify that in [5] the primary and secondary networks are modeled as one-single phase and three-phase models, respectively, and in the model presented in this paper both networks (primary and secondary) are modeled by an one-single phase representation. Therefore, before applying the proposed methodology to the test system, an evaluation of the final configuration presented in [5] is previously performed using the methodology proposed in this paper.

In [5] are proposed three cases of study, where case 2 is the integrated planning without DGs. The published results for this case are 1.789, 0.337, and 0.184 (millions of dollars), for the objective function, and costs of the energy technical losses in the MV and LV networks, respectively. When the final configuration of case 2 in [5] is evaluated with the integrated mathematical model proposed in this paper, the results are 1.773, 0.335, and 0.169 (millions of dollars) for the same aspects (objective function, and the costs of the energy technical losses in the MV and LV networks). From both results, can be seen that the error between the two objective functions is 0.89%. These values allow to conclude that although the

representation of both voltage levels proposed in this article is one-single phase, the results are quite reliable and approximate to those obtained under a three-phase representation.

5.2.2 Results

The algorithm was implemented in Matlab (2017), using an Intel®Core i5-3470 8 GB RAM PC. The CPU time for Cases 1, 2, 3 and 4 are 10160 s (2.82 h), 11451 s (3.18 h), 7806.3 s (2.16 h) and 9732.7 s (2.70 h), respectively. The solutions for Cases 2 and 3 reported in [5] are obtained using a bilevel integrated planning for both networks. Case 2 does not consider DGs and Case 3 does consider DGs. The incumbent behavior for the objective function of all cases is shown in Fig. 5.3.

A comparison of these results is shown in Tables 5.1 and 5.2 in terms of present value, where the term ETL means the costs of the energy technical losses. Figs. B.1–B.8 show the best solutions found for the four studied cases. To facilitate the visualization of the obtained topologies, the primary and secondary networks of each case are presented in separate figures. In these figures, the primary and secondary branches are represented by solid lines.

For all cases of the two networks, the number in parentheses is associated to the type of wire for each branch; branches without a number have type 1 wire. The DTs are represented by black triangles and their types are presented by an underlined number.

In all four cases, the existing substation was not upgraded, and a new type 1 substation was installed. The installation nodes of the DGs and their types for Case 2 are: 23 (type 1), 38 (type 1), 43 (type 1), 88 (type 1), 95 (type 1), 103 (type 1), 110 (type 1), 130 (type 1), 131 (type 1), and 136 (type 2). For Case 4 they are: 23 (type 2), 38 (type 1), 43 (type 1), 88 (type 1), 95 (type 1), 103 (type 1), 110 (type 1), 130 (type 2), 131 (type 1), and 136 (type 2). In all cases the solutions are feasible.

Table 5.1: Comparison of cost of expansion in millions of USD.

Cost	Description	Reported in [5]		Reported in this thesis	
		Case 1	Case 2	Case 1	Case 2
Fixed	Substations	0.336	0.336	0.336	0.336
	MV feeders	0.410	0.397	0.393	0.376
	LV circuits	0.255	0.254	0.283	0.270
	DT	0.265	0.225	0.258	0.215
	DG	—	0.032	—	0.026
	Total	1.267	1.246	1.270	1.223
Variable	ETL in MV	0.337	0.307	0.207	0.194
	ETL in LV	0.184	0.183	0.164	0.183
	Total	0.521	0.490	0.371	0.377
Total cost		1.789	1.737	1.640	1.599

The consolidated results from Table 5.1 show that the total costs found are better than those reported in [5]. The results from Table 5.2 show that the lowest costs were obtained in Cases 2 and 4, which have a penetration of DG.

Table 5.2: Comparison of cost of expansion in millions of USD.

Cost	Description	Case 1	Case 2	Case 3	Case 4
Fixed	Substations	0.336	0.336	0.336	0.336
	MV feeders	0.393	0.376	0.375	0.358
	LV circuits	0.283	0.270	0.283	0.271
	DT	0.258	0.215	0.254	0.237
	DG	—	0.026	—	0.029
	Total	1.270	1.223	1.248	1.231
Variable	ETL in MV	0.207	0.194	0.208	0.196
	ETL in LV	0.164	0.183	0.174	0.178
	ETL in DTs	—	—	0.178	0.129
	Total	0.371	0.377	0.560	0.502
Total cost		1.640	1.599	1.808	1.733

Case 1 achieved a lower variable cost (USD 0.490 M) than that reported for Case 1 in [5] (USD 0.521 M) using almost the same fixed cost. Under this premise, the integrated model proposed can find a topology with lower global cost. Case 2 has lower fixed and variable costs (1.223 and 0.377 millions of USD) than Case 2 reported in [5] (1.256 and 0.490 millions of USD). As a consequence, the sensitivity analysis proposed for the installation of DGs is highly recommended.

Cases 3 and 4 are more detailed because they consider the energy technical losses in the DTs. Note that the penetration of DG in the LV network allows installing DTs, LV circuits, and MV feeders with smaller sizes than Case 3. In addition, the energy technical losses in MV, LV and DTs are also affected, which is reflected in the lowest operative cost.

The lower costs are obtained because the location and sizing of the DTs enhances the power

flow circulation between both systems (MV and LV networks), which decreases the technical losses and the investment costs in the elements of both networks. For all cases, the solutions found have different topologies.

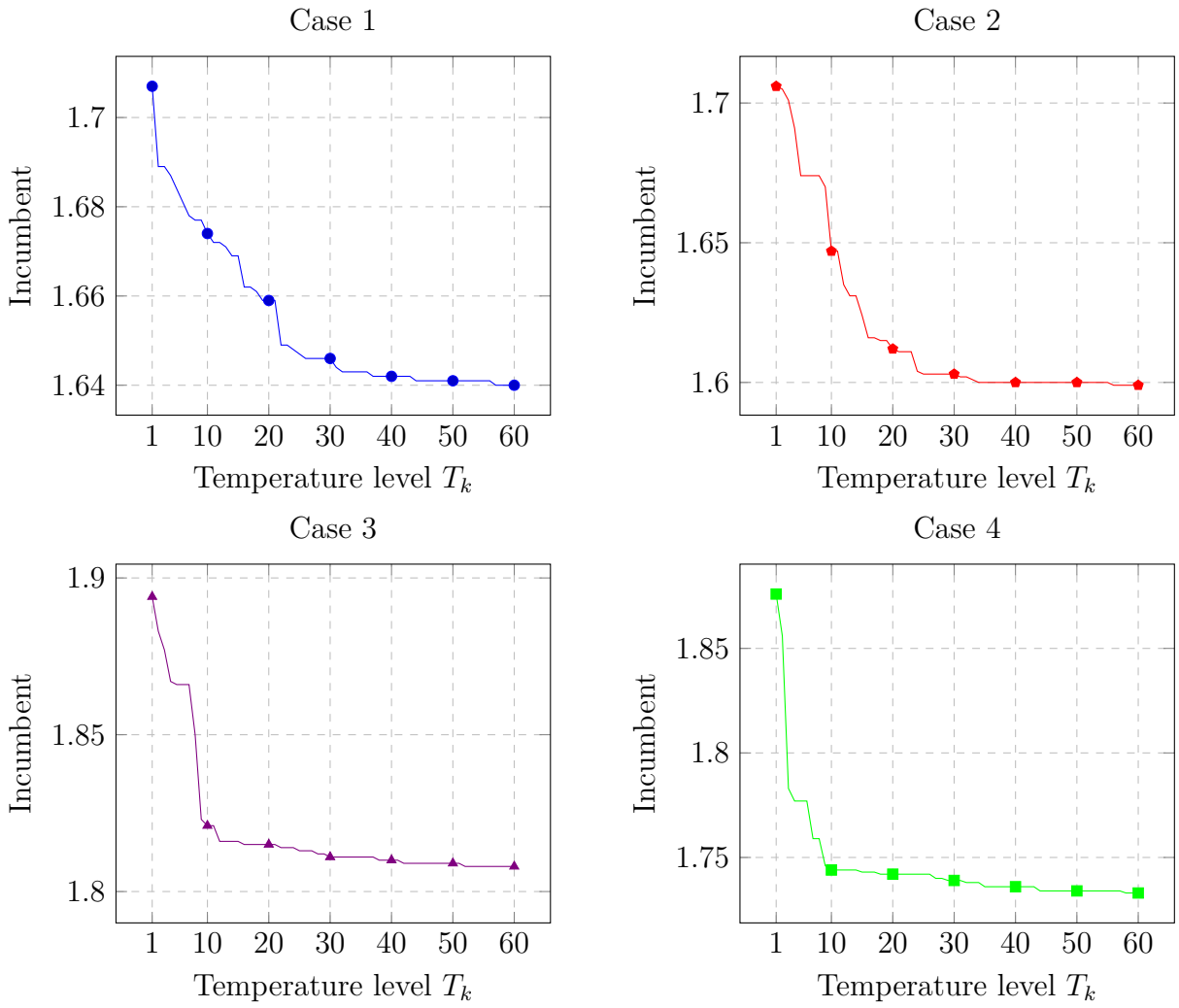

Figure 5.3: Incumbent behavior for the four cases in millions of USD.

5.3 Integrated DSP of both networks considering DGs and ESSs

To solve this problem, the methodology explained in Chapter 4 is used. The cooling scheme factors are 0.5%, 2.365%, 1.1, and 0.95 for μ, Φ, β, and α, respectively. The values of the penalty factors are defined as follows. Factors fpV_{MV} and fpV_{LV} are equal to 660000. Factors fpI_{MV} and fpI_{LV} are equivalent to the cost of the current wire times 10000. Factor fpS_{MV} is a dynamic value equivalent to the difference between the cost of the existing substation and the next upgraded substation, and factor fpS_{LV} is a dynamic value equivalent to the cost of the current DT times 60000. The two stopping criteria used are: 60 temperature levels for the cooling process, and 15 temperature levels if the best solution found is not improved. The test system used is shown in Fig. 5.1 and the full system database is found in Appendix A.2. The sensitivity factor of the Eq. (3.16) is used to reduce the candidate nodes for the ESSs installation. The reduced candidate nodes obtained by using this sensitivity factor are shown in Table 5.3.

Table 5.3: Candidate nodes for installing ESSs in the LV and MV networks.

Network	Nodes
LV	129, 111, 109, 127, 130, 113, 30, 11, 132, 135, 137, 116, 8, 106, 48
MV	157, 139, 158, 168, 109, 142, 104, 156, 106, 159, 111, 169, 146, 160, 151

In order to analyze the benefits of the integration of the ESSs into the DSP problem, the following five cases are studied. Case (A) is the integrated planning without DGs and ESSs. Cases (B) and (C) are: (B) integrated planning with DGs and ESSs in the LV network and (C) integrated planning with DGs in the LV network and ESSs in the MV network. These

two cases consider the losses of the ESSs due the efficiency ($\eta_b = 90\%$). Cases (D) and (E) are the same as (B) and (C) but these cases do not consider the losses of the ESSs ($\eta_b = 100\%$).

5.3.1 Validation of the decomposition method

To validate the proposed decomposition method used to solve the OPF considering DGs and ESSs, the test system of Figs. 5.4 and 5.5 is used. The decomposition method is compared with the nonlinear model presented in Subsection 4.4.1. The database of the system is presented in Appendix A.2.

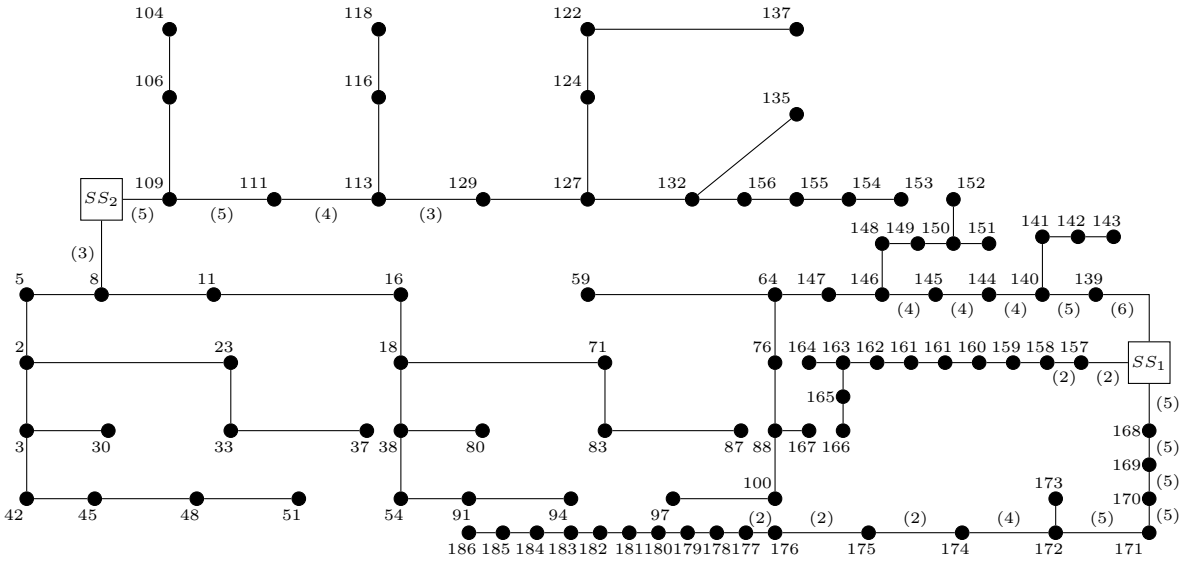

Figure 5.4: Primary Network of the test system.

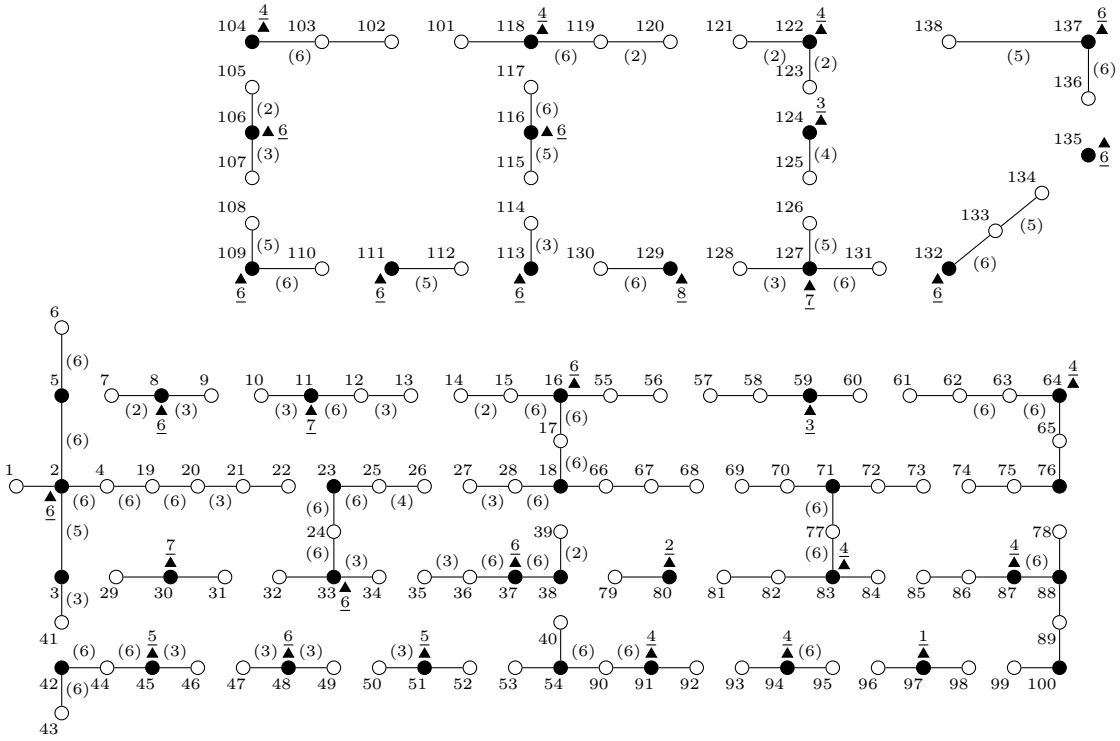

Figure 5.5: Secondary Network of the test system.

The Table 5.4 shows the comparison between both methods. Case (I) do not considered DGs and ESSs. Five cases are used in order to compared the efficiency of the decomposition method. Case (II) has the next DGs and ESSs nodes: 6 (type 4), 43 (type 3), 54 (type 2), 103 (type 4), 110 (type 4), and 131 (type 3) are nodes with DGs; and 111 (type 4), 127 (type 3), 113 (type 4), 11 (type 4), 116 (type 1), and 48 (type 4) are nodes with ESSs. Case (III) has the next DGs and ESSs nodes: 23 (type 1), 38 (type 2), 62 (type 3), 71 (type 3), 95 (type 4), 103 (type 4), 130 (type 3), and 131 (type 2) are nodes with DGs; and 139 (type 4), 109 (type 4), 104 (type 3), 106 (type 1), 169 (type 1), 146 (type 1), and 151 (type 2) are nodes with ESSs. Cases (II) and (III) consider the losses of the ESSs due the efficiency ($\eta_b = 90\%$). Case (IV) has the next DGs and ESSs nodes: 6 (type 3), 43 (type 4), 54 (type 1), 88 (type 2), 117 (type 3), and 136 (type 4) are nodes with DGs; and 111 (type 3), 127 (type 4), 30 (type 2), 11 (type 4), 137 (type 3), and 48 (type 3) are nodes with ESSs. Case (V) has the

next DGs and ESSs nodes: 6 (type 2), 23 (type 2), 38 (type 4), 62 (type 2), 71 (type 3), 95 (type 1), 103 (type 3), 130 (type 4), and 131 (type 1) are nodes with DGs; and 168 (type 3), 142 (type 2), 104 (type 3), 106 (type 3), 111 (type 2), 146 (type 1), and 160 (type 3) are nodes with ESSs. Cases (IV) and (V) do not consider the losses of the ESSs ($\eta_b = 100\%$).

Table 5.4: Comparison of the objective functions for the five cases in millions of USD.

		Case I	Case II	Case III	Case IV	Case V
decomposition	OF	13.6169	16.1772	16.0903	16.3539	16.5507
method	CPU time [s]	0.1092	1.0393	0.8212	0.3296	0.3388
nonlinear	OF	13.6175	16.1773	16.0898	16.3543	16.5507
model	CPU time [s]	59.5858	1014.9358	375.7602	2513.6399	541.5253
	Error between the OFs [%]	0.0043	0.0003	0.0032	0.0025	0.0003

The two methods were implemented using an interface between Matlab (2017b) and GAMS (24.5.4) and an Intel®Core i5-4460S 12 GB RAM PC. The solvers CPLEX and KNITRO were used for the linear and nonlinear model, respectively. The results from Table 5.4 verify the efficiency of the proposed decomposition method. Table 5.4 shows that the computational effort is reduced with the decomposition method and the objective function results are the same. Thus, the results obtained show that the decomposition method achieves the optimal solution in less time.

5.3.2 Results

The algorithm was implemented using an interface between Matlab (2017b) and GAMS (24.5.4) and an Intel®Core i5-4460S 12 GB RAM PC. The solver CPLEX is used to solve the linear problem of the decomposition method. The CPU time for Cases A, B, C, D and E are

7999.87 s (2.22 h), 212339.99 s (58.98 h), 210917.60 s (58.59 h), 203203.75 s (56.45 h), and 200664.16 s (55.74 h), respectively. It is to be expected that these times could be reduced if a production-grade routine such as C++ is applied and a better optimization tool interface is implemented. In any case, planning studies do not require real-time simulations, thus the above timings are considered adequate. The incumbent behavior for the objective function of all cases is shown in Fig. 5.7.

A comparison of these results is shown in Table 5.5 in terms of present value, where the term ETL means the costs of the energy technical losses. Figs. B.9–B.18 show the best solutions found for the five studied cases. To facilitate the visualization of the obtained topologies, the primary and secondary networks of each case are presented in separate figures. In these figures, the primary and secondary branches are represented by solid lines.

For all cases of the two networks, the number in parentheses is associated to the type of wire for each branch; branches without a number have type 1 wire. The DTs are represented by black triangles and their types are presented by an underlined number.

In all five cases, the existing substation was not upgraded, and a new type 1 substation was installed. For all the cases, new DGs and ESSs type 4 were installed in all the candidate nodes. In all cases the solutions are feasible. For all cases, the solutions found have different topologies.

Table 5.5: Comparison of the cost and profit in millions of USD.

Cost	Description	Case A	Case B	Case C	Case D	Case E
Fixed	Substations	0.336	0.336	0.336	0.336	0.336
	MV feeders	0.574	0.571	0.543	0.568	0.539
	LV circuits	0.411	0.512	0.512	0.507	0.514
	DT	0.341	0.324	0.284	0.325	0.280
	DG	—	0.094	0.094	0.094	0.094
	ESS	—	1.920	1.920	1.920	1.920
	O&M of the ESS	—	1.362	1.362	1.362	1.362
	Total cost	1.662	5.119	5.051	5.112	5.044
Variable	ETL in MV, LV and DTs	0.730	0.725	0.739	0.746	0.738
	ETL in ESSs	—	1.064	1.064	0.000	0.000
	Energy purchase	85.563	78.136	77.998	76.982	76.810
	Energy sale	99.167	99.273	99.166	99.285	99.165
	Profit	13.604	21.138	21.168	22.303	22.355
Total profit		11.943	16.019	16.117	17.191	17.310

Case A shows that the only way to maximize the profit from the energy purchase and sale when no DGs and ESSs are considered is minimizing the costs of the energy technical losses in the network and the inversion costs. Thus, the objective value obtained is (USD 11.943 M). Cases B and C show that incorporating DGs and ESSs into the DSP problem improve the profit from the energy purchase and sale but increase the inversion costs. Nevertheless, the objective functions obtained (16.019 and 16.117 millions of USD) show that integrate these elements is desirable. These Cases also show that is better to include the ESSs into the MV network rather than the LV network. Cases D and E show the same behavior than Cases B and C even if the losses of the ESSs are not considered. If the ESSs had not losses,

the profit would have improved (17.191 and 17.310 millions of USD).

Despite the Case B is the only one who improved the costs of the energy technical losses from the reference Case A, the objective functions of the rest of cases are better than Case B. Moreover, the costs of the energy technical losses for Cases C, D and E are just a little bit bigger than Case A.

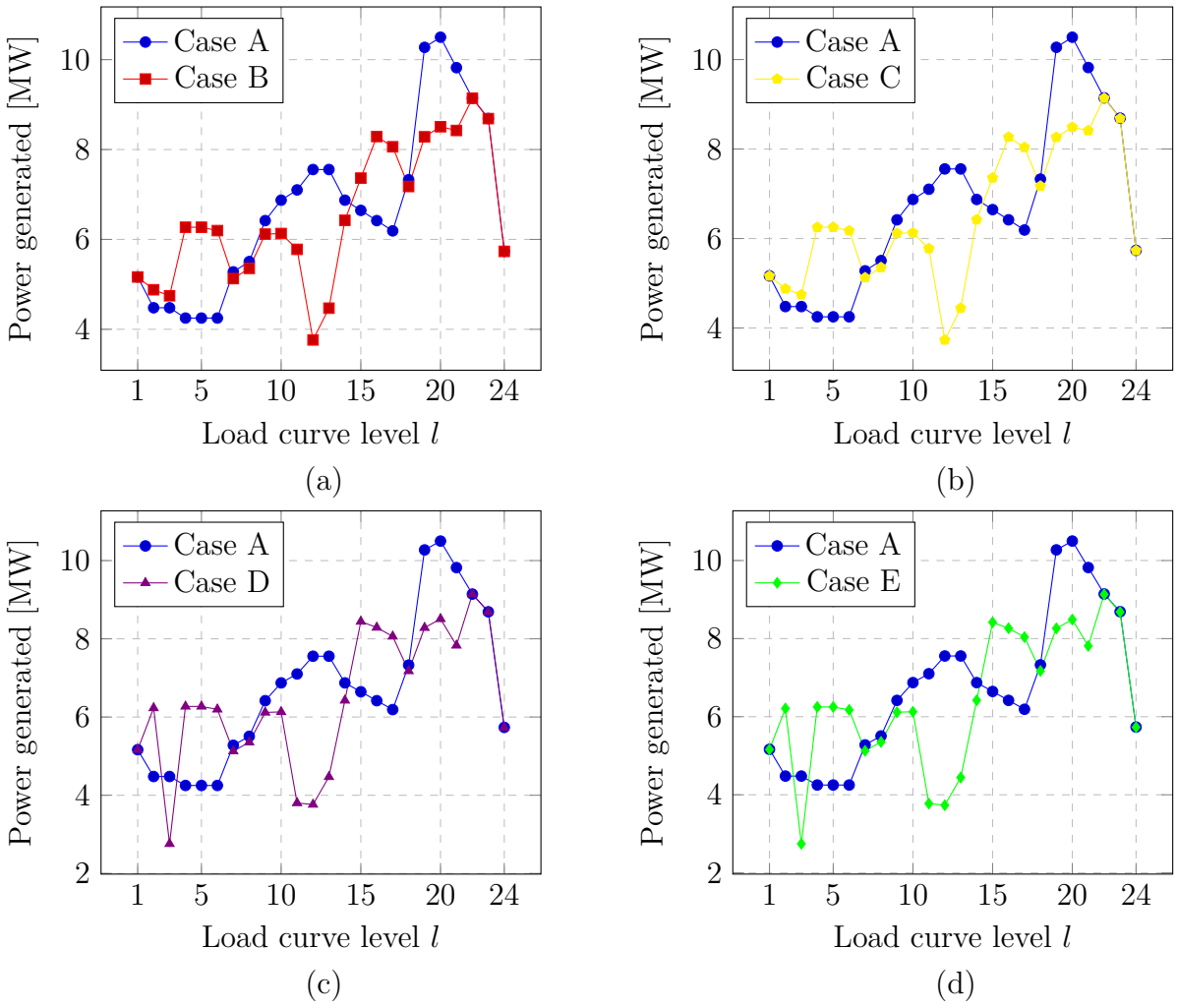

Figure 5.6: Comparison of the generated power by the substations for the five cases.

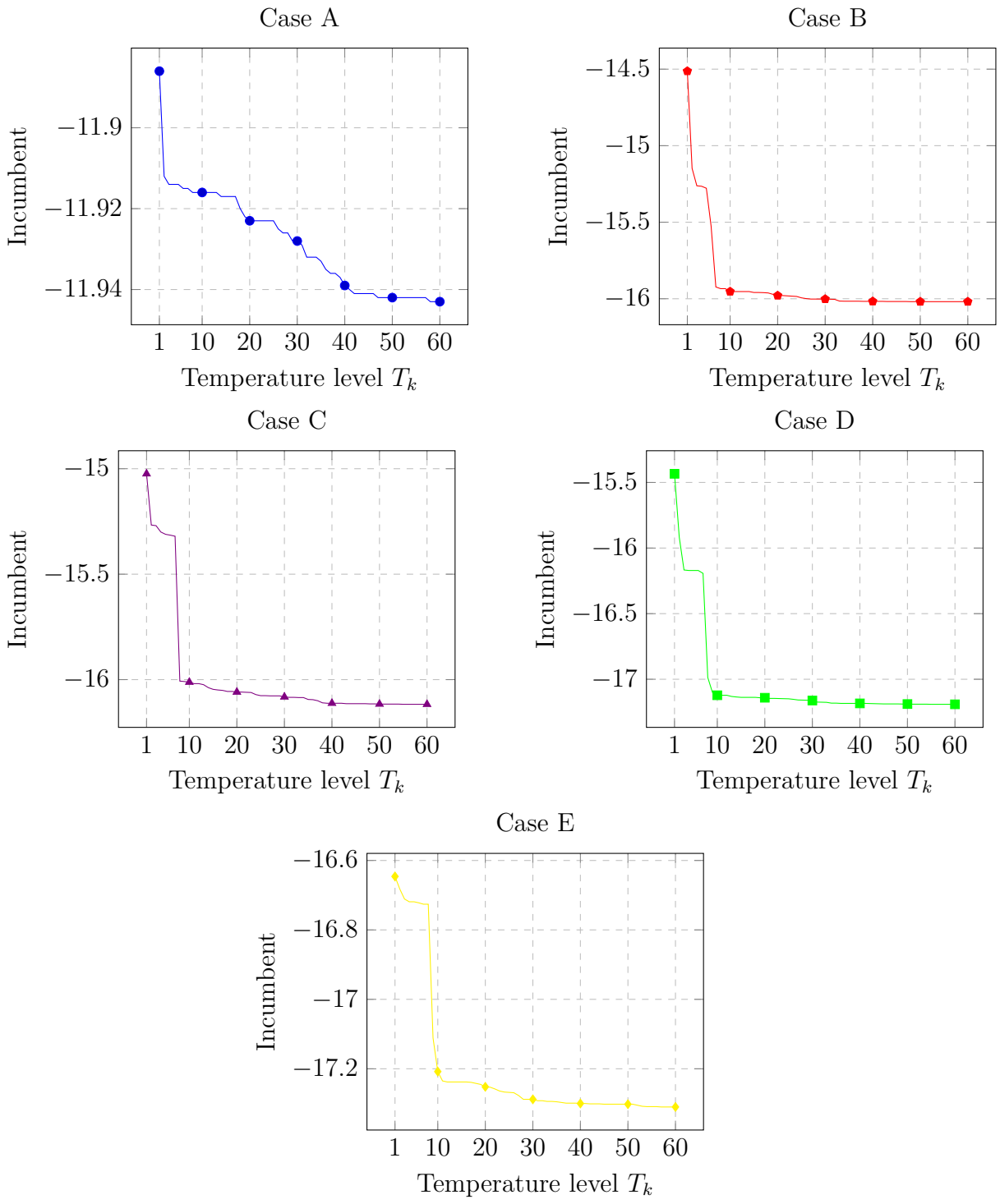

Figure 5.7: Incumbent behavior for the five cases in millions of USD.

Fig. 5.6 shows the behavior of the power generated by the substations and compares the Cases B, C, D, and E which have DGs and ESSs with Case A which has not. Figs. 5.6a–5.6d show that for Cases B, C, D, and E the load curve is modified due DGs and ESSs and that the new peak hour is moved at the hour 22. Figs. 5.6a and 5.6b show that the behavior of the load curve seems to be the same but is different from Figs. 5.6c and 5.6d. As consequence, it is shown that the losses of the ESSs impact the load curve behavior in order to maximize the profit from the energy purchase and sale. Figs. 5.6c and 5.6d show that the behavior of the load curve seems to be the same. Although the behavior seems to be the same for these cases the values are a little bit different due the losses of the network.

When no DGs and ESSs are considered in Case A, the peak hour is presented at the hour 20 with a power value of 10.499 MW. When DGs and ESSs are considered in Cases B, C, D, and E this peak value is reduced to 8.508 MW, 8.488 MW, 8.509 MW, and 8.488 MW, respectively. Due this value is reduced, a new peak hour is presented at the hour 22 in Cases B, C, D, and E with a power value of 8.688 MW, 8.682 MW, 8.689 MW, and 8.682 MW, respectively. In order to measure the efficiency of electrical energy usage due the DGs and ESSs the load factor for all cases is calculated. For Cases A, B, C, D, and E the load factor obtained is 0.638, 0.713, 0.712, 0.703, and 0.702, respectively. As consequence, the increase in this value shows that the integration of ESSs and DGs into the DSP problem is desirable.

Chapter 6

Conclusions and Future work

6.1 Conclusions

This thesis has presented a new methodology which uses a simulated annealing algorithm with a novel neighborhood search method based on the Zbus matrix (NSZM) for the optimal integrated planning of medium and low voltage distribution systems considering distributed generation (DG) and energy storage systems (ESSs). The NSZM method uses a defined neighborhood structure combined with sensitivity factors based on the Zbus matrix in order to find attractive solutions in quick times for the simulated annealing algorithm. The methodology has been validated and tested using a real distribution system of the literature. The results obtained with the proposed methodology are better than the reported in the literature. As consequence, it is demonstrated that the use of a defined neighborhood structure combined with sensitivity factors based on the Zbus matrix for exploring the solution space for a metaheuristic algorithm leads to good quality solutions in relative quick times.

In this thesis, the distribution system planning (DSP) problem of primary and secondary networks was studied with and without DGs. When DGs are considered in the DSP problem,

it has been demonstrated that a reduction in investment and operative costs is achieved. Furthermore, the results obtained with the proposed sensitivity analysis based on the Zbus matrix for solving the allocation and sizing of DGs are better than the reported in the literature. Therefore, it is demonstrated that the use of the Zbus matrix in the analysis of the impact of DGs in the technical losses of both networks is desirable to solve the DSP problem considering DGs.

After this, the DSP problem of primary and secondary networks was studied with and without DGs and ESSs. When DGs and ESSs are considered in the DSP problem, it has been demonstrated that the efficiency of electrical energy usage is improved and the profits from the energy purchase and sale are increased. The results obtained show that it is better to include ESSs into the MV network rather than into the LV network. Moreover, the results show that the decomposition method used for the optimal operation of the ESSs comes to the optimal solution. Hence, the robustness and effectiveness of the methodology proposed to solve the DSP problem considering DGs and ESSs is verified.

The Zbus matrix is a mathematical model which establishes an electrical relation between the primary and secondary nodes. Therefore, a change in one network is reflected in the electrical characteristics of the other one. Under this premise, the Zbus matrix is used in the methodology proposed in this thesis to solve the integrated DSP problem of primary and secondary networks, and its validity has been demonstrated when the results are compared with those reported in the literature.

6.2 Future Work

From the attained results and the drawbacks found along the process, the following topics could be explored.

- Regarding the proposed methodology based on the Zbus matrix, the employment of a three-phase model for the primary and secondary networks.
- Regarding the proposed methodology considering DGs, the employment of different technologies for DGs and the analysis of the conflict when the utility is not the owner of the DGs.
- Regarding the proposed methodology considering DGs and ESSs, the integration of electric vehicles into the DSP problem considering different scenarios is desirable.
- A more efficient implementation could be developed. The usage of a different meta-heuristic combined with the NSZM method to improve the solutions and reduce processing time. Furthermore, these times could be reduced if a production-grade routine such as C++ is applied and a better optimization tool interface is implemented.

Bibliography

[1] S. Wong, K. Bhattacharya, and J. Fuller, "Electric power distribution system design and planning in a deregulated environment," *IET Generation, Transmission & Distribution*, vol. 3, no. 12, p. 1061, 2009.

[2] T. Gönen and I. Ramirez-Rosado, "Review of distribution system planning models: a model for optimal multistage planning," *IEE Proceedings C - Generation, Transmission and Distribution*, vol. 133, no. 7, pp. 397–408, Nov. 1986.

[3] M. Yosef, M. Sayed, and H. K. Youssef, "Allocation and sizing of distribution transformers and feeders for optimal planning of MV/LV distribution networks using optimal integrated biogeography based optimization method," *Electric Power Systems Research*, vol. 128, pp. 100–112, nov 2015.

[4] I. Ziari, G. Ledwich, and A. Ghosh, "Optimal integrated planning of MV–LV distribution systems using DPSO," *Electric Power Systems Research*, vol. 81, no. 10, pp. 1905–1914, oct 2011.

[5] R. A. Hincapíe, R. A. Gallego, and J. Mantovani, "A decomposition approach for integrated planning of primary and secondary distribution networks considering distributed generation," *International Journal of Electrical Power & Energy Systems*, vol. 106, pp. 146–157, mar 2019.

[6] P. S. Georgilakis and N. D. Hatziargyriou, "A review of power distribution planning in the modern power systems era: Models, methods and future research," *Electric Power Systems Research*, vol. 121, pp. 89–100, apr 2015.

[7] K. Aoki, K. Nara, T. Satoh, M. Kitagawa, and K. Yamanaka, "New approximate optimization method for distribution system planning," *IEEE Transactions on Power Systems*, vol. 5, no. 1, pp. 126–132, 1990.

[8] V. Miranda, J. Ranito, and L. Proenca, "Genetic algorithms in optimal multistage distribution network planning," *IEEE Transactions on Power Systems*, vol. 9, no. 4, pp. 1927–1933, 1994.

[9] S. Jonnavithula and R. Billinton, "Minimum cost analysis of feeder routing in distribution system planning," *IEEE Transactions on Power Delivery*, vol. 11, no. 4, pp. 1935–1940, 1996.

[10] I. Ramirez-Rosado and J. Bernal-Agustin, "Genetic algorithms applied to the design of large power distribution systems," *IEEE Transactions on Power Systems*, vol. 13, no. 2, pp. 696–703, may 1998.

[11] I. Ramirez-Rosado and J. Dominguez-Navarro, "New multiobjective tabu search algorithm for fuzzy optimal planning of power distribution systems," *IEEE Transactions on Power Systems*, vol. 21, no. 1, pp. 224–233, feb 2006.

[12] T. El-Fouly, H. Zeineldin, E. El-Saadany, and M. Salama, "A new optimization model for distribution substation siting, sizing, and timing," *International Journal of Electrical Power & Energy Systems*, vol. 30, no. 5, pp. 308–315, jun 2008.

[13] S. Najafi, S. Hosseinian, M. Abedi, A. Vahidnia, and S. Abachezadeh, "A framework for optimal planning in large distribution networks," *IEEE Transactions on Power Systems*, vol. 24, no. 2, pp. 1019–1028, may 2009.

[14] M. Lavorato, M. J. Rider, A. V. Garcia, and R. Romero, "A constructive heuristic algorithm for distribution system planning," *IEEE Transactions on Power Systems*, vol. 25, no. 3, pp. 1734–1742, aug 2010.

[15] B. R. P. Junior, J. R. S. Mantovani, A. M. Cossi, and J. Contreras, "Multiobjective multistage distribution system planning using tabu search," *IET Generation, Transmission & Distribution*, vol. 8, no. 1, pp. 35–45, jan 2014.

[16] R. R. Gonçalves, J. F. Franco, and M. J. Rider, "Short-term expansion planning of radial electrical distribution systems using mixed-integer linear programming," *IET Generation, Transmission & Distribution*, vol. 9, no. 3, pp. 256–266, feb 2015.

[17] M. Jooshaki, A. Abbaspour, M. Fotuhi-Firuzabad, H. Farzin, M. Moeini-Aghtaie, and M. Lehtonen, "A MILP model for incorporating reliability indices in distribution system expansion planning," *IEEE Transactions on Power Systems*, vol. 34, no. 3, pp. 2453–2456, may 2019.

[18] M. Jooshaki, A. Abbaspour, M. Fotuhi-Firuzabad, M. Moeini-Aghtaie, and M. Lehtonen, "MILP model of electricity distribution system expansion planning considering incentive reliability regulations," *IEEE Transactions on Power Systems*, vol. 34, no. 6, pp. 4300–4316, nov 2019.

[19] H. Ghasemi, J. Aghaei, G. B. Gharehpetian, and A. Safdarian, "MILP model for integrated expansion planning of multi-carrier active energy systems," *IET Generation, Transmission & Distribution*, vol. 13, no. 7, pp. 1177–1189, apr 2019.

[20] E. Diaz-Dorado, J. Pidre, and E. M. Garcia, "Planning of large rural low-voltage networks using evolution strategies," *IEEE Transactions on Power Systems*, vol. 18, no. 4, pp. 1594–1600, nov 2003.

[21] A. Cossi, R. Romero, and J. Mantovani, "Planning of secondary distribution circuits through evolutionary algorithms," *IEEE Transactions on Power Delivery*, vol. 20, no. 1, pp. 205–213, jan 2005.

[22] A. Navarro and H. Rudnick, "Large-scale distribution planning – Part I: Simultaneous network and transformer optimization," *IEEE Transactions on Power Systems*, vol. 24, no. 2, pp. 744–751, may 2009.

[23] ——, "Large-scale distribution planning – Part II: Macro-optimization with voronoi's diagram and tabu search," *IEEE Transactions on Power Systems*, vol. 24, no. 2, pp. 752–758, 2009.

[24] A. Cossi, R. Romero, and J. Mantovani, "Planning and projects of secondary electric power distribution systems," *IEEE Transactions on Power Systems*, vol. 24, no. 3, pp. 1599–1608, aug 2009.

[25] C. K. Gan, P. Mancarella, D. Pudjianto, and G. Strbac, "Statistical appraisal of economic design strategies of LV distribution networks," *Electric Power Systems Research*, vol. 81, no. 7, pp. 1363–1372, jul 2011.

[26] V. M. Vélez, R. A. Hincapíe, and R. A. Gallego, "Low voltage distribution system planning using diversified demand curves," *International Journal of Electrical Power & Energy Systems*, vol. 61, pp. 691–700, oct 2014.

[27] P. Paiva, H. Khodr, J. Dominguez-Navarro, J. Yusta, and A. Urdaneta, "Integral planning of primary–secondary distribution systems using mixed integer linear programming," *IEEE Transactions on Power Systems*, vol. 20, no. 2, pp. 1134–1143, may 2005.

[28] R. H. Fletcher and K. Strunz, "Optimal distribution system horizon planning – Part I: Formulation," *IEEE Transactions on Power Systems*, vol. 22, no. 2, pp. 791–799, may 2007.

[29] R. Gholizadeh-Roshanagh, S. Najafi-Ravadanegh, and S. H. Hosseinian, "A framework for optimal coordinated primary–secondary planning of distribution systems considering MV distributed generation," *IEEE Transactions on Smart Grid*, vol. 9, no. 2, pp. 1408–1415, mar 2018.

[30] M. Asensio, P. M. de Quevedo, G. Munoz-Delgado, and J. Contreras, "Joint distribution network and renewable energy expansion planning considering demand response and energy storage – Part I: Stochastic programming model," *IEEE Transactions on Smart Grid*, vol. 9, no. 2, pp. 655–666, mar 2018.

[31] Z. Hu and Y. Song, "Distribution network expansion planning with optimal siting and sizing of electric vehicle charging stations," in *2012 47th International Universities Power Engineering Conference (UPEC)*. IEEE, sep 2012.

[32] E. Naderi, H. Seifi, and M. S. Sepasian, "A dynamic approach for distribution system planning considering distributed generation," *IEEE Transactions on Power Delivery*, vol. 27, no. 3, pp. 1313–1322, jul 2012.

[33] A. Keane, L. F. Ochoa, C. L. T. Borges, G. W. Ault, A. D. Alarcon-Rodriguez, R. A. F. Currie, F. Pilo, C. Dent, and G. P. Harrison, "State-of-the-art techniques and challenges ahead for distributed generation planning and optimization," *IEEE Transactions on Power Systems*, vol. 28, no. 2, pp. 1493–1502, may 2013.

[34] H. Wang and L. Shi, "Optimal distribution network expansion planning incorporating distributed generation," in *2016 IEEE PES Asia-Pacific Power and Energy Engineering Conference (APPEEC)*. IEEE, oct 2016.

[35] H. Wang, L. Shi, and Y. Ni, "A bi-level programming model for distribution network expansion planning with distributed generations and energy storage systems," in *2018 IEEE Power & Energy Society General Meeting (PESGM)*. IEEE, aug 2018.

[36] B. Canizes, J. Soares, F. Lezama, C. Silva, Z. Vale, and J. M. Corchado, "Optimal expansion planning considering storage investment and seasonal effect of demand and renewable generation," *Renewable Energy*, vol. 138, pp. 937–954, aug 2019.

[37] S. Xie, Z. Hu, L. Yang, and J. Wang, "Expansion planning of active distribution system considering multiple active network managements and the optimal load-shedding direction," *International Journal of Electrical Power & Energy Systems*, vol. 115, p. 105451, feb 2020.

[38] J. E. Mendoza, M. E. López, S. C. Fingerhuth, H. E. Peña, and C. A. Salinas, "Low voltage distribution planning considering micro distributed generation," *Electric Power Systems Research*, vol. 103, pp. 233–240, oct 2013.

[39] R. A. Hincapie, M. Granada, and R. A. Gallego, "Optimal planning of secondary distribution systems considering distributed generation and network reliability," in *2016 IEEE ANDESCON*. IEEE, oct 2016.

[40] S. Harnisch, P. Steffens, H. Thies, K. Cibis, M. Zdrallek, and B. Lehde, "New planning principles for low voltage networks with a high share of decentralized generation," in *CIRED Workshop 2016*. Institution of Engineering and Technology, 2016.

[41] D. Rupolo, J. R. S. Mantovani, and B. R. P. Junior, "Medium-and low-voltage planning of electric power distribution systems with distributed generation, energy storage sources, and electric vehicles," in *2019 IEEE Milan PowerTech*. IEEE, jun 2019.

[42] J. Nahman and D. Peric, "Optimal planning of radial distribution networks by simulated annealing technique," *IEEE Transactions on Power Systems*, vol. 23, no. 2, pp. 790–795, may 2008.

[43] Ž. Popović, V. D. Kerleta, and D. Popović, "Hybrid simulated annealing and mixed integer linear programming algorithm for optimal planning of radial distribution networks

with distributed generation," *Electric Power Systems Research*, vol. 108, pp. 211–222, mar 2014.

[44] R. Romero, R. Gallego, and A. Monticelli, "Transmission system expansion planning by simulated annealing," *IEEE Transactions on Power Systems*, vol. 11, no. 1, pp. 364–369, 1996.

[45] J. J. Grainger and W. D. Stevenson, *Power System Analysis*. New York: McGraw-Hill, 1994.

[46] T.-H. Chen, M.-S. Chen, K.-J. Hwang, P. Kotas, and E. Chebli, "Distribution system power flow analysis – Arigid approach," *IEEE Transactions on Power Delivery*, vol. 6, no. 3, pp. 1146–1152, jul 1991.

[47] S. Civanlar, J. Grainger, H. Yin, and S. Lee, "Distribution feeder reconfiguration for loss reduction," *IEEE Transactions on Power Delivery*, vol. 3, no. 3, pp. 1217–1223, jul 1988.

[48] S. Pahwa, D. Weerasinghe, C. Scoglio, and R. Miller, "A complex networks approach for sizing and siting of distributed generators in the distribution system," in *2013 North American Power Symposium (NAPS)*. IEEE, sep 2013.

[49] G. W. Stagg and A. H. El-Abiad, *Computer methods in power systems analysis*. New York: McGraw-Hill, 1968.

[50] G. Kron, *Tensor Analysis of Networks*. London: Macdonald, 1965.

[51] R. A. Gallego, E. M. Toro, and A. H. Escobar, *Tecnicas heuristicas y metaheuristicas*. Editorial UTP, 2015.

[52] G. Caralis, T. Christakopoulos, S. Karellas, and Z. Gao, "Analysis of energy storage systems to exploit wind energy curtailment in crete," *Renewable and Sustainable Energy Reviews*, vol. 103, pp. 122–139, apr 2019.

[53] P. Nikolaidis and A. Poullikkas, "Cost metrics of electrical energy storage technologies in potential power system operations," *Sustainable Energy Technologies and Assessments*, vol. 25, pp. 43–59, feb 2018.

Appendix A

Data Systems

A.1 Data of the distribution system

The real distribution system of Fig. 5.1 is proposed in [5]. This distribution system integrates the primary and secondary networks. The primary distribution network has 48 existing nodes, 1 existing substation (type 2) and 51 existing feeders (type 1). To supply the new power demand, 60 new feeders and 1 new substation can be installed. In order to supply the 138 new secondary demand nodes, there are proposed 33 new DTs, 15 new DGs, and 147 new secondary circuits. Additionally, 5 types of substations, 6 types of wires for primary and secondary, 8 types of DTs, and 4 types of DGs are considered.

The nominal voltage of this system is 13.2 kV (line to line) for the primary network and 440 V (line to neutral) for the secondary network. The maximum voltage regulation for the primary and secondary systems is 10%. The planning horizon is 20 years. The load duration curve is discretized in three load levels: 100%, 60%, and 30% of peak demand, with durations of 1000, 6760, and 1000 h respectively. The ZIP load model coefficients are $a_0 = 0.2$ and $a_2 = 0.8$. The discount rate is 10% and the energy cost is 0.15 USD/kWh. The full system

database can be also find in [**?**].

The candidate nodes for the installation of DTs and DGs are presented in Table A.1.

Table A.1: Candidate nodes for installing DTs and DGs.

Element	Nodes
DT	2, 8, 11, 16, 30, 33, 37, 45, 48, 51, 56, 59, 64, 80, 83, 87, 91, 94, 97, 104, 106, 109, 111, 113, 116, 118, 122, 124, 127, 129, 132, 135, 137
DG	6, 23, 38, 43, 54, 62, 71, 88, 95, 103, 110, 117, 130, 131, 136

Table A.2: Information of the wires used in the distribution system.

	MV Network				LV Network			
Type	R [ohm/km]	X [ohm/km]	Amp	USD/m	R [ohm/km]	X [ohm/km]	Amp	USD/m
1	0.52	0.22	205	26	1.04	0.45	150	14
2	0.32	0.14	275	40	0.65	0.28	180	20
3	0.26	0.12	305	47	0.52	0.22	205	26
4	0.18	0.1	390	57	0.32	0.14	275	40
5	0.14	0.08	460	64	0.26	0.12	305	47
6	0.12	0.07	600	72	0.18	0.1	390	57

Table A.3: Upgrading costs of the wires in [USD/m].

	MV Network						LV Network					
Type	1	2	3	4	5	6	1	2	3	4	5	6
1	0	10	19	26	36	43	0	4	10	22	31	38
2	—	0	5	12	22	29	—	0	4	16	25	32
3	—	—	0	5	15	22	—	—	0	10	19	26
4	—	—	—	0	5	12	—	—	—	0	5	12
5	—	—	—	—	0	5	—	—	—	—	0	5
6	—	—	—	—	—	0	—	—	—	—	—	0

Table A.4: Elements information.

	Substations		DTs				DGs	
Type	kVA	USD	R HV [ohm]	X HV [ohm]	kVA	USD	kW	USD
1	7000	336000	99.704	142.894	30	3177.57	50	2500
2	10000	672000	61.0916	98.7976	45	3953.07	75	3750
3	20000	1344000	33.7638	73.9706	75	5502.69	100	5000
4	30000	2016000	21.2014	49.89	112.5	7439.72	125	6250
5	40000	2688000	15.1782	43.915	150	9376.74	—	—
6	—	—	9.9467	29.3356	225	11053.72	—	—
7	—	—	7.1148	25.149	300	16806	—	—
8	—	—	5.151	18.9131	400	22408	—	—

Table A.5: Information of the circuits of the LV network.

From	To	km	Existing		From	To	km	Existing
1	2	0.1440	0		27	28	0.1824	0
2	3	0.1440	0		28	18	0.1800	0

Table A.5 continued from previous page.

From	To	km	Existing
2	4	0.1344	0
2	5	0.1440	0
5	6	0.1056	0
5	7	0.1632	0
7	8	0.1440	0
8	9	0.1560	0
9	10	0.1440	0
10	11	0.1800	0
11	12	0.1800	0
12	13	0.1800	0
13	14	0.1800	0
14	15	0.1800	0
15	16	0.1800	0
16	17	0.1440	0
18	17	0.1008	0
4	19	0.1056	0
19	20	0.0864	0
20	21	0.0173	0
21	22	0.1344	0
22	23	0.1800	0
23	24	0.1800	0
23	25	0.1800	0
25	26	0.1608	0
26	27	0.1800	0
50	51	0.1728	0

From	To	km	Existing
18	39	0.1440	0
3	29	0.1440	0
29	30	0.1560	0
30	31	0.1920	0
31	32	0.1248	0
32	33	0.1632	0
33	24	0.1800	0
33	34	0.1378	0
34	35	0.1800	0
35	36	0.1195	0
36	37	0.1800	0
37	38	0.1920	0
38	39	0.1800	0
38	40	0.1440	0
3	41	0.1440	0
41	42	0.1584	0
42	43	0.1560	0
42	44	0.1560	0
44	45	0.1008	0
45	46	0.1522	0
46	47	0.1848	0
47	48	0.1800	0
48	49	0.1440	0
49	50	0.1800	0
73	74	0.1800	0

Table A.5 continued from previous page.

From	To	km	Existing
51	52	0.1440	0
52	53	0.1440	0
54	53	0.1800	0
40	54	0.1440	0
18	66	0.1344	0
16	55	0.1632	0
55	56	0.1440	0
56	57	0.1560	0
57	58	0.1440	0
58	59	0.1800	0
59	60	0.1800	0
60	61	0.1800	0
61	62	0.1800	0
62	63	0.1800	0
63	64	0.1800	0
64	65	0.1440	0
76	65	0.1008	0
66	67	0.1056	0
67	68	0.0864	0
68	69	0.0173	0
69	70	0.1344	0
70	71	0.1800	0
71	77	0.1800	0
71	72	0.1800	0
72	73	0.1608	0

From	To	km	Existing
74	75	0.1824	0
75	76	0.1800	0
76	78	0.1440	0
38	79	0.1440	0
79	80	0.1560	0
80	81	0.1920	0
81	82	0.1248	0
82	83	0.1632	0
83	77	0.1800	0
83	84	0.1378	0
84	85	0.1800	0
85	86	0.1195	0
86	87	0.1800	0
87	88	0.1920	0
88	78	0.1800	0
88	89	0.1440	0
54	90	0.1560	0
90	91	0.1008	0
91	92	0.1522	0
92	93	0.1848	0
93	94	0.1800	0
94	95	0.1440	0
95	96	0.1800	0
96	97	0.1728	0
97	98	0.1440	0

Table A.5 continued from previous page.

From	To	km	Existing
98	99	0.1440	0
100	99	0.1800	0
89	100	0.1440	0
101	102	0.1080	0
102	103	0.1080	0
103	104	0.1080	0
104	105	0.1620	0
105	106	0.1620	0
106	107	0.1620	0
107	108	0.1620	0
108	109	0.1620	0
109	110	0.1080	0
110	111	0.1080	0
111	112	0.1080	0
112	113	0.1080	0
113	114	0.1620	0
114	115	0.1620	0
115	116	0.1620	0
116	117	0.1620	0
117	118	0.1620	0
118	101	0.1080	0
118	119	0.1080	0

From	To	km	Existing
119	120	0.1080	0
120	121	0.1080	0
121	122	0.1080	0
122	123	0.1620	0
123	124	0.1620	0
124	125	0.1620	0
125	126	0.1620	0
126	127	0.1620	0
127	128	0.1080	0
128	129	0.1080	0
129	130	0.1080	0
130	113	0.1080	0
127	131	0.1080	0
131	132	0.1080	0
132	133	0.1620	0
133	134	0.1620	0
134	135	0.1620	0
135	136	0.1620	0
136	137	0.1620	0
137	138	0.1080	0
138	122	0.1080	0
—	—	—	—

Table A.6: Information of the feeders of the MV network.

From	To	km	Existing	From	To	km	Existing
SS1	139	0.226404	1	16	18	0.2448000	0
139	140	0.226404	1	64	76	0.2448000	0
140	141	0.153672	1	2	23	0.6580800	0
141	142	0.288000	1	23	18	0.8832000	0
142	143	0.153672	1	18	71	0.6580800	0
140	144	0.258480	1	71	76	0.8832000	0
144	145	0.153672	1	2	3	0.1440000	0
145	146	0.096000	1	23	33	0.3600000	0
146	147	0.360000	1	18	38	0.3240000	0
146	148	0.153672	1	71	83	0.3600000	0
148	149	0.307344	1	76	88	0.3240000	0
149	150	0.153672	1	3	30	0.3000000	0
150	151	0.312000	1	30	33	0.4800000	0
150	152	0.192000	1	33	37	0.6172800	0
152	153	0.307344	1	37	38	0.1920000	0
153	154	0.288000	1	38	80	0.3000000	0
154	155	0.153672	1	80	83	0.4800000	0
155	156	0.192000	1	83	87	0.6172800	0
SS1	157	0.258480	1	87	88	0.1920000	0
157	158	0.258480	1	3	42	0.3024000	0
158	159	0.258480	1	38	54	0.2880000	0
159	160	0.258480	1	88	100	0.2880000	0
160	161	0.153672	1	42	45	0.2568000	0
161	162	0.153672	1	45	48	0.5169600	0
162	163	0.240000	1	48	51	0.4968000	0

Table A.6 continued from previous page.

From	To	km	Existing
163	164	0.226404	1
163	165	0.120000	1
165	166	0.360000	1
166	167	0.360000	1
SS1	168	0.240000	1
168	169	0.240000	1
169	170	0.374880	1
170	171	0.258480	1
171	172	0.096000	1
172	173	0.153672	1
172	174	0.258480	1
174	175	0.120000	1
175	176	0.192000	1
176	177	0.153672	1
177	178	0.192000	1
178	179	0.096000	1
179	180	0.120000	1
180	181	0.153672	1
181	182	0.153672	1
182	183	0.096000	1
183	184	0.120000	1
184	185	0.120000	1
185	186	0.153672	1
SS2	8	0.340000	0
5	8	0.307200	0

From	To	km	Existing
51	54	0.4680000	0
54	91	0.2568000	0
91	94	0.5169600	0
94	97	0.4968000	0
97	100	0.4680000	0
94	183	0.2300000	0
100	176	0.2100000	0
88	167	0.4699636	0
76	164	0.4516364	0
64	147	0.4254545	0
104	106	0.3236763	0
106	109	0.4855145	0
109	111	0.2157842	0
111	113	0.2157842	0
113	116	0.4855145	0
116	118	0.3236763	0
118	104	0.4315684	0
118	122	0.4315684	0
122	124	0.3236763	0
124	127	0.4855145	0
127	129	0.2157842	0
129	113	0.2157842	0
127	132	0.2157842	0
132	135	0.4855145	0
135	137	0.3236763	0

Table A.6 continued from previous page.

From	To	km	Existing
5	2	0.144000	0
8	11	0.480000	0
11	16	0.900000	0
16	56	0.307200	0
56	59	0.480000	0
59	64	0.900000	0

From	To	km	Existing
137	122	0.2157842	0
156	132	0.1000000	0
153	135	0.3400000	0
152	137	0.3490909	0
SS2	109	0.2500000	0
—	—	—	—

Table A.7: Nodal information of the LV network.

Node	kVA	Existing
1	0.8550	0
2	8.7300	0
3	17.1675	0
4	8.7300	0
5	23.4675	0
6	7.9650	0
7	29.2950	0
8	43.5150	0
9	43.5150	0
10	43.5150	0
11	57.7350	0
12	43.5150	0
13	43.5150	0
14	32.4225	0
15	43.0875	0
16	29.2950	0
17	0.8550	0

Node	kVA	Existing
70	3.5900	0
71	5.4400	0
72	8.2900	0
73	9.9100	0
74	9.9100	0
75	6.6700	0
76	0.1900	0
77	0.1900	0
78	6.6700	0
79	5.4400	0
80	35.7750	0
81	5.4400	0
82	5.4400	0
83	5.4400	0
84	9.9100	0
85	9.9100	0
86	9.9100	0

Table A.7 continued from previous page.

Node	kVA	Existing	Node	kVA	Existing
18	0.8550	0	87	9.2900	0
19	24.4800	0	88	8.8900	0
20	24.4800	0	89	1.8100	0
21	24.4800	0	90	1.7700	0
22	16.1550	0	91	8.0900	0
23	24.4800	0	92	9.6700	0
24	0.8550	0	93	9.6700	0
25	37.3050	0	94	12.8300	0
26	44.5950	0	95	9.6700	0
27	44.5950	0	96	9.6700	0
28	30.0150	0	97	9.6700	0
29	24.4800	0	98	5.2150	0
30	160.9875	0	99	4.9300	0
31	24.4800	0	100	0.1900	0
32	24.4800	0	101	15.4700	0
33	24.4800	0	102	17.2800	0
34	44.5950	0	103	22.6600	0
35	44.5950	0	104	17.2800	0
36	44.5950	0	105	30.9700	0
37	41.8050	0	106	15.4700	0
38	40.0050	0	107	38.6700	0
39	30.0150	0	108	57.4300	0
40	8.1450	0	109	57.4300	0
41	36.4050	0	110	57.4300	0
42	22.1850	0	111	76.2100	0

Table A.7 continued from previous page.

Node	kVA	Existing	Node	kVA	Existing
43	7.9650	0	112	57.4300	0
44	7.9650	0	113	57.4300	0
45	36.4050	0	114	42.8000	0
46	43.5150	0	115	56.8700	0
47	43.5150	0	116	38.6700	0
48	57.7350	0	117	15.4700	0
49	43.5150	0	118	15.4700	0
50	43.5150	0	119	32.3200	0
51	43.5150	0	120	32.3200	0
52	23.4675	0	121	32.3200	0
53	22.1850	0	122	21.3300	0
54	0.8550	0	123	32.3200	0
55	6.5100	0	124	15.4700	0
56	9.6700	0	125	49.2500	0
57	9.6700	0	126	58.8700	0
58	9.6700	0	127	58.8700	0
59	12.8300	0	128	39.6200	0
60	9.6700	0	129	32.3200	0
61	9.6700	0	130	212.5000	0
62	7.2050	0	131	32.3200	0
63	9.5750	0	132	32.3200	0
64	6.5100	0	133	32.3200	0
65	0.1900	0	134	58.8700	0
66	1.9400	0	135	58.8700	0
67	5.4400	0	136	58.8700	0

Table A.7 continued from previous page.

Node	kVA	Existing	Node	kVA	Existing
68	5.4400	0	137	55.1900	0
69	5.4400	0	138	52.8100	0

Table A.8: Nodal information of the MV network.

Node	kVA	Existing	Node	kVA	Existing
139	387.197	1	186	121.994	1
140	121.994	1	5	0	0
141	73.479	1	23	0	0
142	387.197	1	18	0	0
143	121.994	1	71	0	0
144	18.370	1	76	0	0
145	73.479	1	3	0	0
146	387.197	1	38	0	0
147	293.911	1	88	0	0
148	18.370	1	42	0	0
149	121.994	1	54	0	0
150	73.479	1	100	0	0
151	387.197	1	2	0	0
152	293.911	1	8	0	0
153	121.994	1	11	0	0
154	18.370	1	16	0	0
155	73.479	1	30	0	0
156	387.197	1	33	0	0
157	121.994	1	37	0	0
158	387.197	1	45	0	0
159	73.479	1	48	0	0

Table A.8 continued from previous page.

Node	kVA	Existing	Node	kVA	Existing
160	18.370	1	51	0	0
161	121.994	1	56	0	0
162	18.370	1	59	0	0
163	121.994	1	64	0	0
164	293.911	1	80	0	0
165	18.370	1	83	0	0
166	293.911	1	87	0	0
167	387.197	1	91	0	0
168	121.994	1	94	0	0
169	293.911	1	97	0	0
170	18.370	1	104	0	0
171	73.479	1	106	0	0
172	387.197	1	109	0	0
173	121.994	1	111	0	0
174	387.197	1	113	0	0
175	18.370	1	116	0	0
176	73.479	1	118	0	0
177	387.197	1	122	0	0
178	121.994	1	124	0	0
179	73.479	1	127	0	0
180	18.370	1	129	0	0
181	73.479	1	132	0	0
182	73.479	1	135	0	0
183	18.370	1	137	0	0
184	73.479	1	SS1	0	1

Table A.8 continued from previous page.

Node	kVA	Existing
185	387.197	1

Node	kVA	Existing
SS2	0	0

A.2 Data of the modified distribution system

Some data of the real distribution system of Fig. 5.1 proposed in Appendix A.1 is modified and added in order to incorporated the ESSs.

The nominal voltage of this system is 13.2 kV (line to line) for the primary network and 440 V (line to line) for the secondary network. The maximum voltage regulation for the primary and secondary systems is 10%. The planning horizon is 20 years. The ZIP load model coefficients are $a_0 = 0.2$ and $a_2 = 0.8$. The discount rate is 10%. The energy sale cost is 0.2 USD/kWh. The Tables A.1–A.8 show the rest of the database system.

Table A.9: Load and DG curves information.

Load level [l]	Load curve [pu]	Energy purchase cost [USD/kWh]	DG curve [pu]
1	0.489130	0.084	0.0002
2	0.423913	0.080	0.0002
3	0.423913	0.080	0.0002
4	0.402174	0.075	0.0002
5	0.402174	0.075	0.0002
6	0.402174	0.075	0.0400
7	0.500000	0.085	0.0800
8	0.521739	0.090	0.0800
9	0.608696	0.105	0.1600

Table A.9 continued from previous page

Load level [l]	Load curve [pu]	Energy purchase cost [USD/kWh]	DG curve [pu]
10	0.652174	0.135	0.4000
11	0.673913	0.145	0.7200
12	0.717391	0.185	1.0000
13	0.717391	0.185	0.6000
14	0.652174	0.135	0.2400
15	0.630435	0.125	0.1200
16	0.608696	0.105	0.0800
17	0.586957	0.098	0.0800
18	0.695652	0.175	0.0800
19	0.978261	0.305	0.0003
20	1.000000	0.325	0.0003
21	0.934783	0.285	0.0003
22	0.869565	0.275	0.0003
23	0.826087	0.265	0.0003
24	0.543478	0.100	0.0003

Table A.10: ESS information.

Type	Capacity [kWh]	kW	USD	$O_{\&}M_b^{fx}$ [USD/year]	ϕ_b [%/kWh]
1	100	33.333	32000	2666.667	1.000
2	200	66.667	64000	5333.333	0.500
3	300	100	96000	8000.000	0.333
4	400	133.333	128000	10666.667	0.250

Appendix B

Final configurations of primary and secondary networks

B.1 Integrated DSP considering DGs

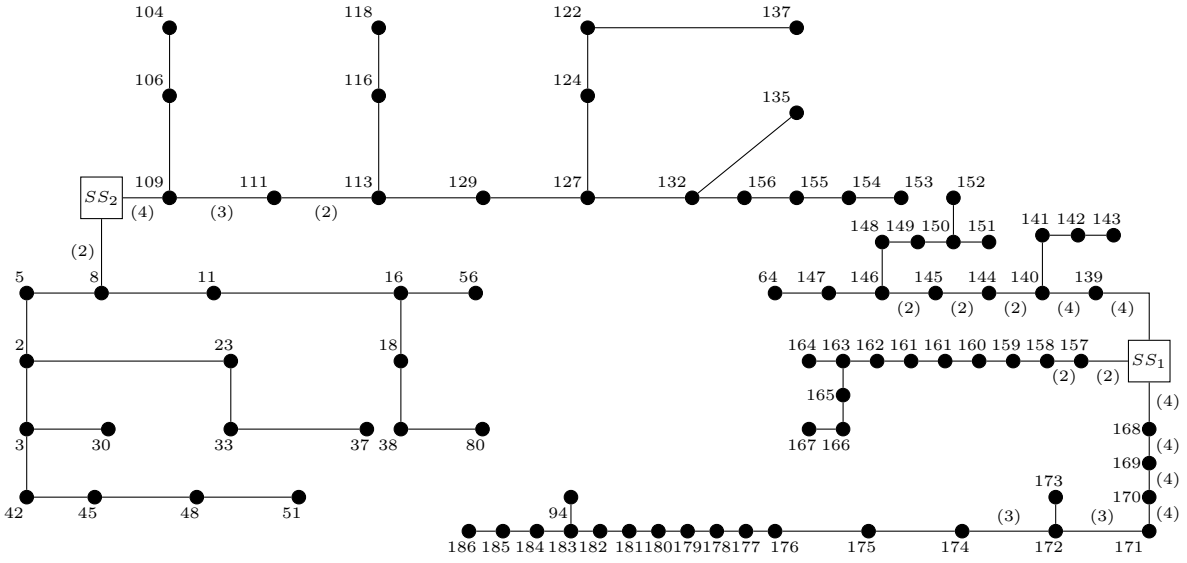

Figure B.1: Case 1 - Primary Network.

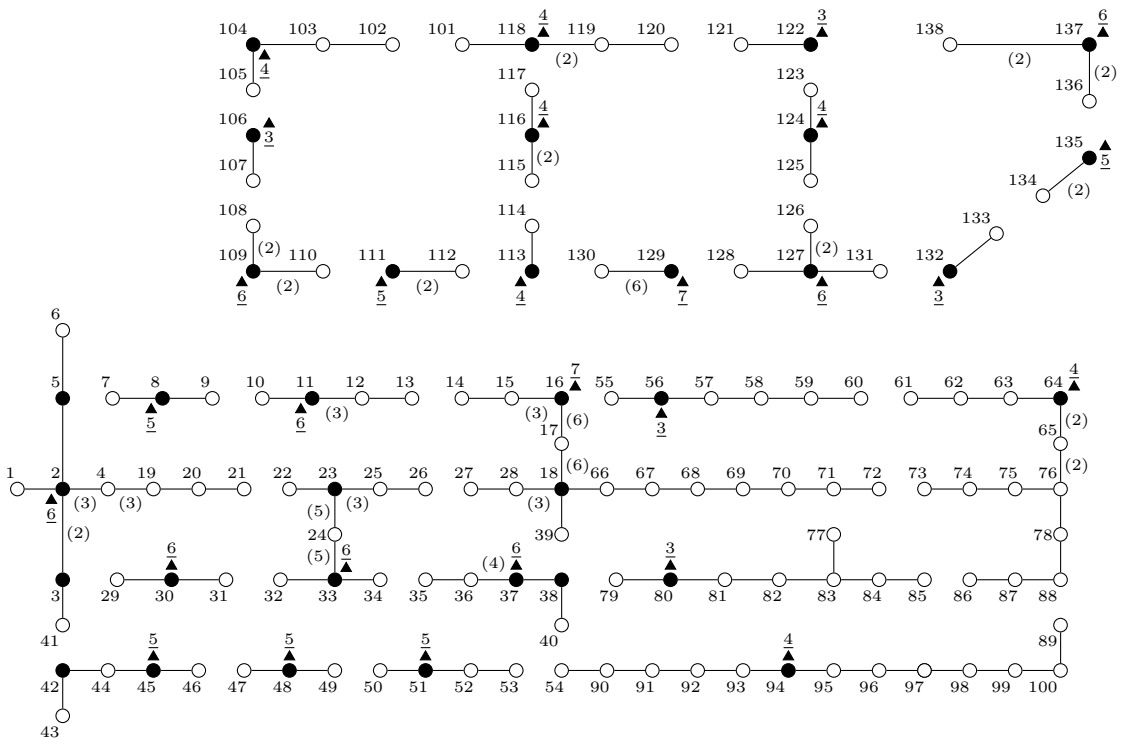

Figure B.2: Case 1 - Secondary Networks.

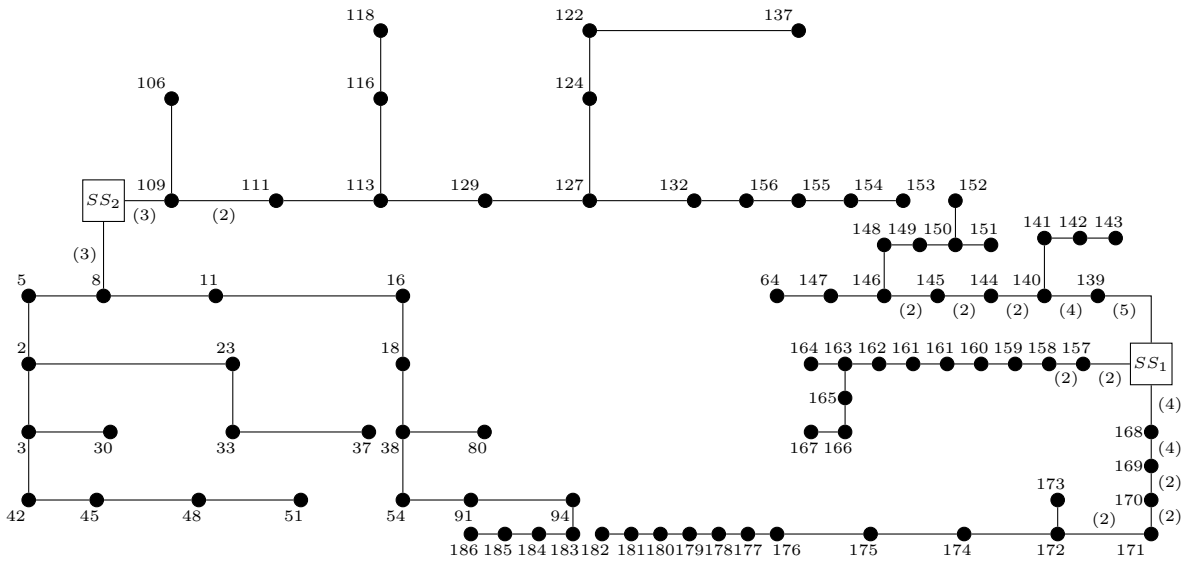

Figure B.3: Case 2 - Primary Network.

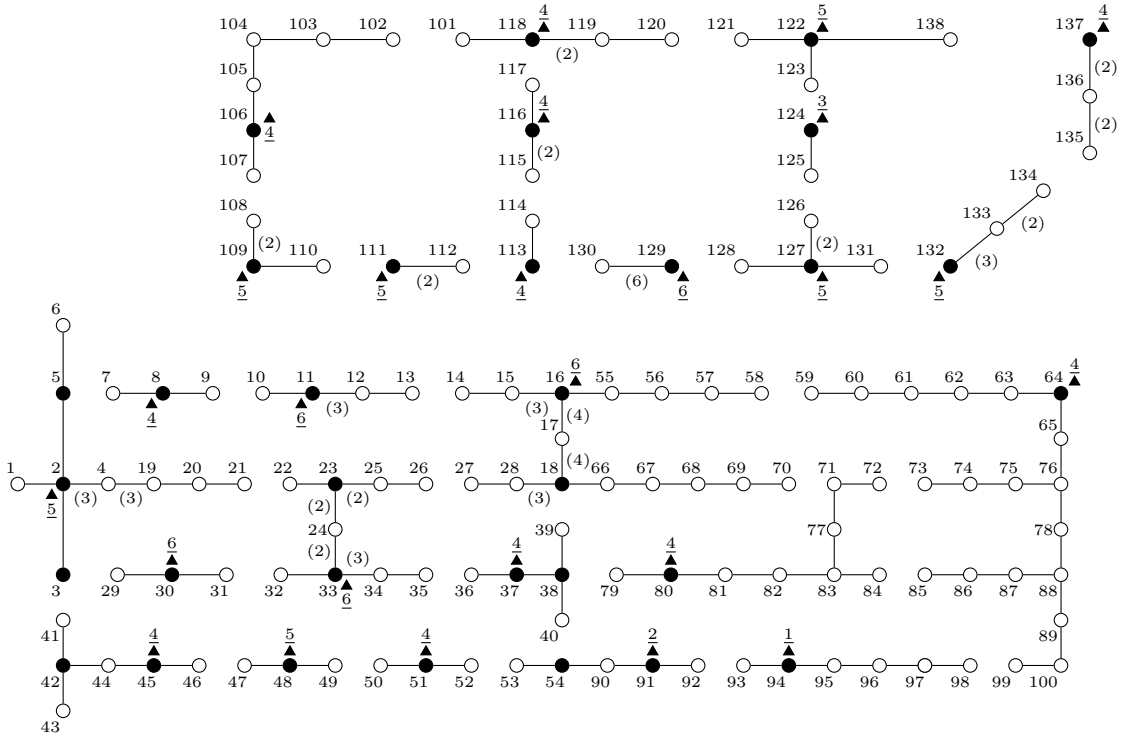

Figure B.4: Case 2 - Secondary Networks.

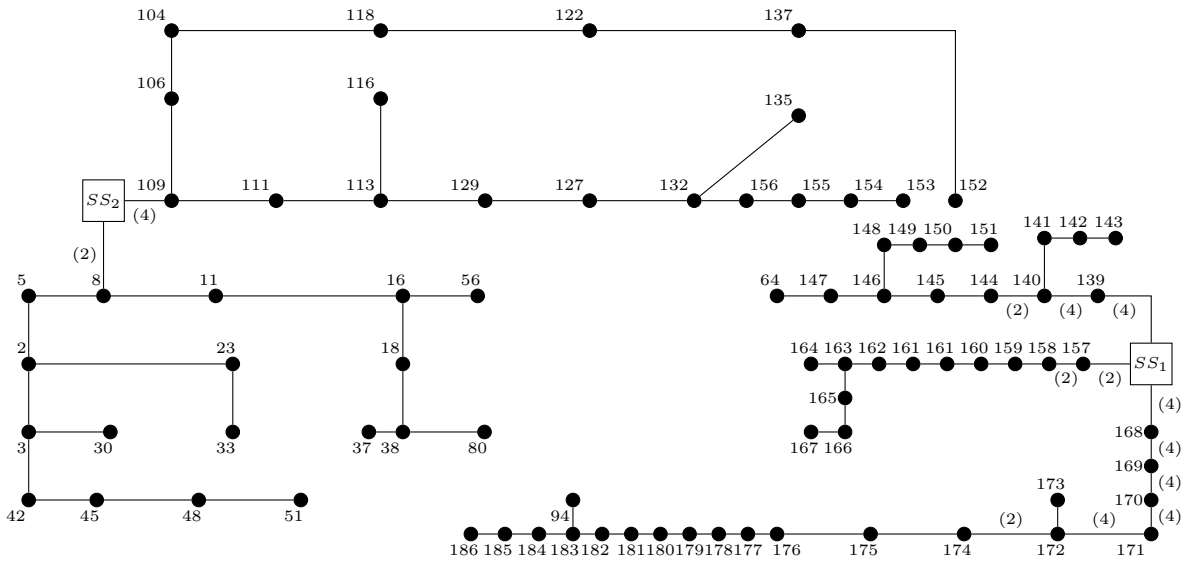

Figure B.5: Case 3 - Primary Network.

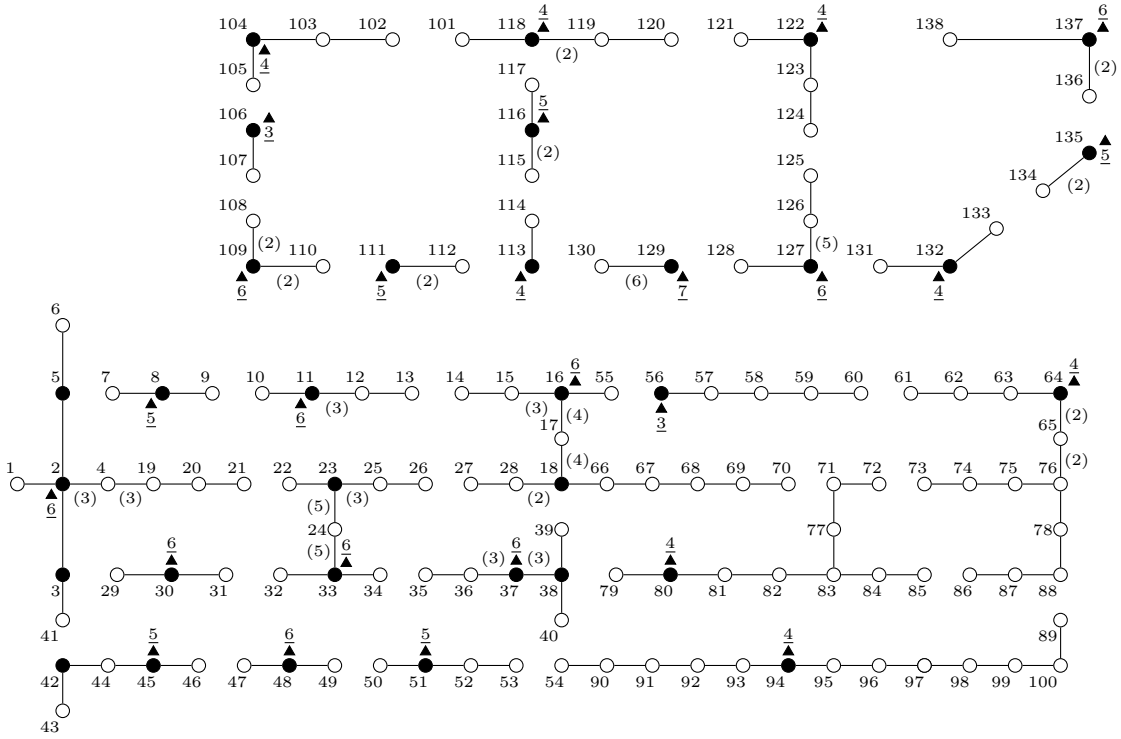

Figure B.6: Case 3 - Secondary Networks.

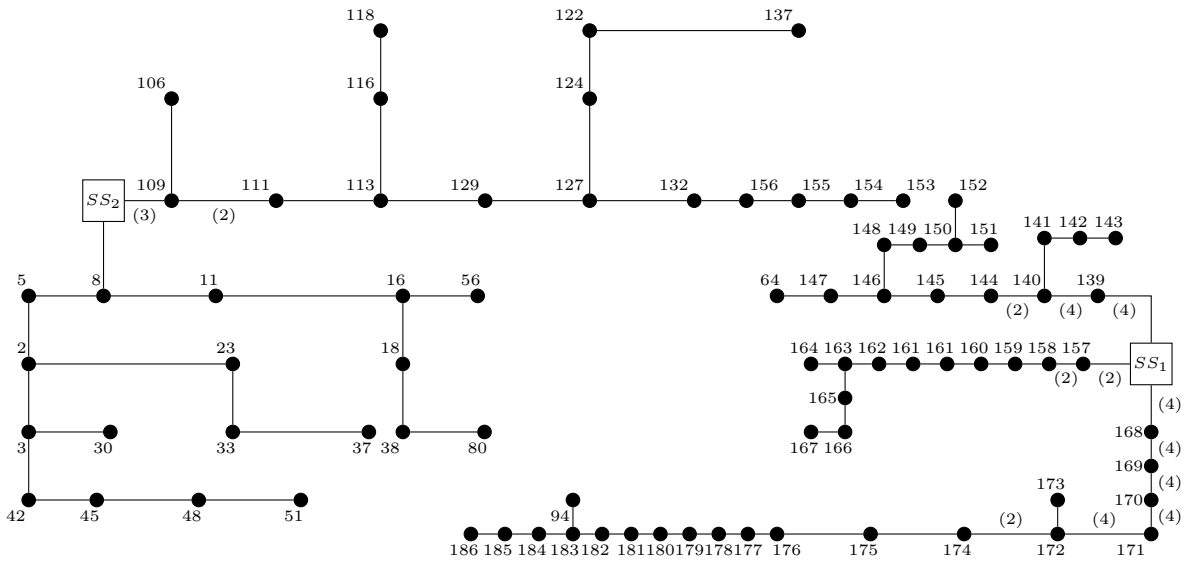

Figure B.7: Case 4 - Primary Network.

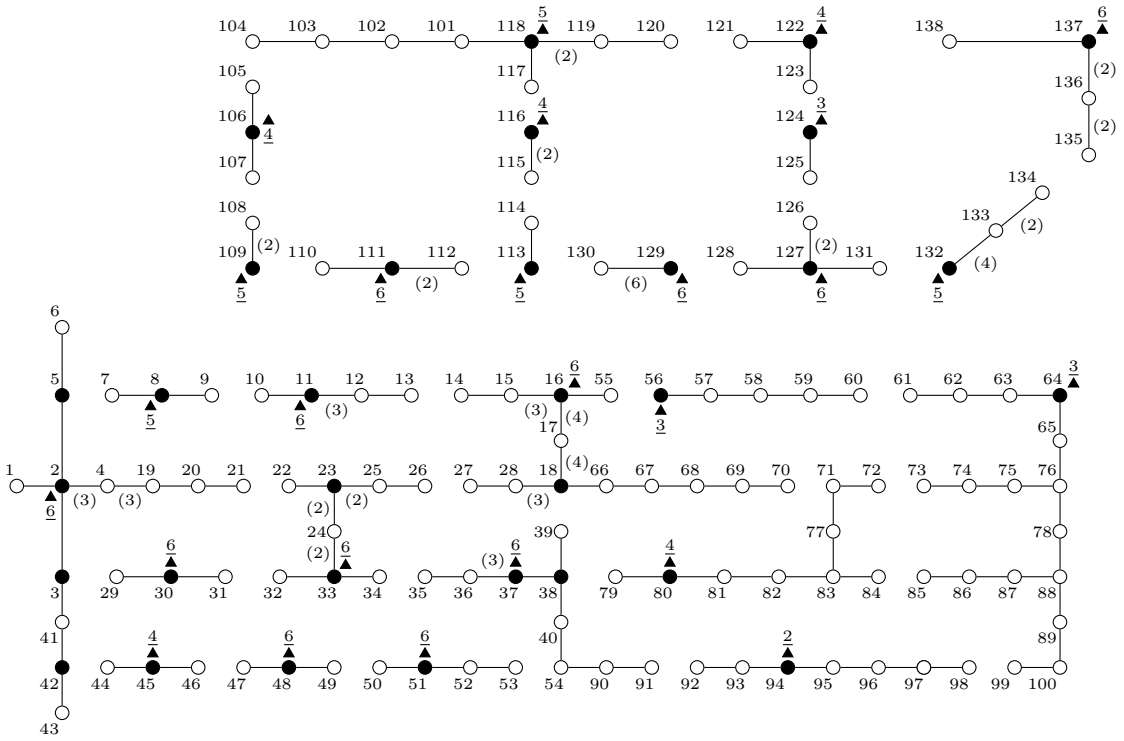

Figure B.8: Case 4 - Secondary Networks.

B.2 Integrated DSP considering DGs and ESSs

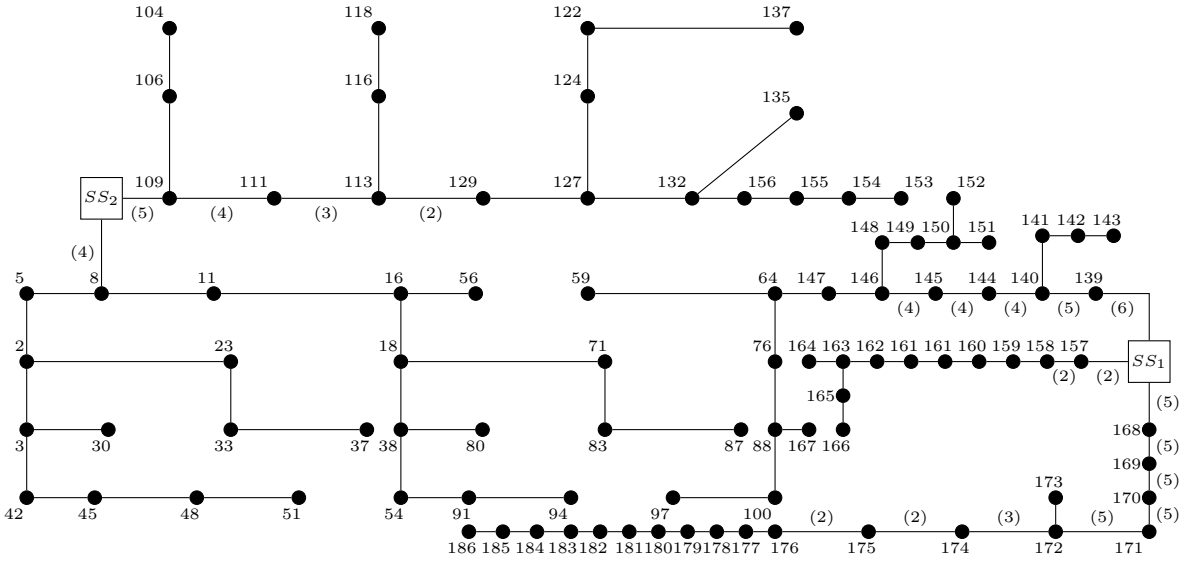

Figure B.9: Case A - Primary Network.

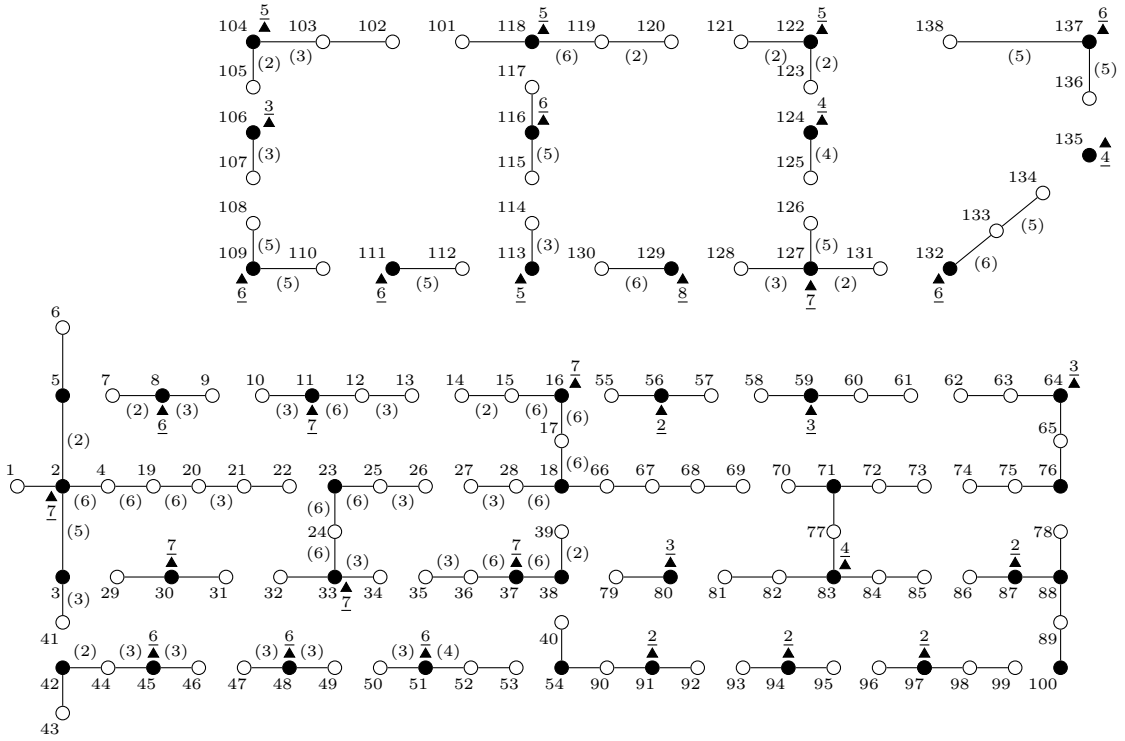

Figure B.10: Case A - Secondary Networks.

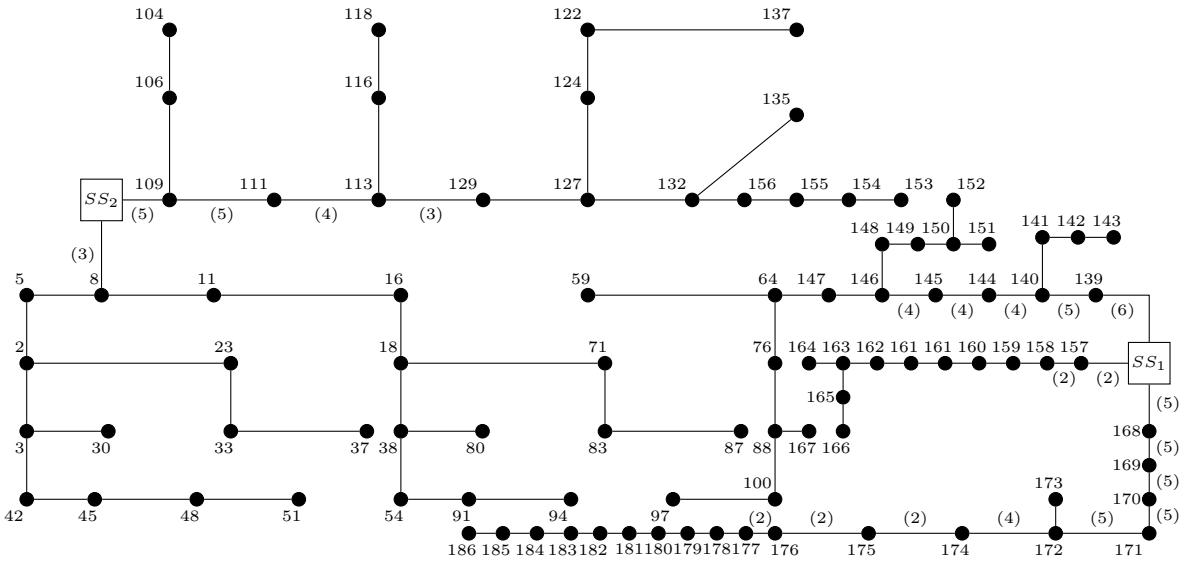

Figure B.11: Case B - Primary Network.

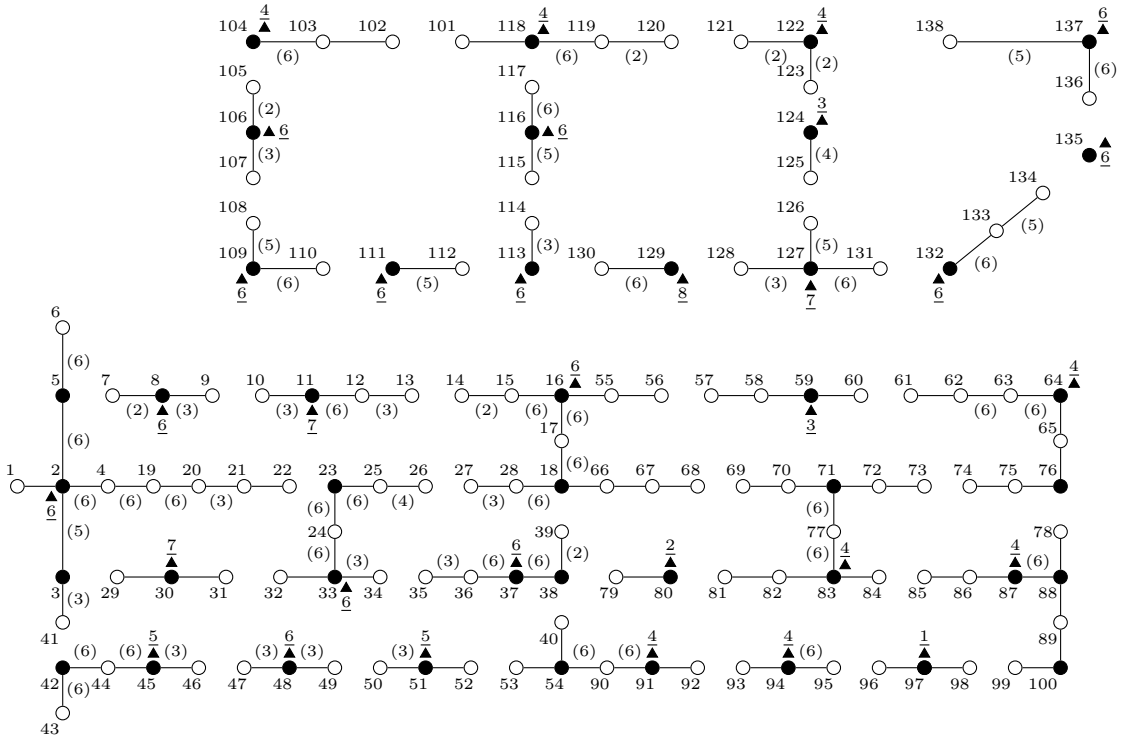

Figure B.12: Case B - Secondary Networks.

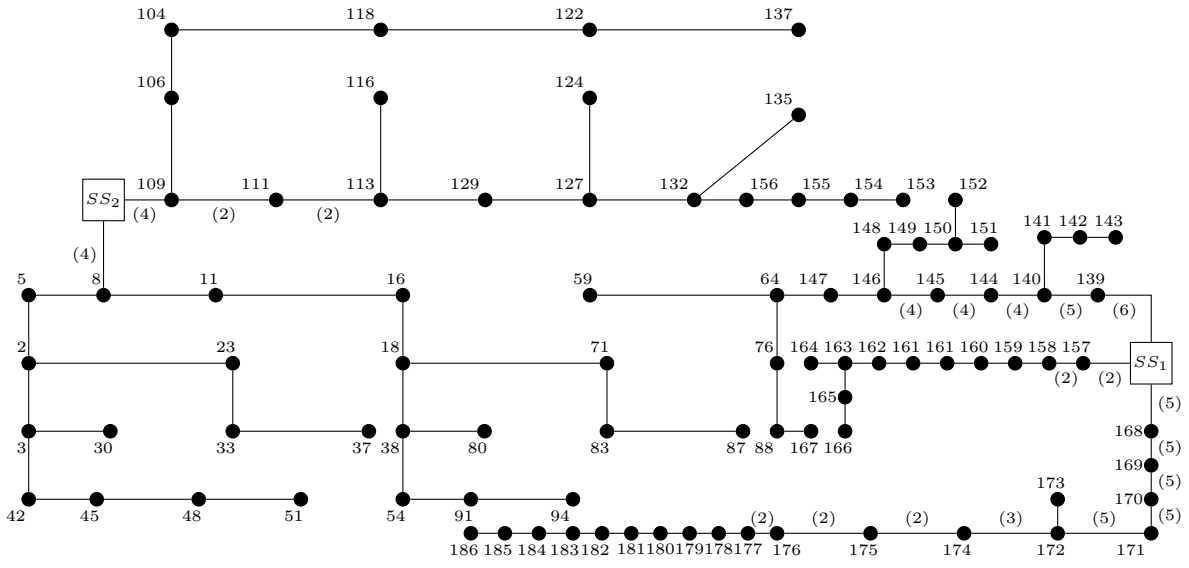

Figure B.13: Case C - Primary Network.

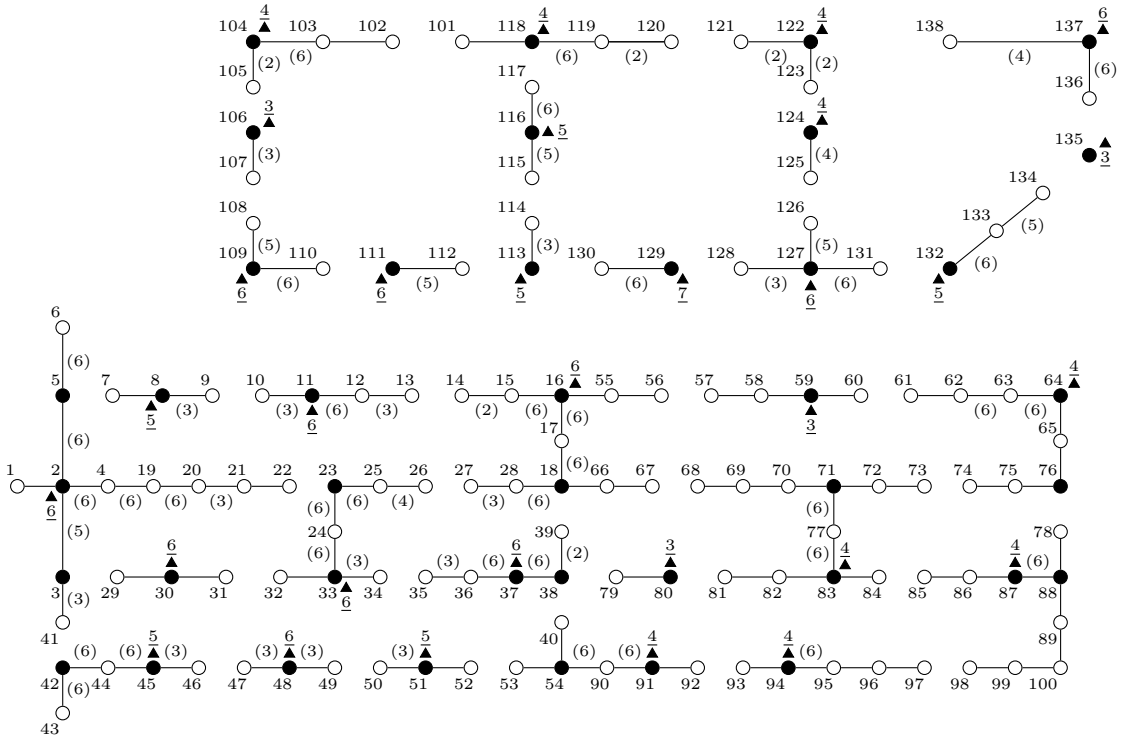

Figure B.14: Case C - Secondary Networks.

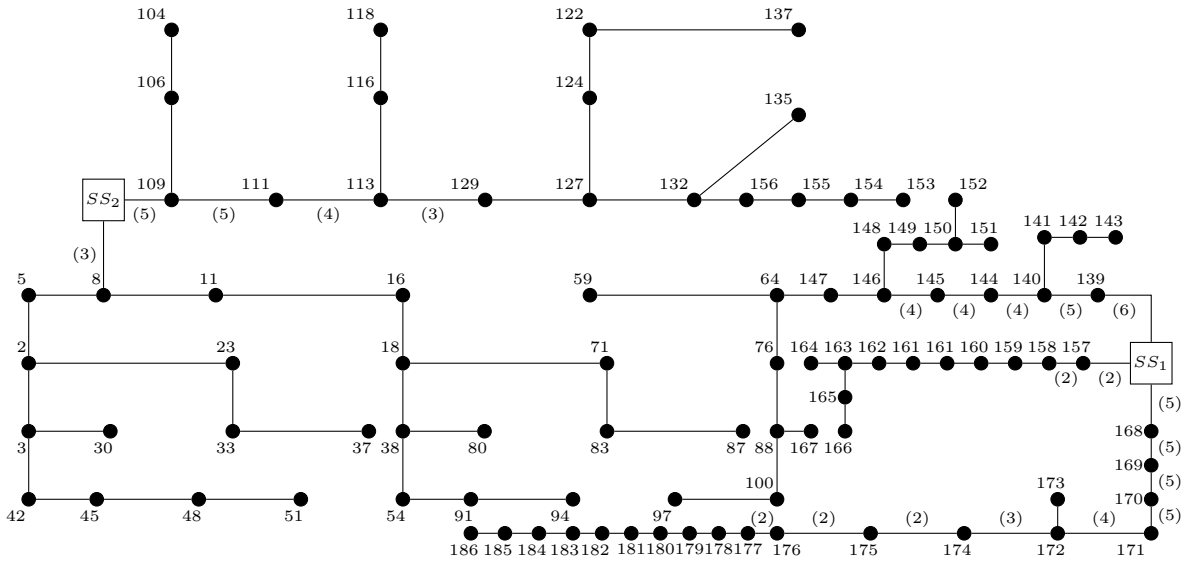

Figure B.15: Case D - Primary Network.

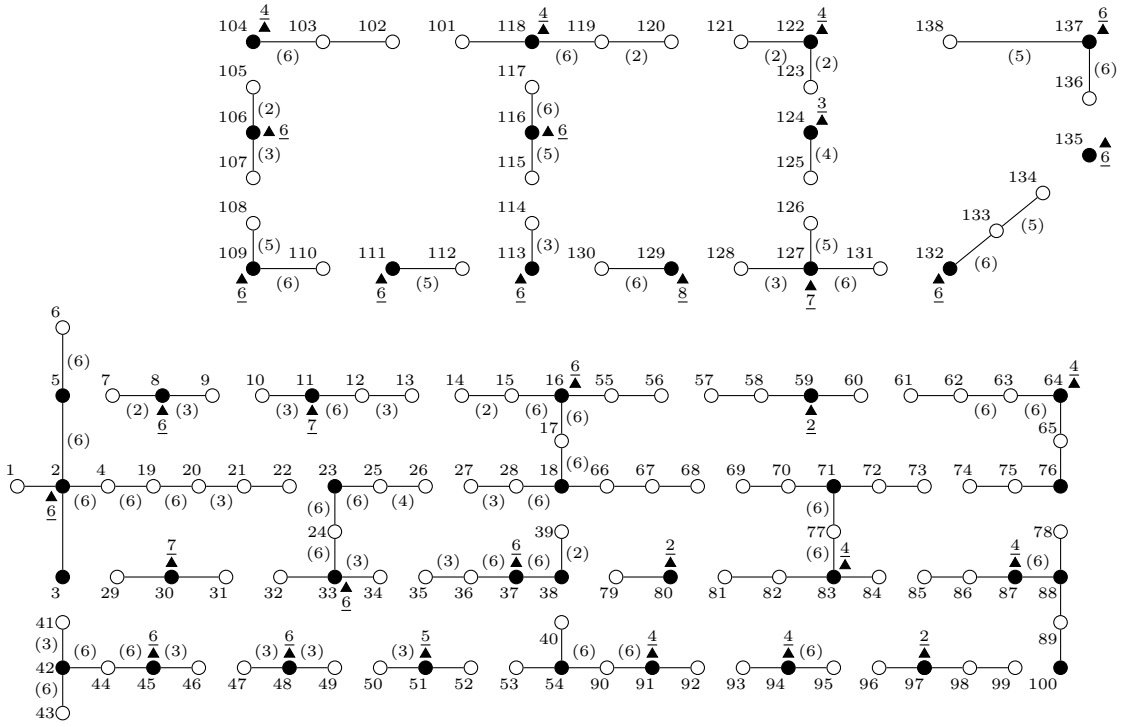

Figure B.16: Case D - Secondary Networks.

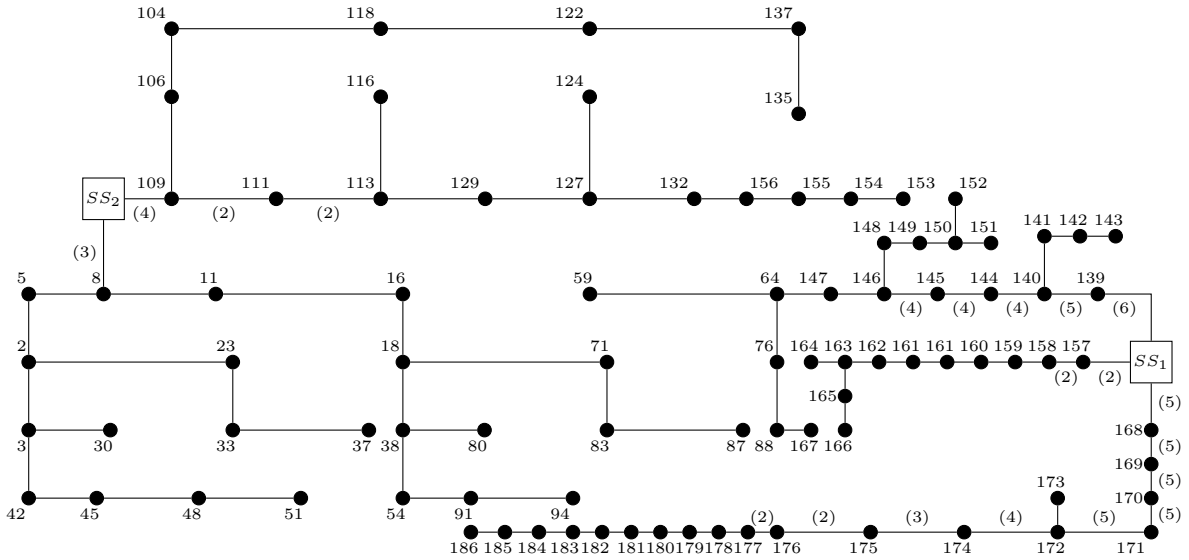

Figure B.17: Case E - Primary Network.

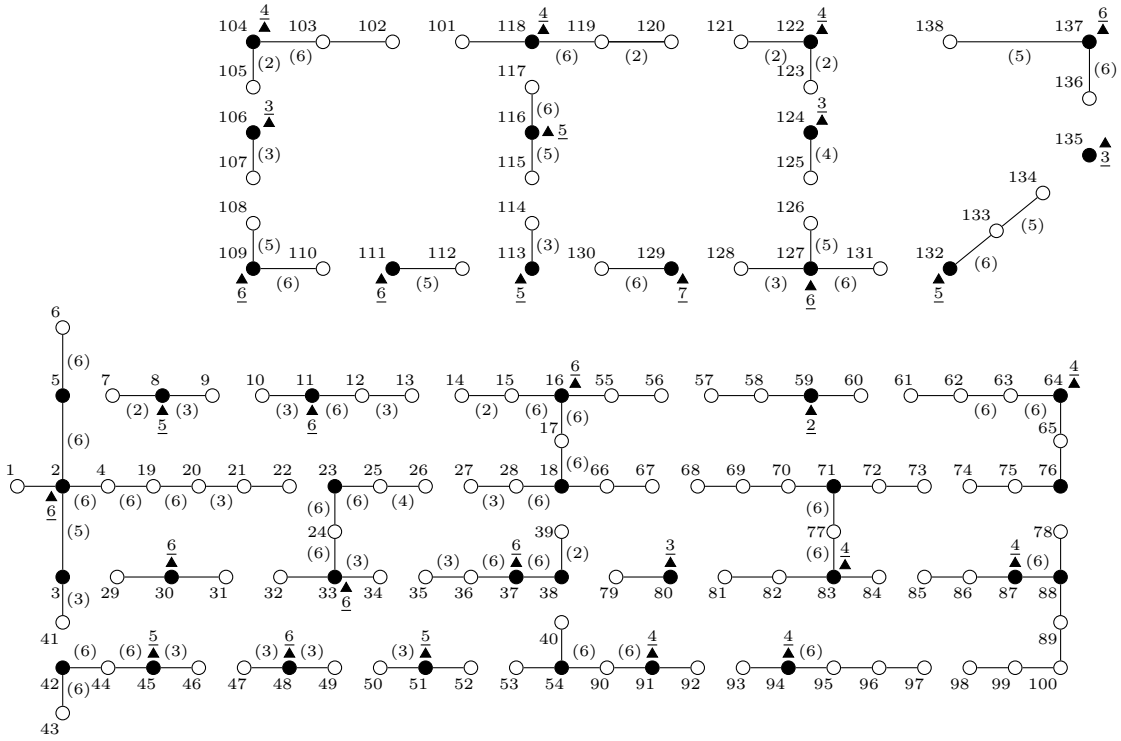

Figure B.18: Case E - Secondary Networks.